DOT/FAA/AR-05/24

Office of Aviation Research
Washington, D.C. 20591

An Inferred European Climatology of Icing Conditions, Including Supercooled Large Droplets

June 2005

Final Report

U.S. Department of Transportation
Federal Aviation Administration

NOTICE

Technical Report Documentation Page

1. Report No.	2. Government Accession No.	3. Recipient's Catalog No.
DOT/FAA/AR-05/24		

4. Title and Subtitle	5. Report Date
AN INFERRED EUROPEAN CLIMATOLOGY OF ICING CONDITIONS, INCLUDING SUPERCOOLED LARGE DROPLETS	June 2005
	6. Performing Organization Code

7. Author(s)	8. Performing Organization Report No.
Ben C. Bernstein	

9. Performing Organization Name and Address	10. Work Unit No. (TRAIS)
Research Applications Program National Center for Atmospheric Research 3450 Mitchell Lane Boulder, CO 80301	11. Contract or Grant No.

12. Sponsoring Agency Name and Address	13. Type of Report and Period Covered
U.S. Department of Transportation Federal Aviation Administration Office of Aviation Research Washington, DC 20591	Final Report
	14. Sponsoring Agency Code AIR-100

15. Supplementary Notes

The FAA William J. Hughes Technical Center Technical Monitor was Dr. James Riley.

16. Abstract

The need for new regulations concerning flight into supercooled large droplet (SLD) icing conditions is currently under consideration. One aspect of determining the need for such regulations is to assess frequency of occurrence, spatial distribution, temporal distribution, and extent of icing conditions, including those from SLD. Little information on these topics is available, due to a lack of regular, direct measurements. Research aircraft provide in situ observations, but the sample set is small and can be biased. Other techniques must be used to infer the presence of such conditions to create a more unbiased climatology. Their presence and absence can be inferred using surface weather observations in conjunction with vertical profiles of temperature and moisture. Such a technique was successfully undertaken for the North American continent. In this study, a similar climatology of icing and SLD was created for Europe and surrounding areas using 15 years of coincident, 12-hour surface weather reports and balloon-borne soundings. Icing conditions were found to be most common across northern and central Europe, especially over Scandinavia, Germany, and nearby locales. SLD was most common over the northern portions of the continent. Prime locations mostly moved latitudinally and vertically with changes in season. Most events appeared to occur below 15,000 ft. SLD events were typically less than 2000 ft deep and formed via the nonclassical mechanism.

17. Key Words	18. Distribution Statement
Icing, Freezing drizzle, Freezing rain, Supercooled large droplet, Climatology	This document is available to the public through the National Technical Information Service (NTIS) Springfield, Virginia 22161.

19. Security Classif. (of this report)	20. Security Classif. (of this page)	21. No. of Pages	22. Price
Unclassified	Unclassified	68	

TABLE OF CONTENTS

LIST OF FIGURES

LIST OF ACRONYMS

CIP	Current icing potential
CTT	Cloud top temperature
DZ	Drizzle
FZDZ	Freezing drizzle
FZRA	Freezing rain
NCAR	National Center for Atmospheric Research
NCDC	National Climatic Data Center
PL	Ice pellets
RA	Rain
RH	Relative humidity
SLD	Supercooled large droplet
SN	Snow
TH	Thunder
UK	United Kingdom

EXECUTIVE SUMMARY

Little information has been available about the frequency of occurrence, spatial distribution, temporal distribution, and extent of icing conditions, including those from supercooled large droplets (SLD), due to a lack of regular, direct measurements. Research aircraft provide in situ observations, but the sample set is small and can be biased. Other techniques must be used to infer the presence of such conditions to create a more unbiased climatology. Their presence and absence can be inferred using surface weather observations in conjunction with vertical profiles of temperature and moisture. In this study, a climatology of icing and SLD was created using 15 years of coincident, 12-hourly surface weather reports and balloon-borne soundings taken across Europe and the surrounding areas. Icing conditions were found to be most common across northern and central Europe, especially over Scandinavia, Germany, and nearby locales. SLD was most common over the northern United Kingdom, Iceland, the Faeroe and Shetland Islands, western Norway, and northern Germany. Prime locations mostly moved latitudinally and vertically with changes in season. Most events appeared to occur below 15,000 ft. SLD events were typically less than 2000 ft deep and formed via the nonclassical mechanism.

1. INTRODUCTION.

1.1 PURPOSE.

The need for new regulations concerning flight into supercooled large droplet (SLD) icing conditions is currently under consideration. One aspect of determining need is to assess how frequently these conditions and all icing conditions exist in the atmosphere. Actual measurements of natural icing and SLD have been done using research aircraft over the last ~20 years. The data sets are cumbersome to analyze, but researchers have examined data from recent flight programs, primarily sampling clouds and precipitation over North America. The results showed that the SLD icing was more prevalent than once thought, occurring in 5% or more of the data set, depending on criteria applied to it. The fact that many of the missions were made in icing-prone areas, for the purpose of finding icing (and in some cases SLD) conditions, indicated that the values might be biased high when compared to random flights. It would be of great value to have an indication of the frequency of icing and SLD for all locations, all times of the year, and all altitudes. The cost of pursuing such a flight program is prohibitive, so such information must be inferred using other methods. This can be accomplished using coincident observations of temperature and dew point from balloon-borne soundings and surface reports of cloud cover and precipitation type. One such climatology was completed for North America. The North American results were consistent with research aircraft findings, suggesting higher than expected SLD frequencies in some areas. Analysis of European data sets has been undertaken in part to extend this analysis to, and test for consistency in the results over, another continent with large amounts of air traffic.

1.2 BACKGROUND.

In-flight icing can pose a significant hazard to aircraft and has been implicated in a number of accidents. SLD, in particular, was noted as a contributing factor in the crash of an ATR-72 on 31 October 1994 [1]. SLD icing-related incidents and accidents continue to this day, but little information is available about the frequency, spatial and temporal distribution, and extent of icing, including that which is associated with SLD, due to a lack of regular, unbiased, direct measurements. Although pilot reports provide sporadic, inconsistent information about the occurrence of icing, research aircraft provide essentially the only direct observations of SLD aloft. However, geographic coverage is limited, the sample set is small and it may be biased by the purpose of the flight program (i.e., to find icing) [2 and 3]. Surface-based climatologies can provide some clues about SLD, but no information about the vertical extent of the phenomenon or its presence aloft when freezing precipitation does not reach the surface. Thus, other techniques must be used to create a more unbiased climatology. By properly combining coincident surface weather observations and vertical profiles of temperature and moisture from balloon-borne instruments, the potential for the presence of icing and SLD can be inferred. Such a climatology was completed for Canada and the United States [4], supplying geographic and altitude distributions as well as estimates of SLD layer depth. In this report, the same approach was used to extend the climatology to cover Europe and some surrounding areas. The North American climatology included information about spatial coverage and persistence of SLD events, using gridded diagnoses. Such data was not available for Europe, so this analysis was not done.

Researchers have attempted to estimate icing and SLD frequencies aloft over parts of the globe using a variety of data sets. Icing climatologies were constructed using pilot reports [5 and 6], icing algorithm output [5 and 7], soundings [8 and 9], surface observations [6, 10, 11, and 12], combinations of soundings and surface observations [3], ice detectors on mountains [13], in situ reports from reconnaissance aircraft [14] and research aircraft [15], manually generated icing forecasts [3], and computer-generated weather model output [16]. Some approaches are two-dimensional, while others include information on occurrence versus altitude or pressure. Most cover specific regions (e.g., North America or Europe), while others cover the entire northern hemisphere. Results vary with data sets and methodologies employed, location, time of year, and altitude, but some were reasonably consistent [e.g., 3, 4, and 9]. It is beyond the scope of this document to intercompare the results of the climatologies, but comparisons between them and the results described here are made in section 4.

Most SLD climatologies have depended solely on surface reports of freezing drizzle (FZDZ) and freezing rain (FZRA), which strongly imply the presence of SLD aloft, since the droplets had to have fallen from above. Ice pellets also imply the presence of SLD aloft, since they are typically formed from FZRA droplets that have frozen before impacting the surface. While such analyses can provide a first cut at the frequency, location, time of year, and even time of day, SLD commonly occur aloft in the absence of FZDZ, FZRA, or ice pellets (PL) at the surface [4]. Thus, this approach results in an underestimate of SLD frequencies aloft. For example, FZDZ or FZRA aloft may fall into above-freezing air, resulting in drizzle (DZ) or rain (RA) at the surface. One could examine DZ and RA observations, but far from all DZ and RA result from FZDZ and FZRA aloft. Most RA is formed from snow that has melted before reaching the surface. A significant percentage of DZ at the surface results from clouds that are at above freezing temperatures throughout their depth. Thus, a surface-based analysis using FZDZ, FZRA, PL, DZ, and RA would result in an overestimate of SLD frequency aloft.

However, given additional information about the temperature and moisture profile that exists above such observations, one can infer the process that formed the precipitation aloft and determine whether or not SLD was likely aloft and at what altitudes. Automated icing algorithms have been developed by the National Center for Atmospheric Research (NCAR) to accomplish this task. One special version was designed to perform this task using climatological data sets of coincident surface observations and balloon-borne soundings of temperature and moisture. This technique has been applied successfully to large data sets taken across North America [4].

2. DATA SETS AND METHODOLOGY.

This section describes the climatological data sets and methods used to create the European SLD icing climatology.

2.1 SOUNDINGS.

Vertical profiles of temperature and moisture were derived from a National Climatic Data Center (NCDC) database of balloon-borne soundings taken at 336 sites across Europe and surrounding areas between 1980 and 1994 (see figure 1a for site locations and figure 1b for identification of countries). Quality control was applied to the sounding data exceeding NCDC standards to only include those that had good temperature and moisture data up to at least T = -35°C, reached 400 mb, and had at least 10 data points at or below this level. This limited the database to profiles that were of relatively good quality, had adequate resolution, and were deep enough to reach temperatures where ice-phase (rather than liquid-phase) cloud tops were very likely to dominate. The ten vertical level minimum was less than ideal, but adequate for analysis. Most soundings had significantly more vertical resolution.

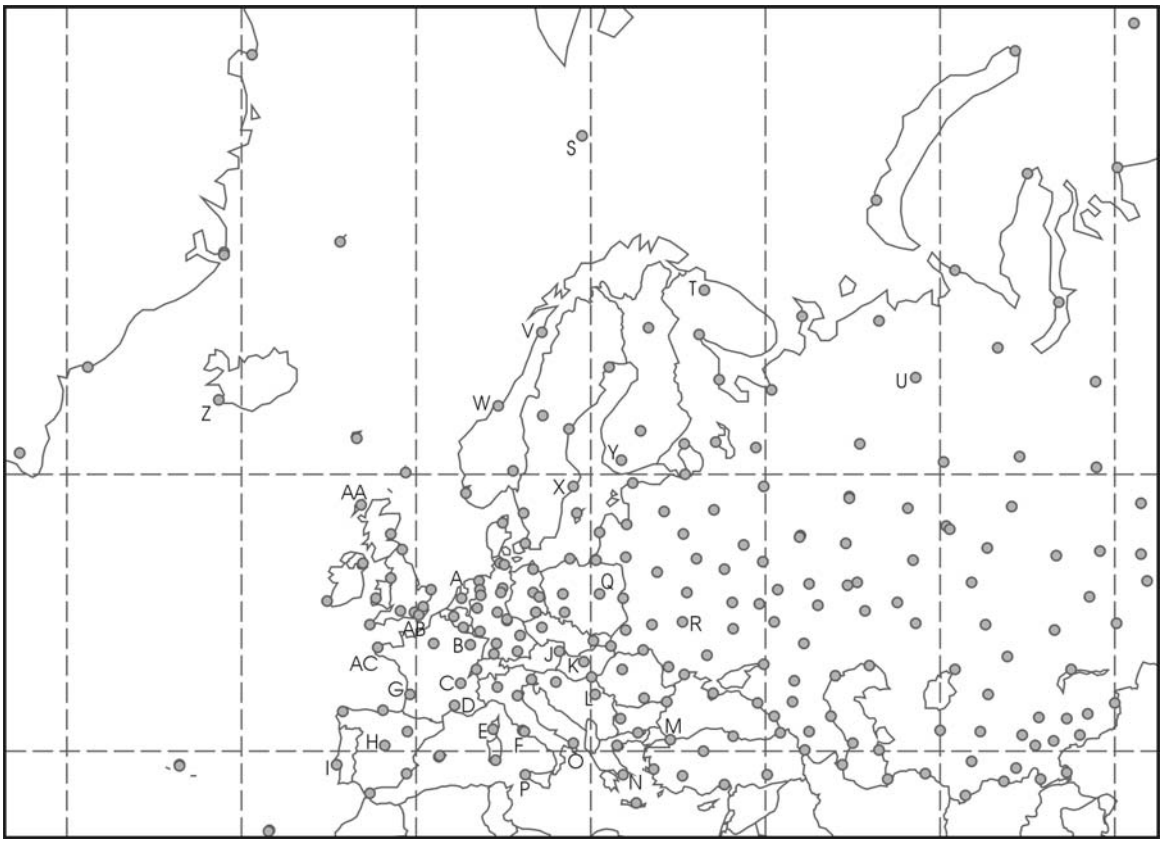

Note that political changes in far eastern Europe and the former Soviet Union are not depicted on this or any other map. Letters match figures 9a through 9ac.

FIGURE 1a. LOCATION OF SOUNDING SITES (GREY DOTS) ACROSS EUROPE AND SOME SURROUNDING COUNTRIES

FIGURE 1b. GEOPOLITICAL MAP OF EUROPE

Soundings were launched at 1100 and 2300 (all times coordinated universal time). The 15-year data set resulted in up to ~10,500 soundings per site. Horizontal coverage was fairly uniform across the domain, eliminating most geographic biases. Interpolation of results between sites was reasonable except in areas where local effects are important, such as near mountain ranges and large water bodies. Local maxima and minima may exist in these areas but will not be captured here.

2.2 SURFACE OBSERVATIONS.

Surface Observations were derived from NCAR and NCDC archives. At each sounding site, all observations made within a 100 km radius were considered in the diagnosis of cloud cover and precipitation type. Station elevations had to be within 2000 ft (609 m) of the sounding site to eliminate the use of irrelevant observations in areas of steep terrain. The number of surface stations available varied from site to site, with several sites having only one surface station (e.g., Jan Mayen, Norway), while others had ten or more (e.g., London, England). Sounding sites with more nearby stations had a better chance of identifying spotty or sporadic precipitation.

The presence or absence of clouds was determined using the maximum cloud cover reported at all stations within 100 km. If all of the stations reported either clear or scattered sky cover, then it was considered to be a cloud free sounding for icing purposes. Nearly all icing occurs in places where at least broken sky cover is reported [17]. If any of the stations within the 100 km radius reported broken, overcast, or obscured sky cover, then the ceiling height was set to the height of the lowest deck that met these criteria (all heights are in meters above mean sea level). Precipitation observations were checked for the presence of the following precipitation types: FZDZ, FZRA, PL, RA, snow (SN), and DZ. The system also searches for observations of thunder (TH), which provide an indication of the presence of deep convection. For ceiling and precipitation reports, data from the valid time of the launch (0 or 12 UTC) were used because they were the most reliably available and were still representative of the conditions present during the balloon flight. Icing and SLD associated with TH were not included in the results shown here.

2.3 CURRENT ICING POTENTIAL AND THE CIP SOUNDING TECHNIQUE.

Meteorologists at the NCAR developed a multiple data source, hybrid approach to the diagnosis of icing, the current icing potential (CIP) [18]. In March 2002, CIP became an official Federal Aviation Administration and National Weather Service product. The latest version of CIP combines satellite, radar, surface, and lightning observations with numerical model output and pilot reports of icing to create an hourly, three-dimensional diagnosis of the potential for icing, and SLD. CIP uses observations to diagnose the locations of clouds and precipitation, and then combines them with numerical model output in a situationally based, fuzzy logic system. It also divides the ground surface into regions and associate a vertical column of the atmosphere with each region. The physical structure of each atmospheric column is assessed, and an icing scenario is identified using a decision tree. Data are treated differently for each scenario, and fuzzy logic membership functions are applied to fields such as temperature and relative humidity in an appropriate manner. The algorithm determines icing and SLD potentials for each level in the sounding. The potential is essentially a confidence or likelihood that such conditions were present. Their presence becomes increasingly more (less) likely at the higher (lower) thresholds, and the algorithm was more (less) efficient at capturing pilot reports while warning for a relatively small (large) volume of airspace in this range. Throughout this report, the threshold of 0.4 will be used. Locations where potentials exceeded 0.4 were considered to have had a good potential for the conditions, while experience indicates that this threshold is fairly efficient in avoiding overwarning or overdiagnosing. Regardless of threshold choice, geographic patterns and vertical distributions in the results were essentially the same (see section 3 for an example).

Sensitivity tests indicated that the use of higher (lower) thresholds resulted in lower (higher) frequencies, and shallower (deeper) layers. A more complete description of CIP, its components and application of fuzzy logic, is found in reference 18.

A special version of CIP was developed that diagnoses icing and SLD potentials in a column using the vertical profile of temperature and moisture from a balloon-borne sounding in combination with coincident surface observations. Such an approach can be applied to historical data sets to determine the frequency at which icing and SLD can be expected above a given site as well as across a region, continent, or even the globe. The CIP sounding technique essentially mirrors that of the real-time CIP described in reference 18. The technique is quite complex, so only the aspects that are unique to the CIP sounding system are described here. In short, the cloud top height and temperature are determined using the moisture profile in the sounding, rather than satellite data, while the occurrence of precipitation and precipitation type are determined solely from surface observations, rather than both surface observations and radar reflectivity. Pilot reports of icing and forecasts of vertical velocity and explicit supercooled liquid water are not available for climatological studies, so they are not used in the sounding CIP. Stricter versions of the relative humidity and cloud top temperature membership functions are applied because the improved quality of moisture data in soundings (as compared to numerical weather model forecasts) provides more accurate estimates of cloud locations and cloud top temperatures.

2.3.1 Determining Cloud Presence and Candidate Altitudes.

The first step in finding icing and SLD is to see if clouds and precipitation are present. If the surface observations indicate that the sounding ascended through a cloud-free environment, then the icing and SLD potentials are set to zero throughout the column. If clouds are present, then the altitudes that are likely to contain clouds and precipitation are identified and all other altitudes are considered to be free of icing and SLD. The lowest altitude considered for icing and SLD is set to ground level when any form of liquid or freezing precipitation is present, since it is possible for icing and SLD to exist from cloud base down to the ground.

Cloud top height is estimated by searching downward through the profile until relative humidity (RH) with respect to water or ice either (1) meets or exceeds 87% or (2) meets or exceeds 84% and the RH of the level above is at least 3% lower [19]. The presence of multiple cloud layers is inferred if the dry layer beneath a cloud deck appears to be adequate for complete sublimation or evaporation of any particles falling from it. If adequate dry air is present and an additional layer meeting the RH thresholds is found beneath the dry layer, then a new cloud deck is identified (see example in figure 2). The cloud top temperature (CTT) of each layer is set to the temperature where the RH threshold is first met. All altitudes above the highest cloud top are indicated as free of icing and SLD. SLD potential is only determined for the lowest cloud layer and altitudes between it and the surface, since only this layer is likely to form precipitation reported at the surface.

Once cloudy and/or precipitating altitudes are found, the sounding structure and precipitation are examined to determine the meteorological situation that is present. This situational approach is

critical, since the meaning of an individual piece of data can be very different for different situations.

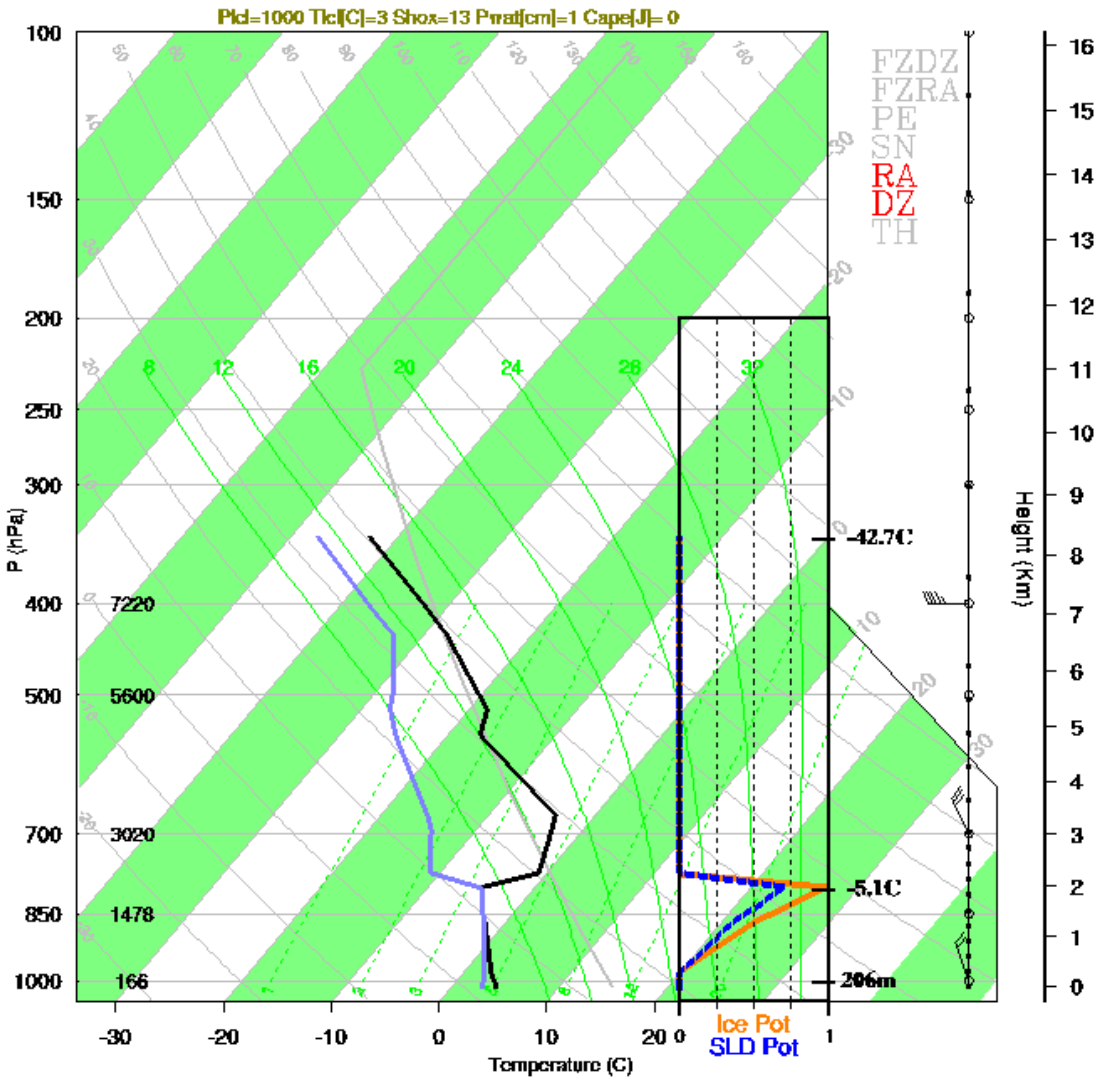

Boxed area to the right of temperature profile contains the diagnosed icing (orange line) and SLD potentials (dark blue line) on a 0 to 1 scale. Reported precipitation types are indicated in red. The solid blue and black curves are for temperature and dew point.

FIGURE 2. EXAMPLE SKEW-T PLOT FOR SOUNDING TAKEN AT EMDEN, GERMANY THROUGH A TWO-LAYER CLOUD WITH ABOVE-FREEZING PRECIPITATION AT THE SURFACE

2.3.2 Icing and SLD Scenarios.

While icing forms via several mechanisms, two primary mechanisms are responsible for the formation of SLD: classical and nonclassical. By determining the mechanism and examining the temperature and moisture profiles as well as the observed precipitation type, the sounding CIP can be used to diagnose the SLD potential. The classical and nonclassical mechanisms are

described below because of their criticality for SLD. Alternative icing mechanisms are described in reference 18. They include single- and multilayer nonprecipitating clouds and deep convection.

2.3.2.1 Classical.

Classical icing and SLD occurs when a layer of temperature (T) T>0°C (warm nose) is located between two layers with T<0°C, surface freezing or liquid precipitation is observed and the CTT (cloud top temperature) is less than -12°C (figure 3(a)). The relatively cold CTTs indicate that an ice process is likely to be active above the warm nose. Snow falls into the warm nose, melts to form liquid precipitation, which subsequently falls into the lower subfreezing layer to form classical SLD, usually in the form of FZRA. The precipitation typically reaches the surface in the form of FZRA, PL, or RA, depending on the strength of the warm nose and the T and RH within and beneath the lower subfreezing layer [20]. It occasionally reaches the surface in the form of FZDZ or DZ when very light snow starts the process above the melting zone or the process is entirely nonclassical, but this is uncommon.

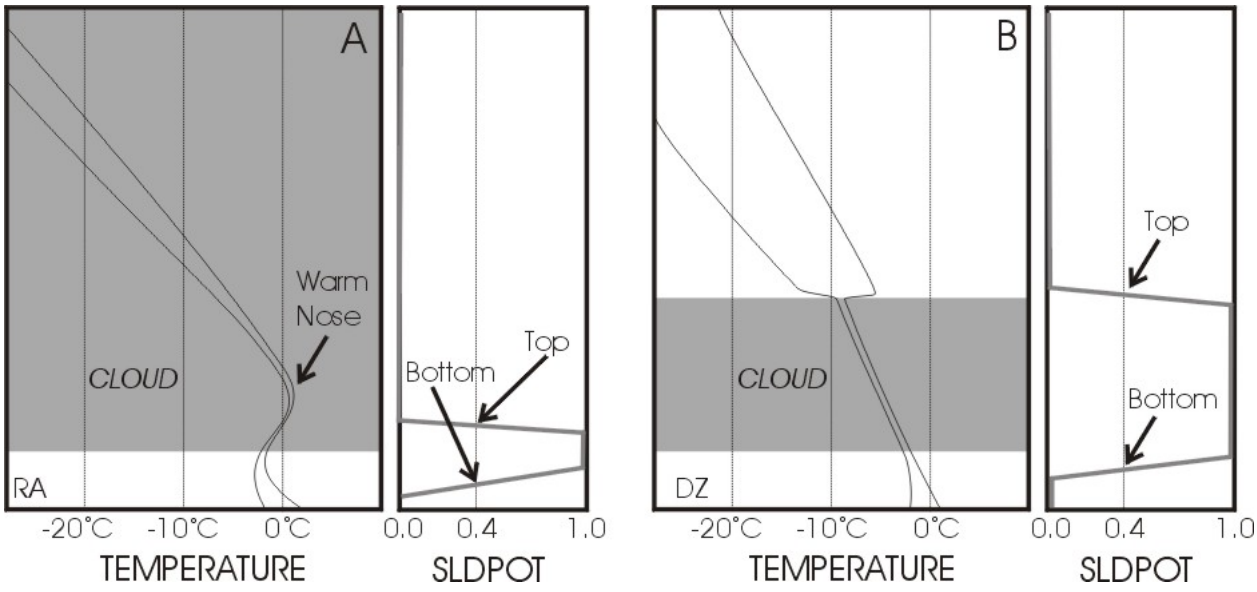

FIGURE 3. EXAMPLES OF (a) CLASSICAL AND (b) NONCLASSICAL SLD

2.3.2.2 Nonclassical.

Nonclassical (collision-coalescence) icing and SLD occurs in one of three situations (figure 3(b)): (a) freezing or liquid precipitation is observed when a classical warm nose is present, but CTT is greater than -12°C, indicating a good chance that an all-liquid process is responsible for the precipitation formation; (b) no warm nose is present, only RA and/or DZ are observed at the surface, and CTT is greater than -12°C; and (c) no warm nose is present and freezing precipitation (FZDZ, FZRA, and PL) is observed at the surface. CTT is not a factor in case (c), since the precipitation has been formed via collision-coalescence.

2.4 FREQUENCY AND LAYER DEPTH CALCULATIONS.

Each sounding was examined for its icing and SLD potential at every level. Frequencies (%) were calculated by dividing the number of soundings that had SLD potential ≥ 0.4 at any level by the total number of soundings examined. Layer depths were calculated by finding the lowest altitude with a value ≥ 0.4 then checking each level above this until a value < 0.4 was found (figure 3). The top and bottom of the layers with SLD potential ≥ 0.4 layer were found using linear interpolation. SLD (but not icing) layer depth was the difference between those altitudes.

Using this approach, the top of the icing and SLD layer was often at the top of the lowest cloud deck. While SLD often forms at cloud top, and proliferates through all subfreezing levels below, this is not always the case. SLD may have only existed through a portion of the cloud deck that produced the precipitation [21]. It was impossible to determine with certainty what the height of the top of the SLD layer was using sounding data for nonclassical SLD situations. Thus, the nonclassical layer depth represented the greatest possible vertical extent of the SLD, and was likely an overestimate of the actual SLD depth. For classical SLD, the depth of the layer was easily determined from the location of the upper and lower 0^{o}C levels, so layer depths were expected to be quite accurate.

3. RESULTS.

3.1 GEOGRAPHIC DISTRIBUTION.

Figures 4a and 4b show the full-year geographic distribution of icing and SLD frequencies for most of Europe and some surrounding areas, using a threshold of 0.4. Maximum frequencies were on the order of 45% for icing and 15% for SLD, but were significantly lower when a threshold of 0.6 was applied to the icing and SLD potentials (figures 4c and 4d). Clearly, absolute frequencies depend heavily on threshold choice. For the remainder of this report, the results found using a threshold of 0.4 will be discussed, but this sensitivity should be borne in mind.

The primary icing maxima were found over Scandinavia, Germany, and the nearby surrounding areas. The primary SLD maxima were somewhat more confined to the United Kingdom (UK), western Scandinavia, and around northern Germany. Most areas had icing <30% and SLD <5% of the time, with minimum frequencies over southern Europe, especially near the Mediterranean Sea, as well as large portions of Russia (SLD only, see later discussion). While the frequencies may sound large, recall (section 2.3) that this number was calculated using a low-to-moderate threshold (0.4) and that it indicates that there was a chance of icing or SLD at any altitude, somewhere within 100 km of the sounding site. It does not imply that icing and SLD would be encountered by 30% and 5% of all flights into that area, respectively. Peak frequencies found using the same methodology over North America were on the order of 40% for icing and 5%-10% for SLD, so European peak areas appear to have similar icing frequency but somewhat more frequent SLD.

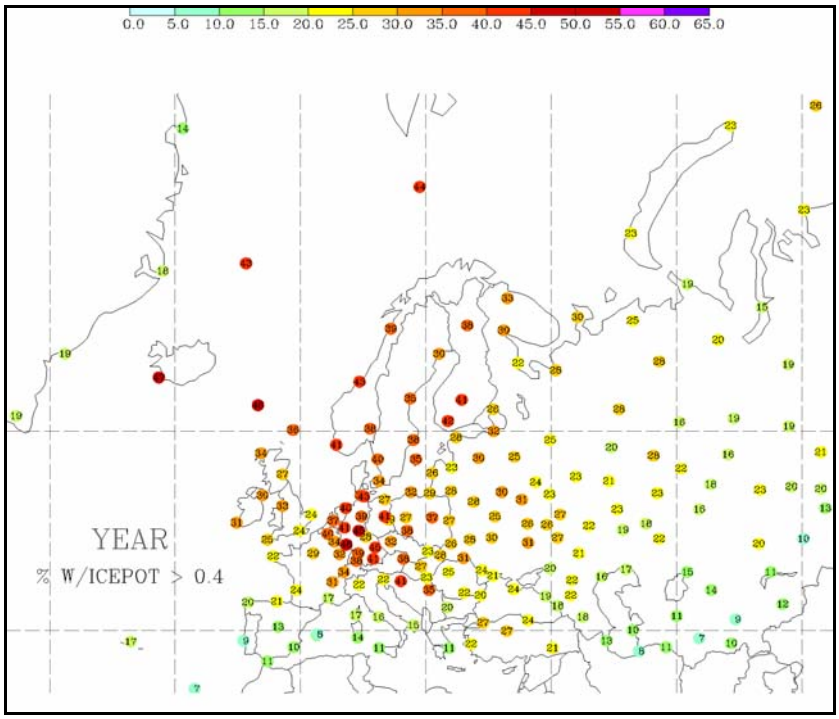

FIGURE 4a. ANNUAL AVERAGE COLUMN ICING FREQUENCIES (%) OVER EUROPE, USING A THRESHOLD OF 0.4

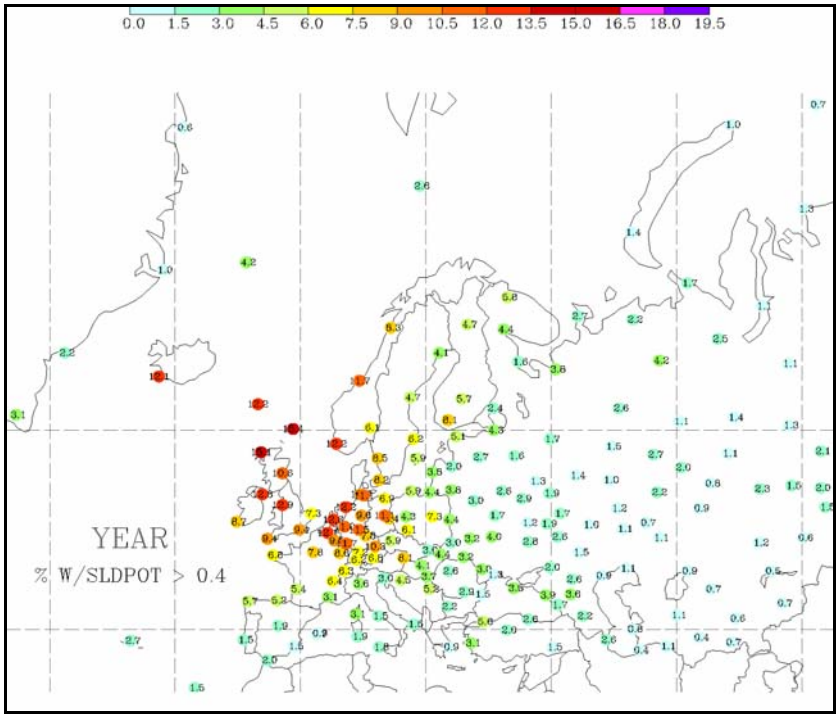

FIGURE 4b. ANNUAL AVERAGE COLUMN SLD FREQUENCIES (%) OVER EUROPE, USING A THRESHOLD OF 0.4

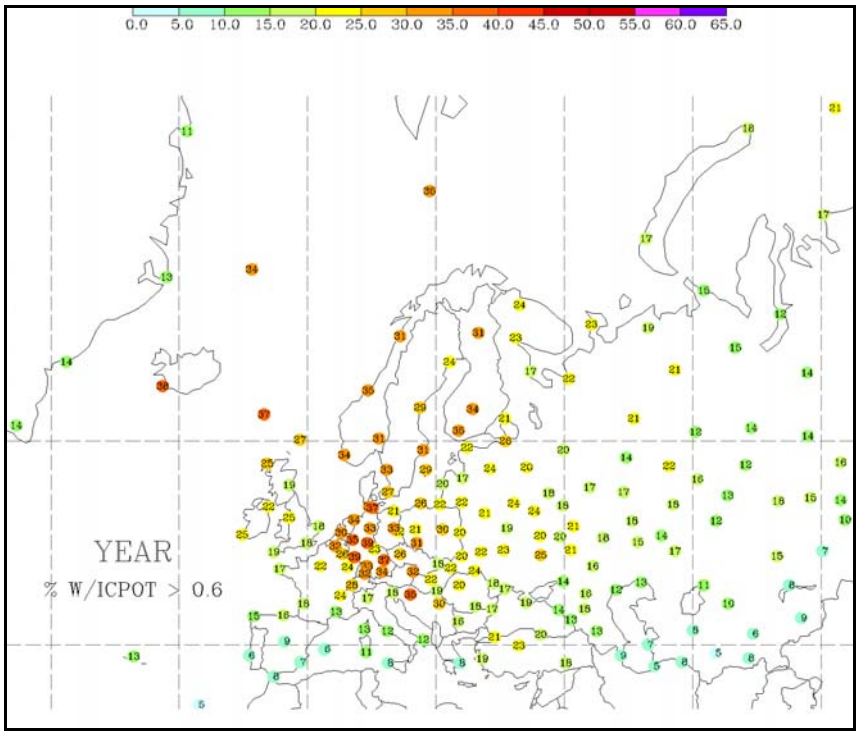

FIGURE 4c. ANNUAL AVERAGE COLUMN ICING FREQUENCIES (%) OVER EUROPE, USING A THRESHOLD OF 0.6

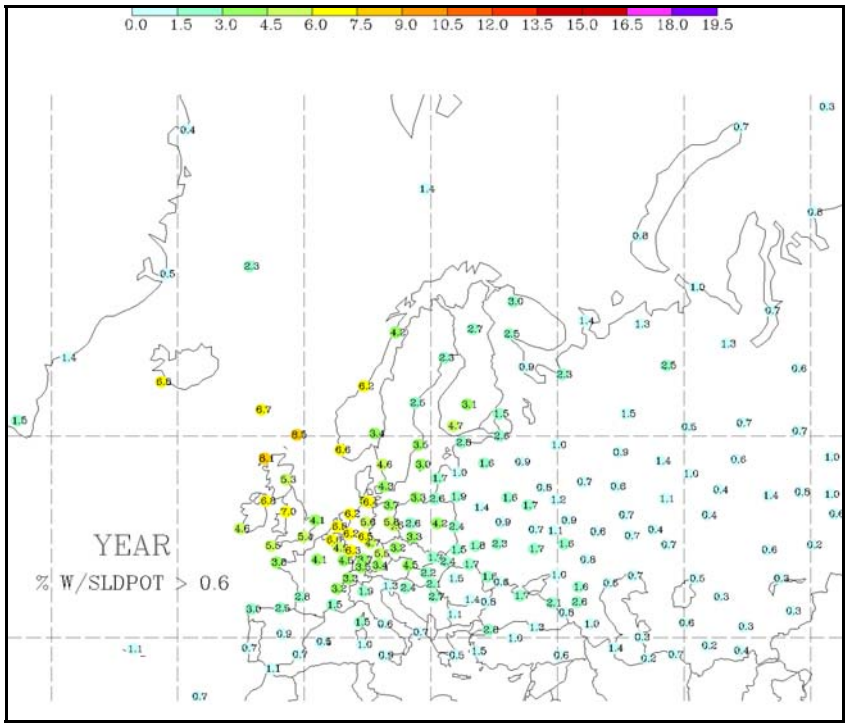

FIGURE 4d. ANNUAL AVERAGE COLUMN SLD FREQUENCIES (%) OVER EUROPE, USING A THRESHOLD OF 0.6

Icing is found most often in places where overcast skies are common (figure 5a) and the clouds have a combination of ideal temperatures within them and at their tops. The locations of the primary SLD maxima are ones where icing clouds with relatively clean source air are expected. These are usually downstream of large fetches of airflow over oceans. Iceland, western Norway, and most of the UK are excellent examples, since their predominant wind directions come off the Atlantic and Arctic Oceans. Such clean source air was found to be conducive to the formation of FZDZ and has been observed in research flights made along the coasts of Newfoundland, the Arctic, and southeastern Alaska [2 and 22]. Long fetches over the ocean are not expected for Germany, Denmark, and the Benelux regions, where the nearest large water body (the North Sea) is relatively small. However, these areas are still quite cloudy and often receive drizzle or light rain (see figures 5b and 5c) in combination with warm cloud tops (> -12ºC), a combination that is often associated with the presence of SLD aloft. Note that surface FZDZ and FZRA are uncommon across all of Europe (figures 5d and 5e), so little of the SLD aloft reaches the surface. For the most part, only elevated stations observed FZDZ or FZRA with significant frequency [11], which matches the lack of SLD below 3000 ft across most of Europe, (discussed in section 3.2). Icing minima occur in areas where skies tend to be less cloudy and SLD minima occur in these same areas and where surface drizzle and light rain is uncommon, such as across most of Russia.

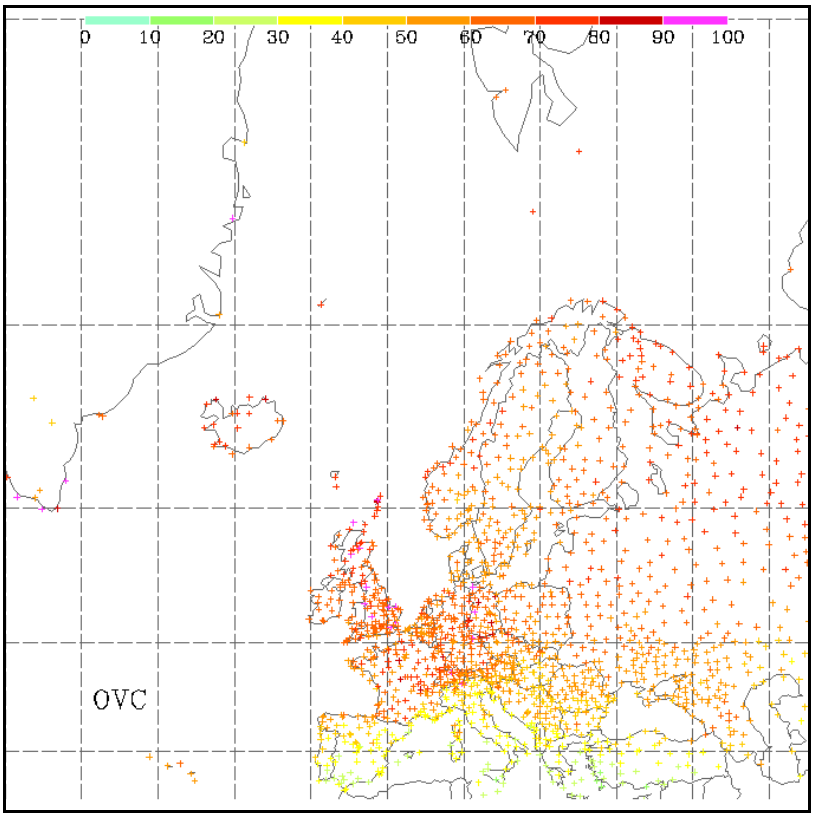

(Scale is shown at the top. Gradations are every 10%.)

FIGURE 5a. PERCENTAGE OF ALL SURFACE OBSERVATIONS THAT HAD OVERCAST SKY COVER

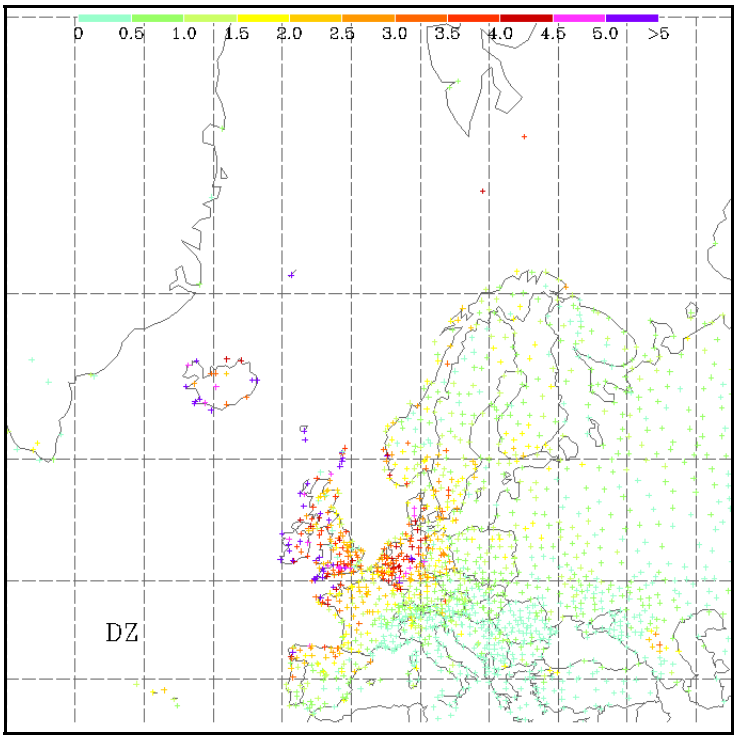

(Scale is shown at the top. Gradations are every 0.5%.)

FIGURE 5b. PERCENTAGE OF ALL SURFACE OBSERVATIONS THAT HAD DZ

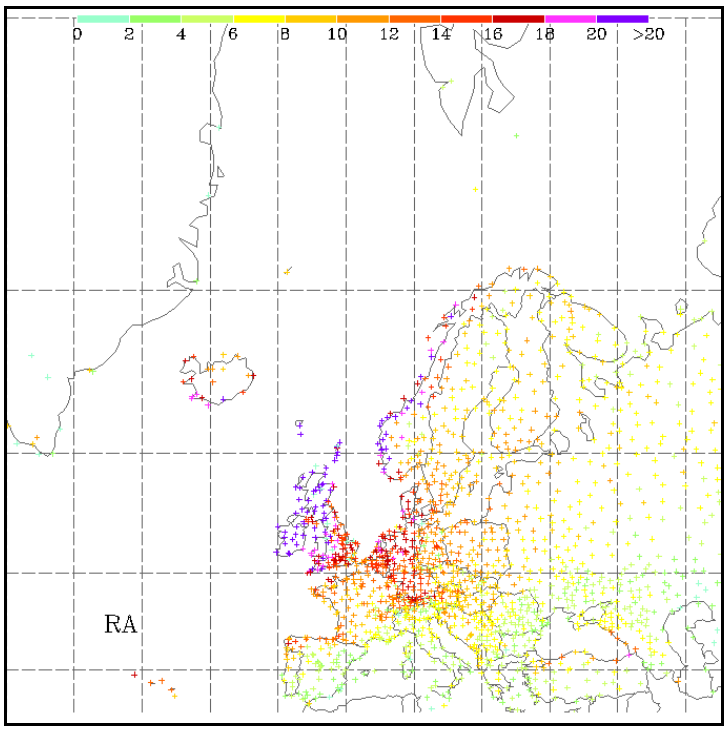

(Scale is shown at the top. Gradations are every 2%.)

FIGURE 5c. PERCENTAGE OF ALL SURFACE OBSERVATIONS THAT HAD RA

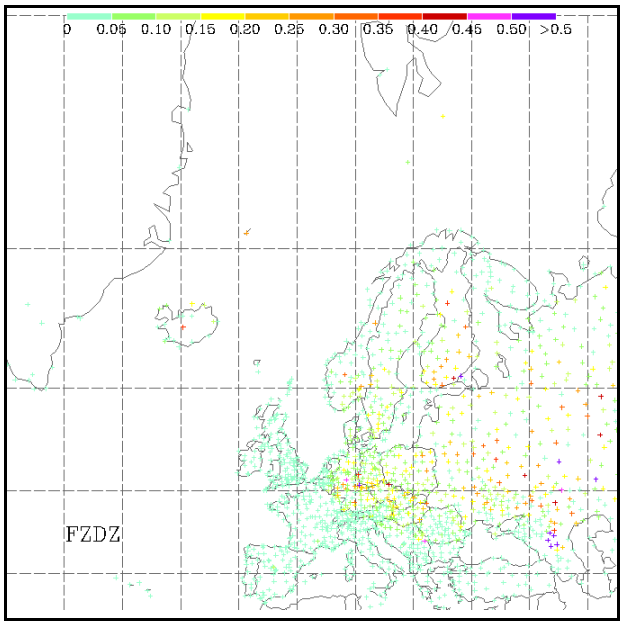

(Scale is shown at the top. Gradations are every 0.05%.)

FIGURE 5d. PERCENTAGE OF ALL SURFACE OBSERVATIONS THAT HAD FZDZ

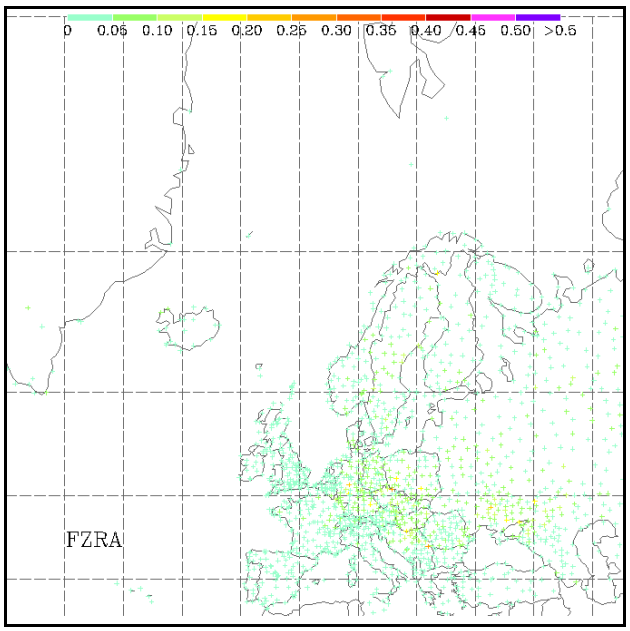

(Scale is shown at the top. Gradations are every 0.05%.)

FIGURE 5e. PERCENTAGE OF ALL SURFACE OBSERVATIONS THAT HAD FZRA

Monthly maps show that the icing and SLD maxima and minima move during the year (figures 6a-6f and 7a-7f). Significant icing frequencies (35%+) cover a broad area at many times of the year. During winter, they can be found across most of central Europe, southern Scandinavia, and from the Baltics and Balkans down to parts of Turkey. Peak frequencies of

50%+ are focused around Germany and parts of southern Scandinavia. By summer, two distinct maxima are present, with one in central Europe and another in the Arctic. This pattern persists into early fall, and central Russia becomes active toward the end of this period. By late fall, the peak icing area contracts back toward its cool season centers.

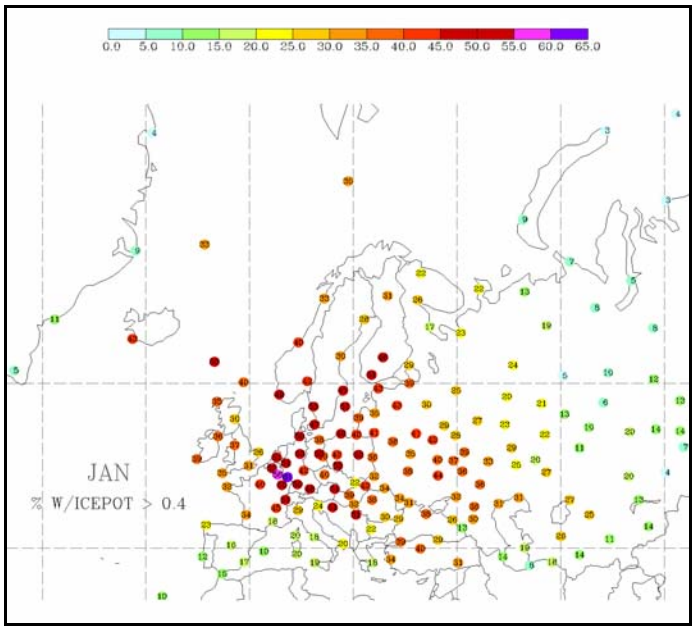

FIGURE 6a. MAP OF FULL-COLUMN ICING FREQUENCIES FOR JANUARY, USING A THRESHOLD OF 0.4

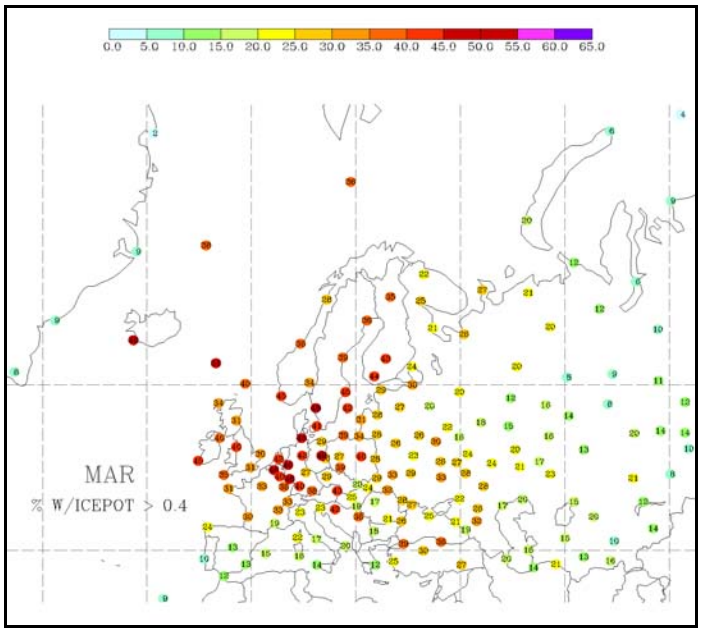

FIGURE 6b. MAP OF FULL-COLUMN ICING FREQUENCIES FOR MARCH, USING A THRESHOLD OF 0.4

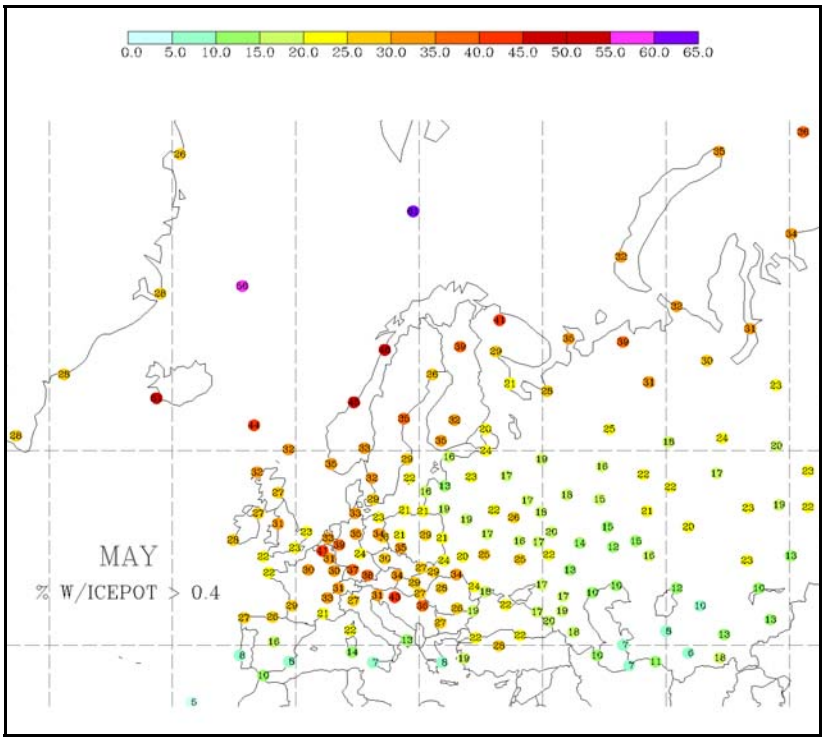

FIGURE 6c. MAP OF FULL-COLUMN ICING FREQUENCIES FOR MAY, USING A THRESHOLD OF 0.4

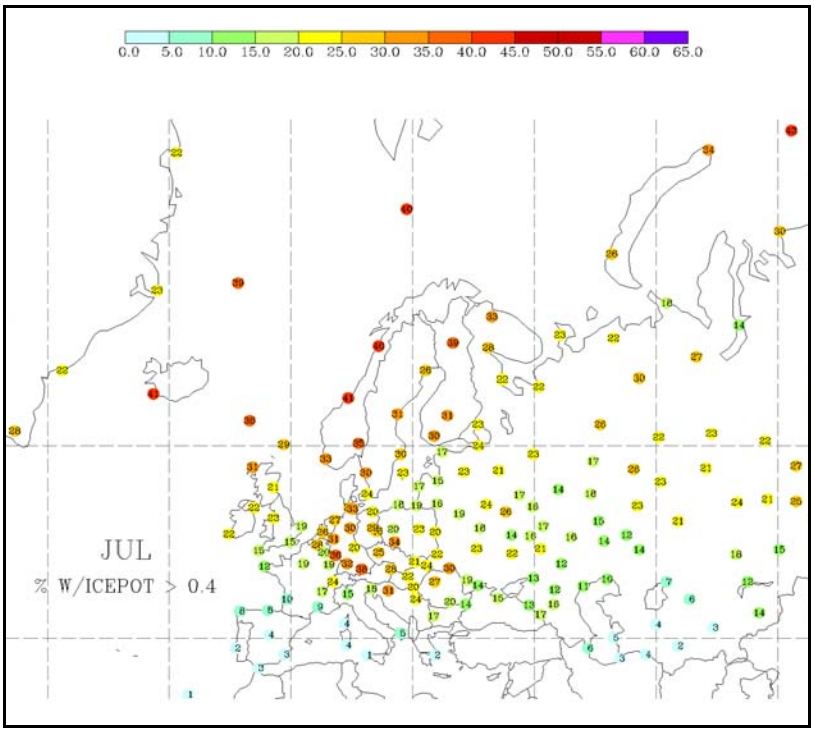

FIGURE 6d. MAP OF FULL-COLUMN ICING FREQUENCIES FOR JULY, USING A THRESHOLD OF 0.4

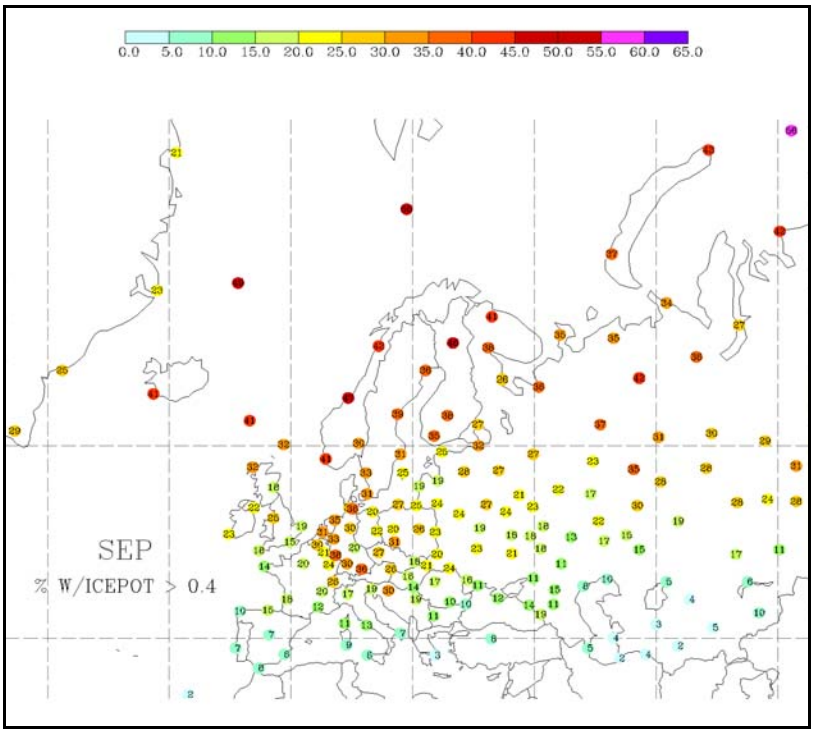

FIGURE 6e. MAP OF FULL-COLUMN ICING FREQUENCIES FOR SEPTEMBER, USING A THRESHOLD OF 0.4

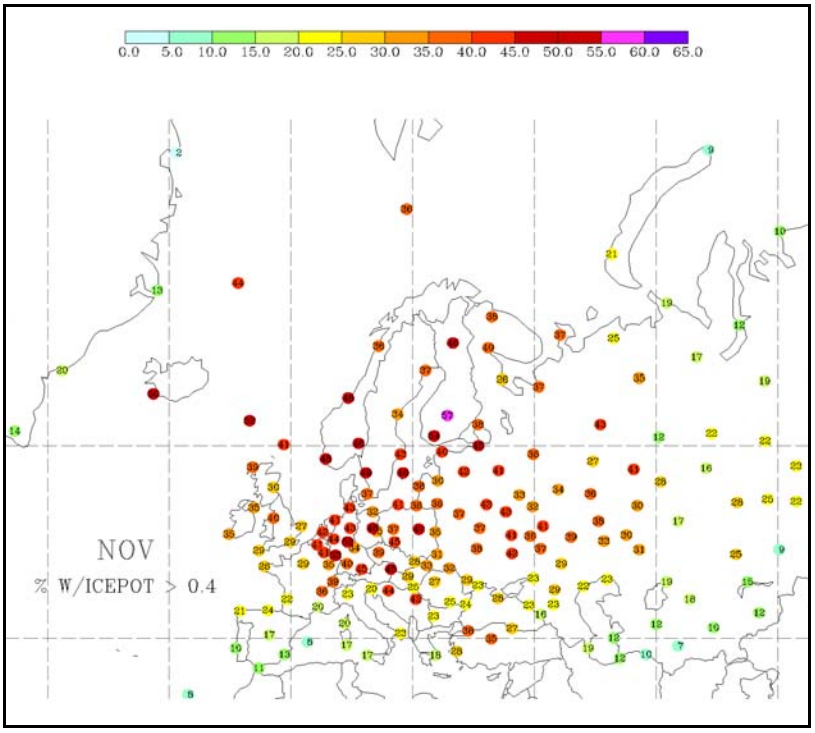

FIGURE 6f. MAP OF FULL-COLUMN ICING FREQUENCIES FOR NOVEMBER, USING A THRESHOLD OF 0.4

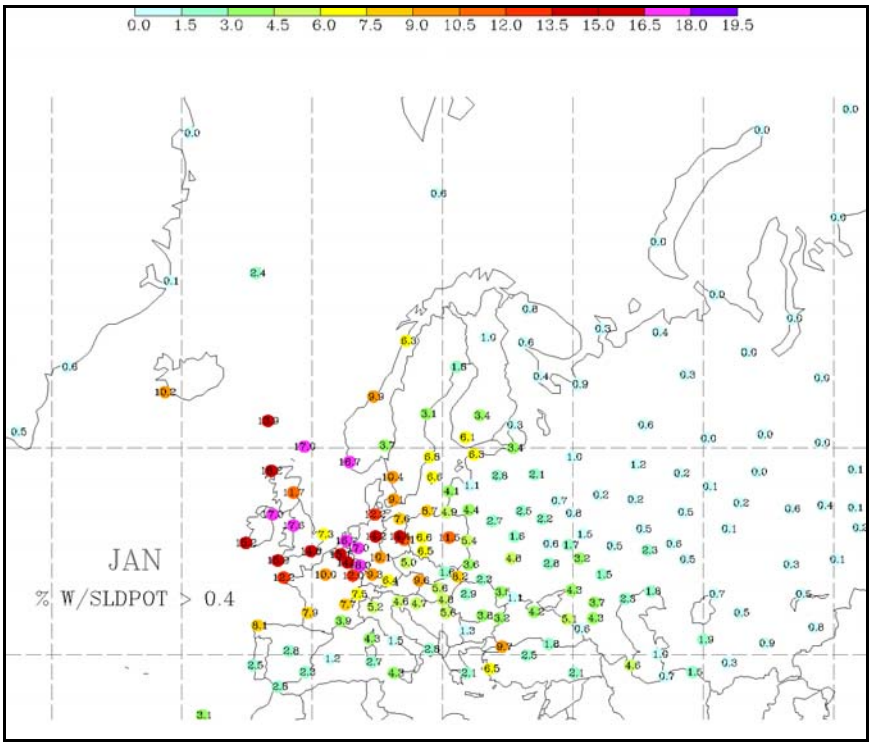

FIGURE 7a. MAP OF FULL-COLUMN SLD FREQUENCIES FOR JANUARY, USING A THRESHOLD OF 0.4

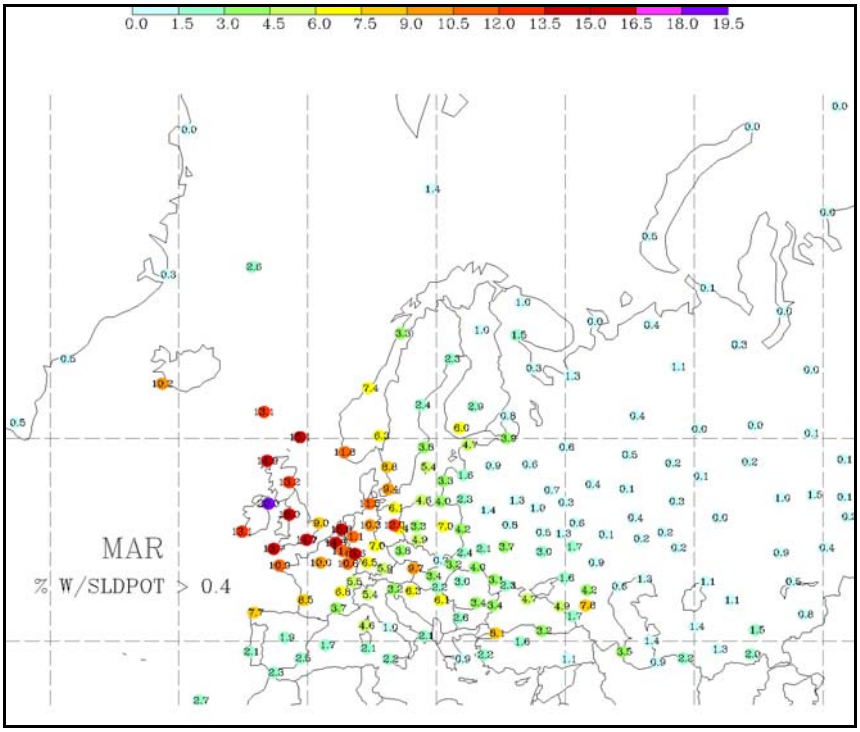

FIGURE 7b. MAP OF FULL-COLUMN SLD FREQUENCIES FOR MARCH, USING A THRESHOLD OF 0.4

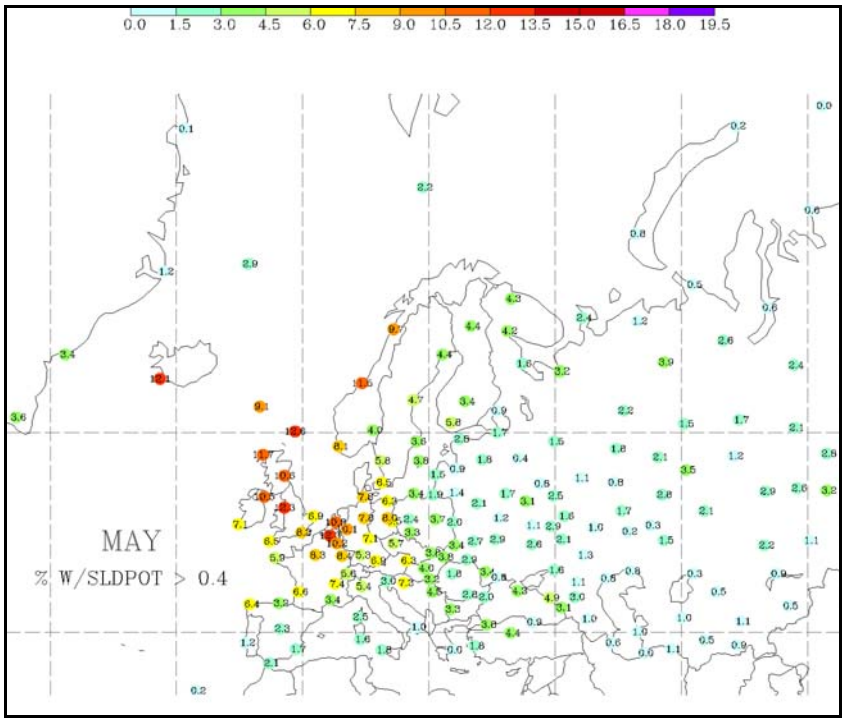

FIGURE 7c. MAP OF FULL-COLUMN SLD FREQUENCIES FOR MAY, USING A THRESHOLD OF 0.4

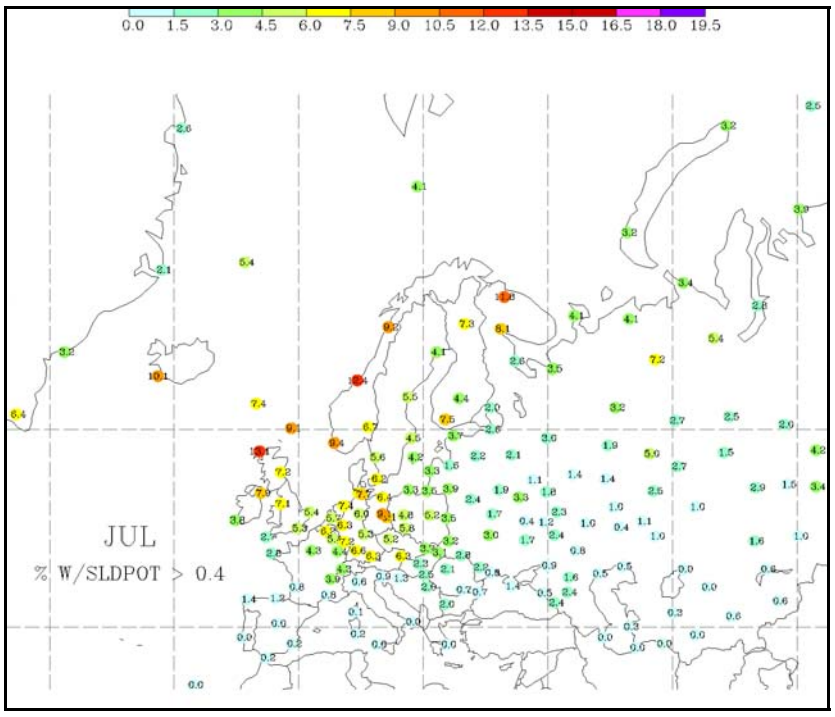

FIGURE 7d. MAP OF FULL-COLUMN SLD FREQUENCIES FOR JULY, USING A THRESHOLD OF 0.4

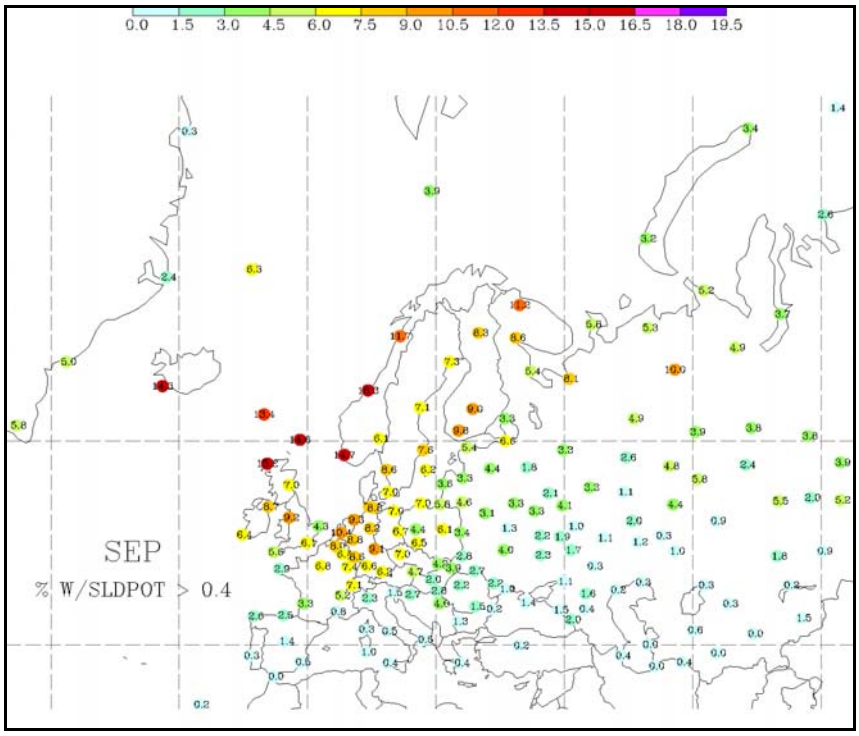

FIGURE 7e. MAP OF FULL-COLUMN SLD FREQUENCIES FOR SEPTEMBER, USING A THRESHOLD OF 0.4

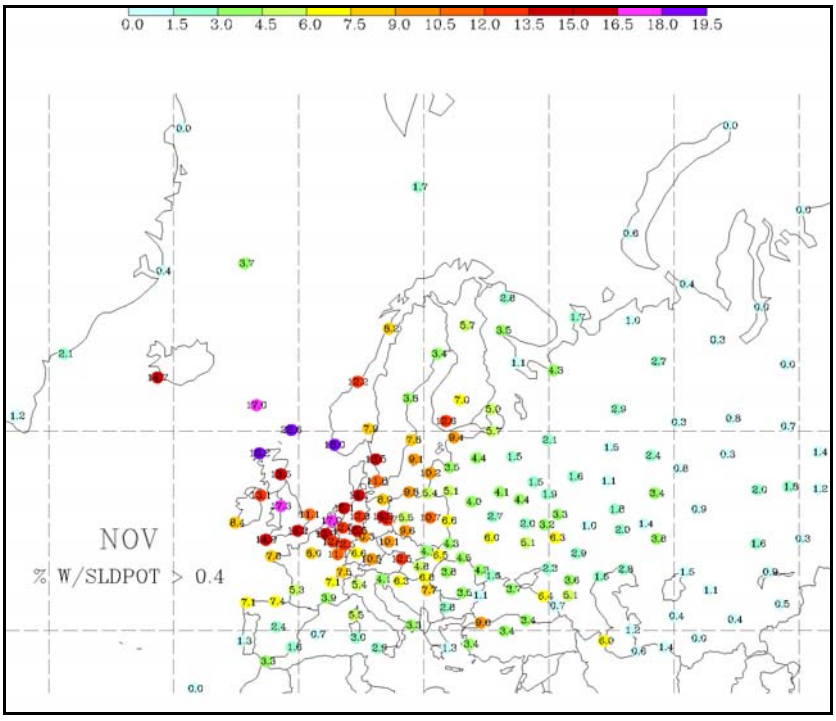

FIGURE 7f. MAP OF FULL-COLUMN SLD FREQUENCIES FOR NOVEMBER, USING A THRESHOLD OF 0.4

Significant SLD frequencies (5%+) extend as far south as northern Spain, southern France, the Alps, and Ukraine during the winter, then move northward during the summer, returning southward in the fall. The southward movement in the fall is more dramatic than the gradual northward movement in the late spring. Maxima found in places like the UK and Germany remain in place throughout most of the year, through the frequencies wax and wane. Maximum values reach 15%-20% during the peak of the winter, when particularly cloudy, drizzly conditions settle into these areas. In contrast, northern Norway has most of its SLD during the summer and relatively little during the winter, when clouds are more likely to be glaciated. Though they do not show up well in the full-year SLD chart, a few stations surrounding the Black Sea have peaks during the fall and winter. Examples from individual stations will be discussed in section 3.2.

3.2 TIME-HEIGHT DISTRIBUTIONS.

The altitudes at which icing and SLD occurred most frequently also changed during the year. Figures 8a and 8b show frequencies with both height and time of year for all stations combined. The peaks in icing (12%-15%) and SLD (1.6%-2.0%) frequency occurred during late fall and early winter, when they were most often found below ~6,000 ft (~2 km, all heights MSL) for icing and ~3000-9000 ft (~1-3 km) for SLD. The SLD peaks are more elevated than those for icing because much of the SLD occurred with above-freezing surface temperatures in maritime regions. Recall that FZDZ, FZRA, and PL are relatively unusual at the surface in Europe, except at mountain stations and in some parts of central and southeastern Europe. This nicely matches the vertical distribution of SLD at low altitudes. Icing also extends upward to slightly higher altitudes than SLD because of the occurrence of multilayer clouds (SLD is only attributed to the lowest cloud deck in this climatology) and the fact that nonclassical SLD can only be diagnosed with CTT of -12°C or greater, mostly precluding SLD from being diagnosed at temperatures colder than -12°C in this climatology, except when strong inversions existed. Icing potentials > 0.4 were possible with colder CTTs and thus, colder temperatures, which were sometimes found at higher altitudes. Seasonal transitions were quite evident as frequencies decreased and began to elevate during the spring, which had a secondary peak during June in the 9,000- to 12,000-ft range. The icing and SLD maxima descended in the fall and frequencies gradually increased to reach their overall maxima in December between 3000 and 6000 ft.

The time-height distributions for individual stations sometimes had patterns that were very similar to the European average, while others had very different patterns. A good match occurred at De Bilt, The Netherlands (figure 9a; see letters in figure 1a for the location of station 4), which was located within the continental SLD maximum. Because stations in this region had the highest frequencies of icing and SLD and quite a few stations were clustered there, the pattern at these sites likely had a significant influence on the European average. Note that SLD was relatively unusual below 3000 ft, even in the heart of the maximum. Low-altitude temperatures tended to remain slightly above freezing there, even in winter.

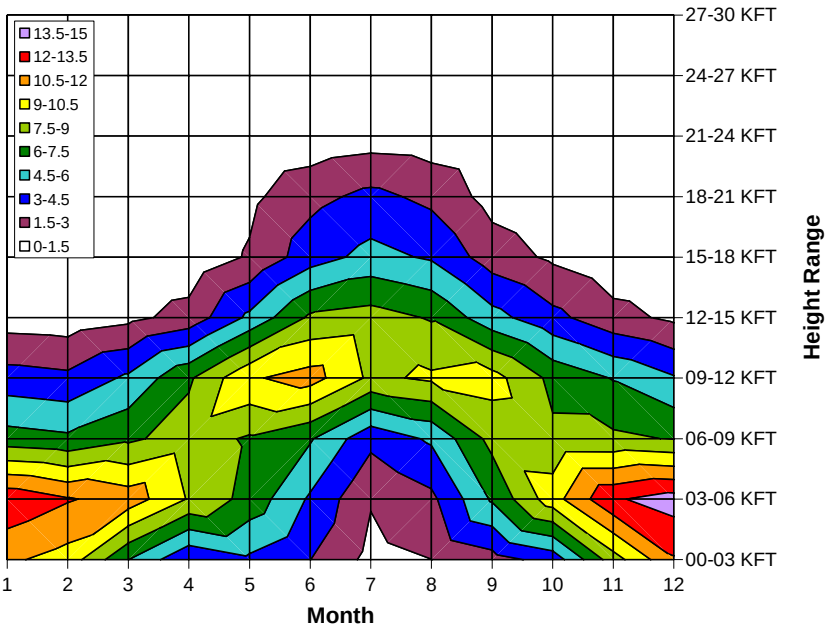

Months are indicated numerically along the x axis. Altitude ranges were binned in 3000-ft intervals. Values for each month and altitude range combination are valid at the intersection of horizontal and vertical lines. Contours are drawn around these points every 1.5% for icing.

FIGURE 8a. TIME-HEIGHT DISTRIBUTION OF INFERRED ICING FREQUENCY (%) FOR ALL EUROPEAN STATIONS COMBINED

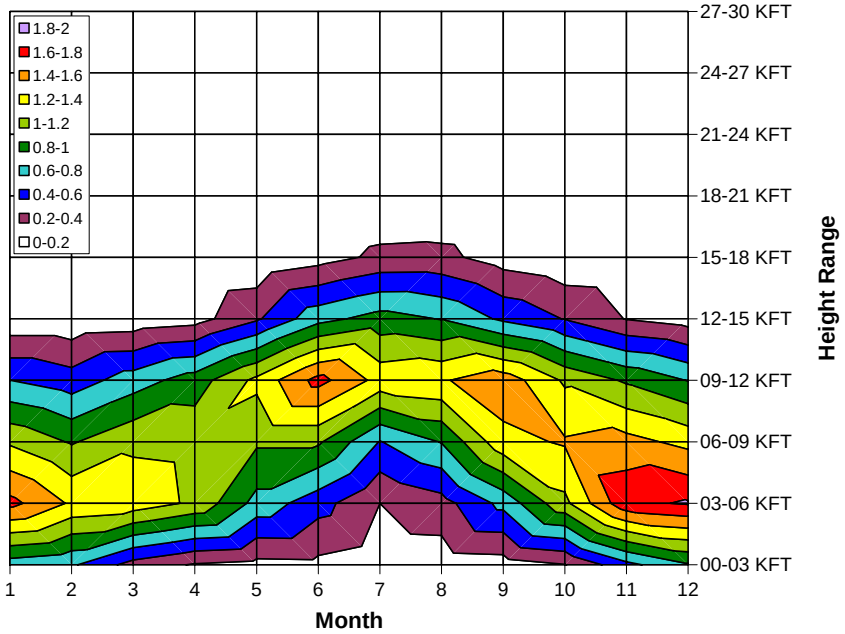

Contours are drawn every 0.2%.

FIGURE 8b. TIME-HEIGHT DISTRIBUTION OF INFERRED SLD FREQUENCY (%) FOR ALL EUROPEAN STATIONS COMBINED

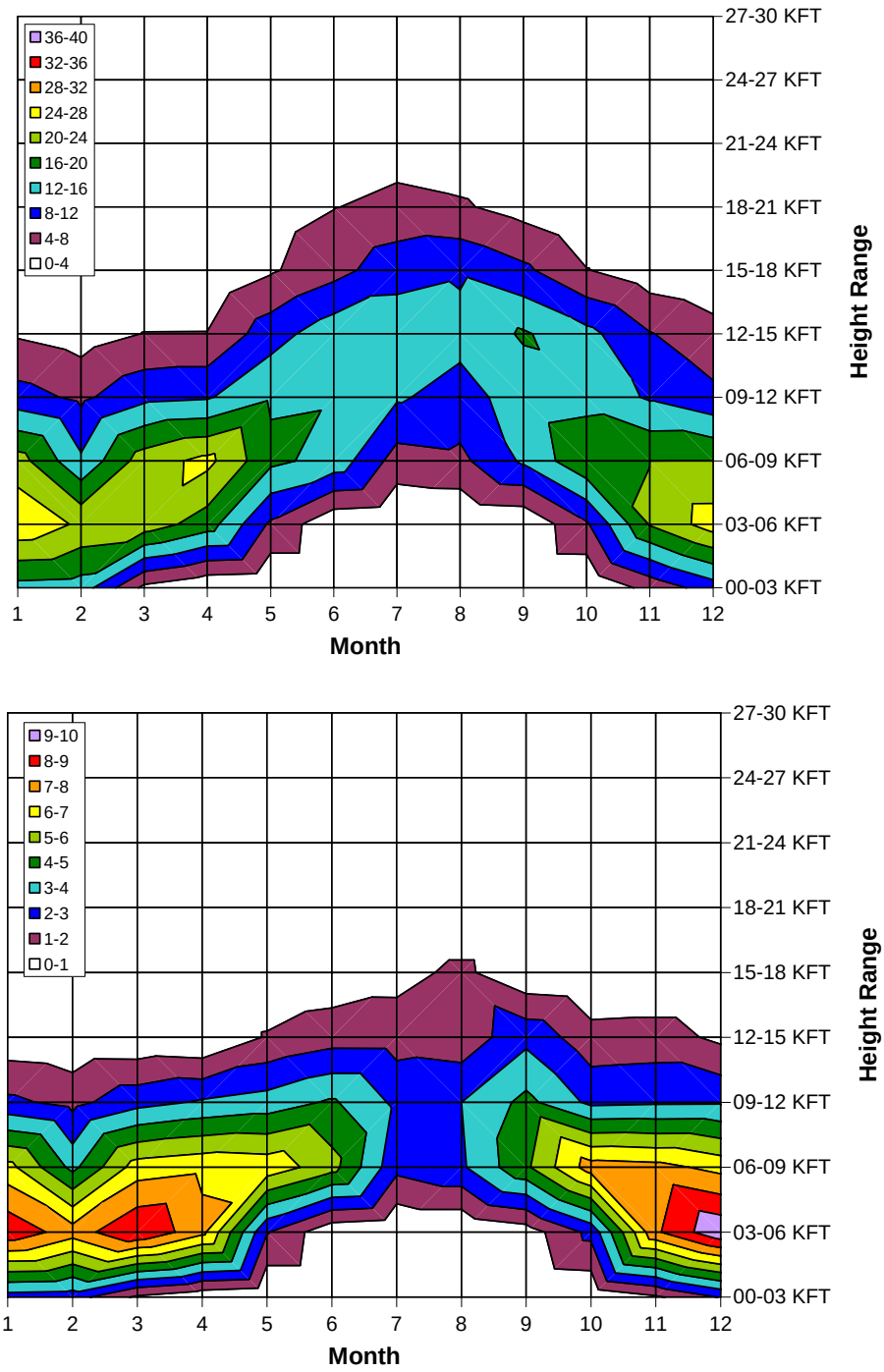

Color intervals are every 4% for icing and 1% for SLD.

FIGURE 9a. TIME-HEIGHT DISTRIBUTION OF INFERRED ICING AND SLD FREQUENCY (%) FOR THE INDIVIDUAL STATION OF DE BILT, THE NETHERLANDS

To the south of the continental maximum, frequencies decreased with decreasing latitude across France and Germany into Italy. Nearly all of the SLD to the south occurred during the cool season, and their lower extents became more elevated, following the freezing level. This transition is particularly evident across France, from Nancy (northeast corner) to Ajaccio, which is located on Corsica, to west of Rome (figures 9b-9e; see figure 1a for the location of stations B, C, D, and E). Though icing still occurred there, Rome appeared to only have very infrequent SLD that only occurred during the cool season (figure 9f; see figure 1a for the location of station F).

To the southwest of the continental maximum the same sort of transition was found. Frequencies dropped off very quickly toward southwestern France (Bordeaux) and central and southern Spain, as well as Portugal (Madrid and Lisbon), where conditions tended to be sunnier and drier (figures 9g-9i, see figure 1a for the location of stations G, H, and I). Toward the southeast, a similar transition occurred, but summertime icing and SLD were still evident above 9000 ft in Vienna, Austria, and Budapest, Hungary (figures 9j and 9k; see figure 1a for the location of stations J and K), though frequencies were markedly decreased. This was also evident through June in Yugoslavia and northwestern Turkey (figures 9l and 9m; see figure 1a for the location of stations L and M), but not in Athens, Greece (figure 9n; see figure 1a for the location of station N), where very low frequencies and a pattern similar to that seen in Rome (figure 9f; see figure 1a for the location of station F), Brindisi, located in southeastern Italy (figure 9o; see figure 1a for the location of station O) and Trapani, Sicily (figure 9p; see figure 1a for the location of station P) existed. This same initial transition was found toward the east in Warsaw, Poland and Kiev, Ukraine (figures 9q and 9r; see figure 1a for the location of stations Q and R). Though SLD appears to be rare, icing still appears to occur in Italy and Greece, with peak frequencies exceeding 12% in the 6000- to 12,000-ft range during the cool season.

Further to the east, SLD frequencies were quite low across most of Russia. It was not clear if the low values were real, or if there were quality control issues with the precipitation observations taken across the old Soviet Union (figures 5b to 5e). Icing clouds were quite common there, but there was little indication of liquid precipitation with these clouds. Snow was frequently observed, so precipitation was certainly not absent, but observations of drizzle, in particular, were lacking (figures 5b and 5d). Geopolitical discontinuities may be an issue due to differences in measurement techniques. A good example may be the relatively large number of drizzle and rain observations in Germany compared to neighboring countries (figures 5c and 5e). A sharp transition might be expected across the Alps or near coastlines of major water bodies, but not along the Germany and Poland border, where no major land or water features are present. Perhaps the German weather service did a better job of observing and reporting such precipitation types. Geopolitical discontinuities are not evident in the frequencies of snow or overcast skies. In fact, there was a very gradual rise in snow frequency in the eastward direction from France to Russia. The topic of surface observation quality may need to be explored further, as it could have a significant effect on the results shown here.

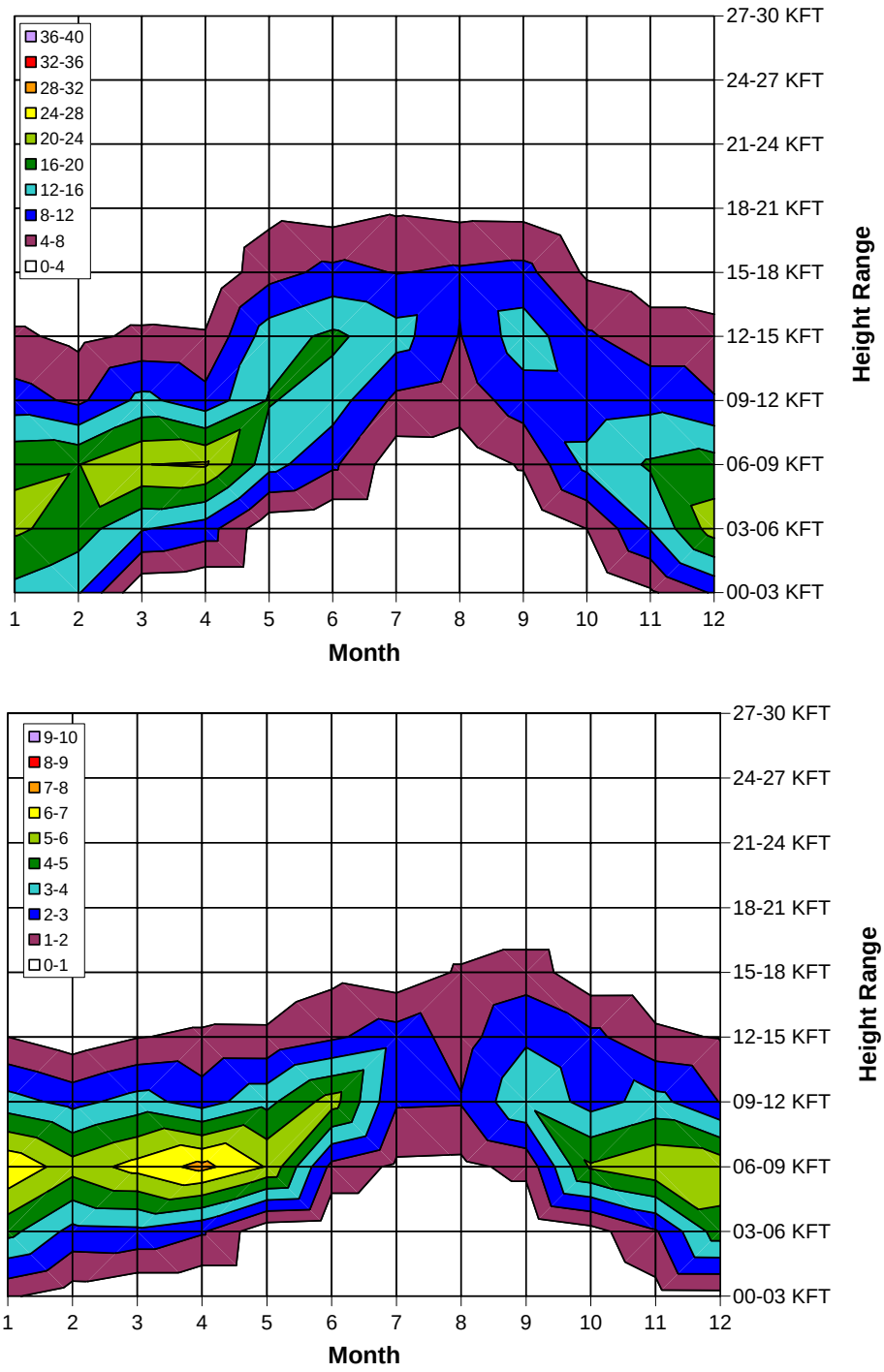

Color intervals are every 4% for icing and 1% for SLD.

FIGURE 9b. TIME-HEIGHT DISTRIBUTION OF INFERRED ICING AND SLD FREQUENCY (%) FOR THE INDIVIDUAL STATION OF NANCY, FRANCE

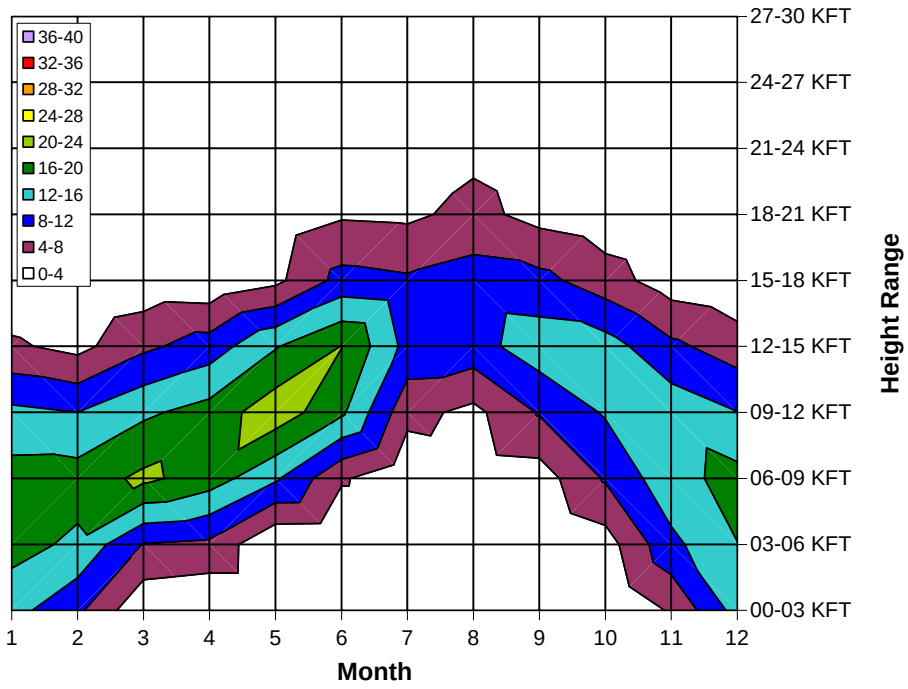

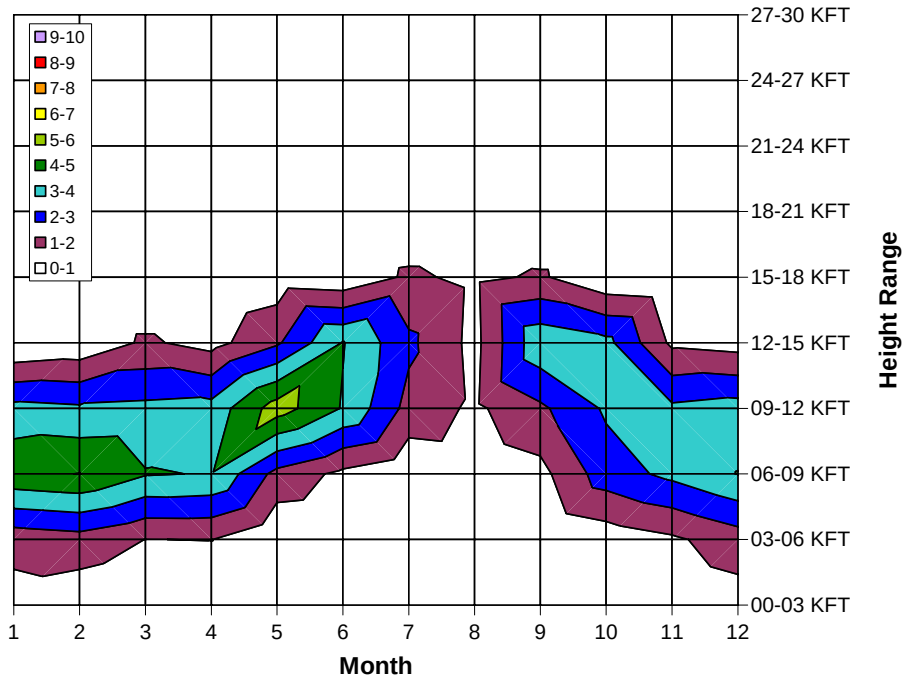

Color intervals are every 4% for icing and 1% for SLD.

FIGURE 9c. TIME-HEIGHT DISTRIBUTION OF INFERRED ICING AND SLD FREQUENCY (%) FOR THE INDIVIDUAL STATION OF LYON, FRANCE

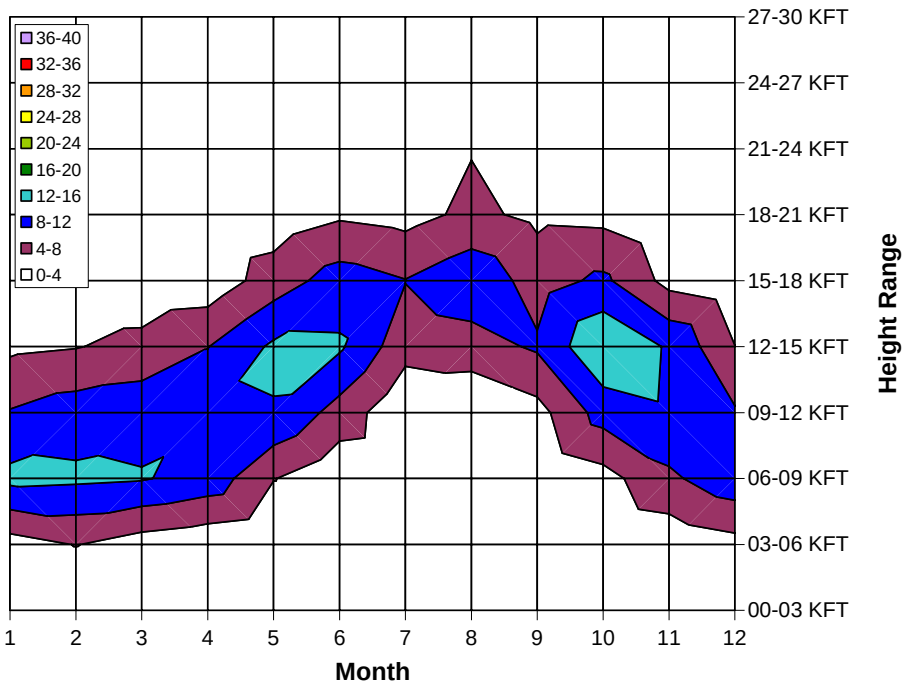

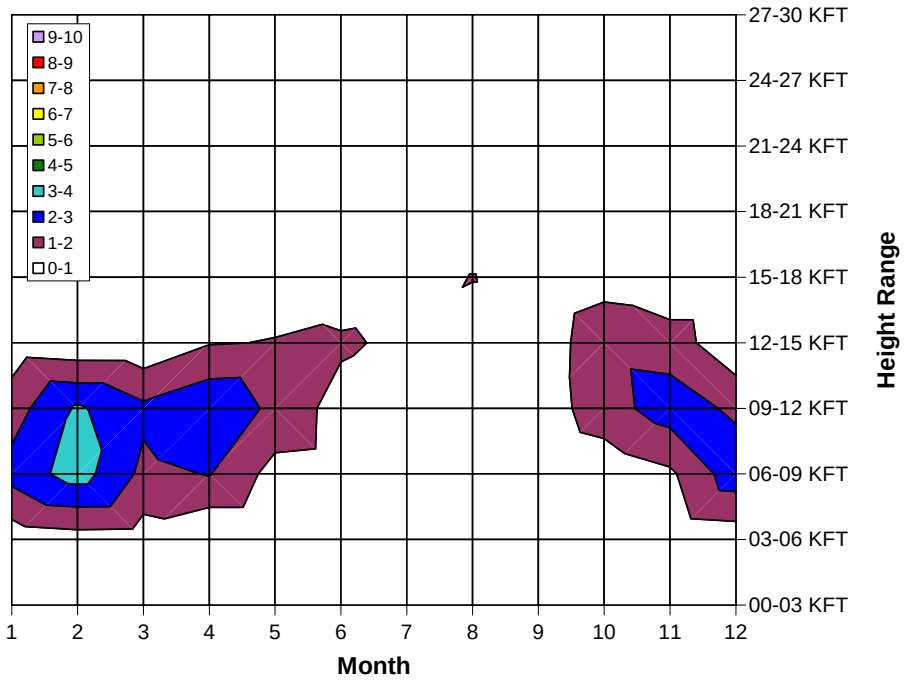

Color intervals are every 4% for icing and 1% for SLD.

FIGURE 9d. TIME-HEIGHT DISTRIBUTION OF INFERRED ICING AND SLD FREQUENCY (%) FOR THE INDIVIDUAL STATION OF NIMES, FRANCE

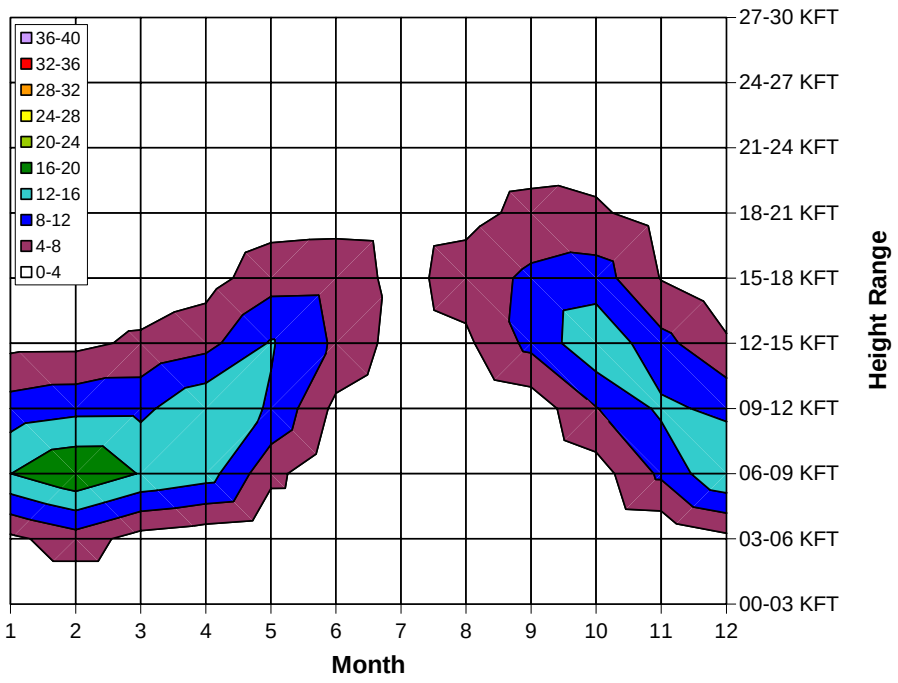

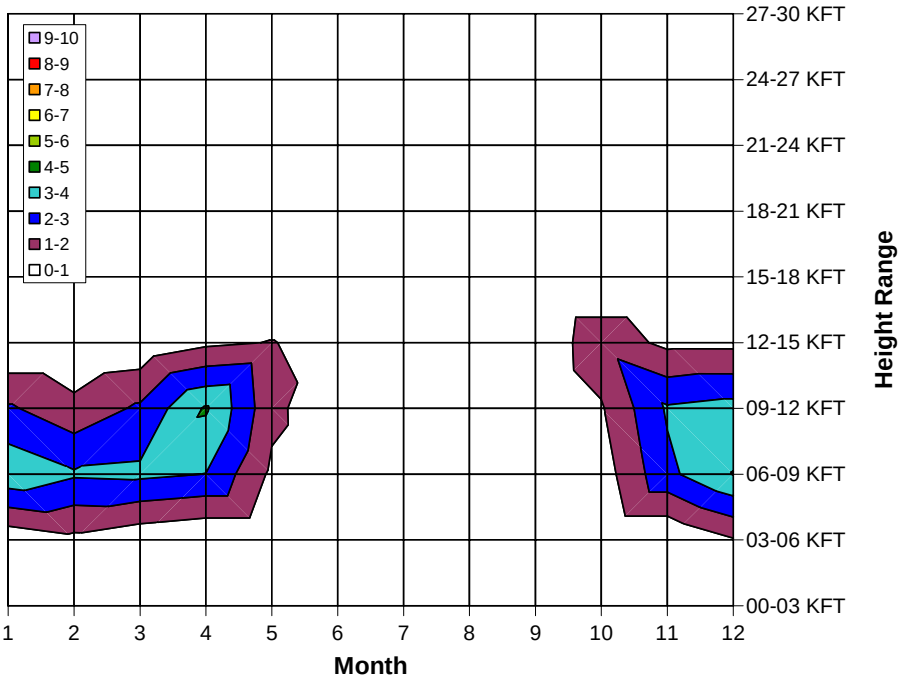

Color intervals are every 4% for icing and 1% for SLD.

FIGURE 9e. TIME-HEIGHT DISTRIBUTION OF INFERRED ICING AND SLD FREQUENCY (%) FOR THE INDIVIDUAL STATION OF AJACCIO, FRANCE

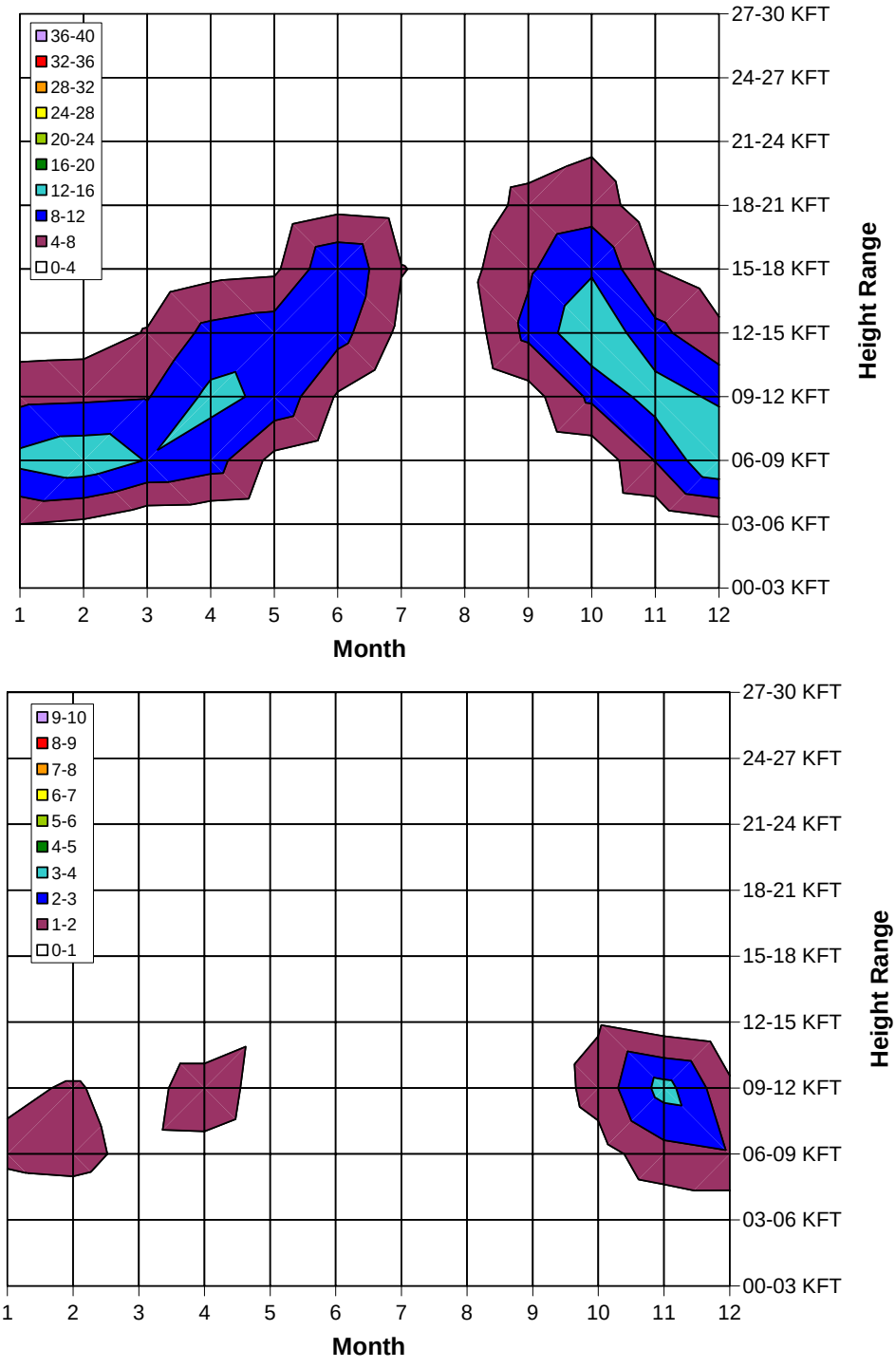

Color intervals are every 4% for icing and 1% for SLD.

FIGURE 9f. TIME-HEIGHT DISTRIBUTION OF INFERRED ICING AND SLD FREQUENCY (%) FOR THE INDIVIDUAL STATION OF ROME, ITALY

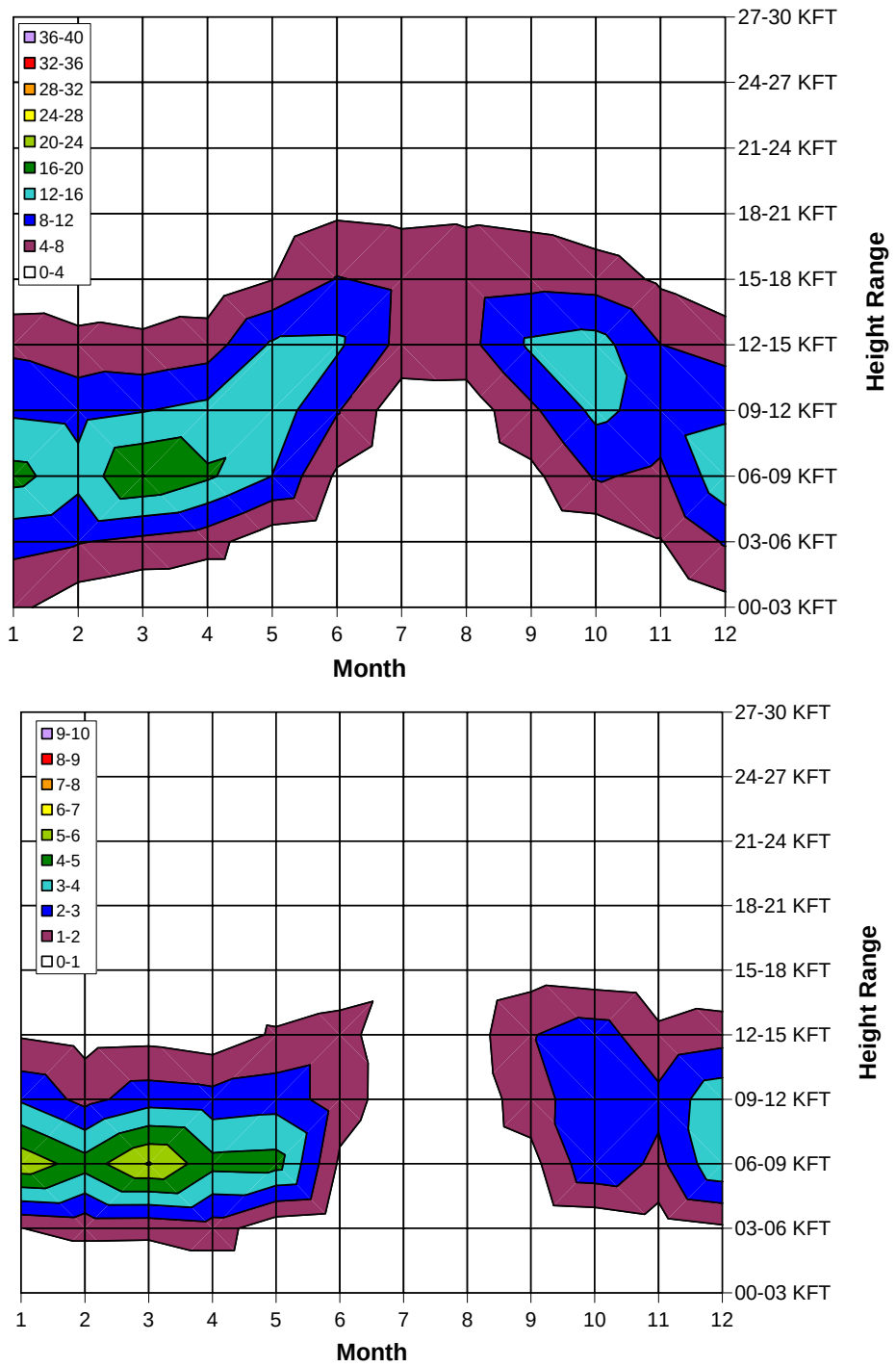

Color intervals are every 4% for icing and 1% for SLD.

FIGURE 9g. TIME-HEIGHT DISTRIBUTION OF INFERRED ICING AND SLD FREQUENCY (%) FOR THE INDIVIDUAL STATION OF BORDEAUX, FRANCE

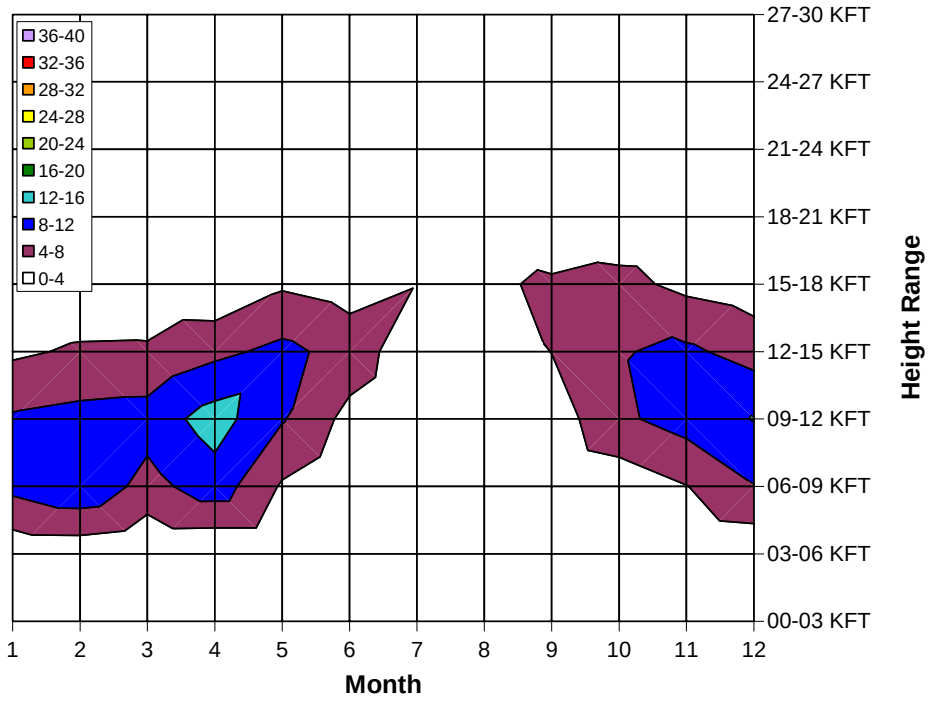

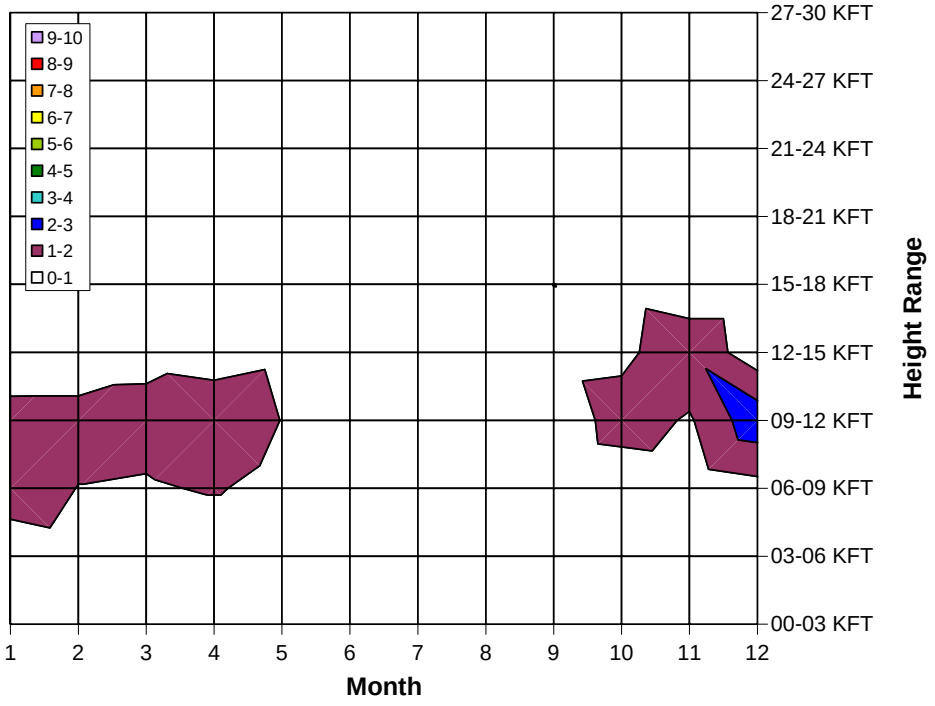

Color intervals are every 4% for icing and 1% for SLD.

FIGURE 9h. TIME-HEIGHT DISTRIBUTION OF INFERRED ICING AND SLD FREQUENCY (%) FOR THE INDIVIDUAL STATION OF MADRID, SPAIN

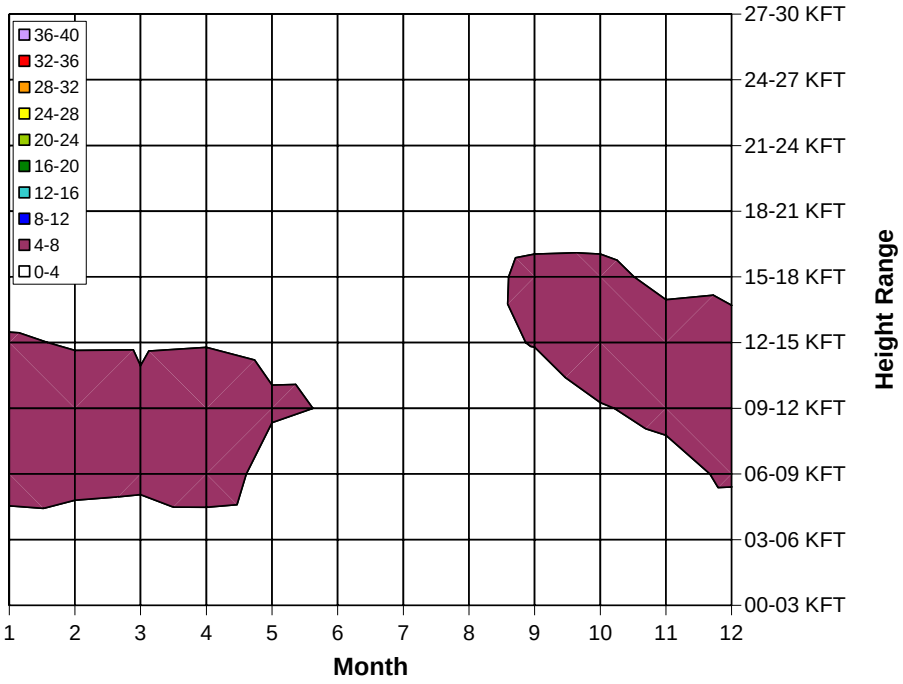

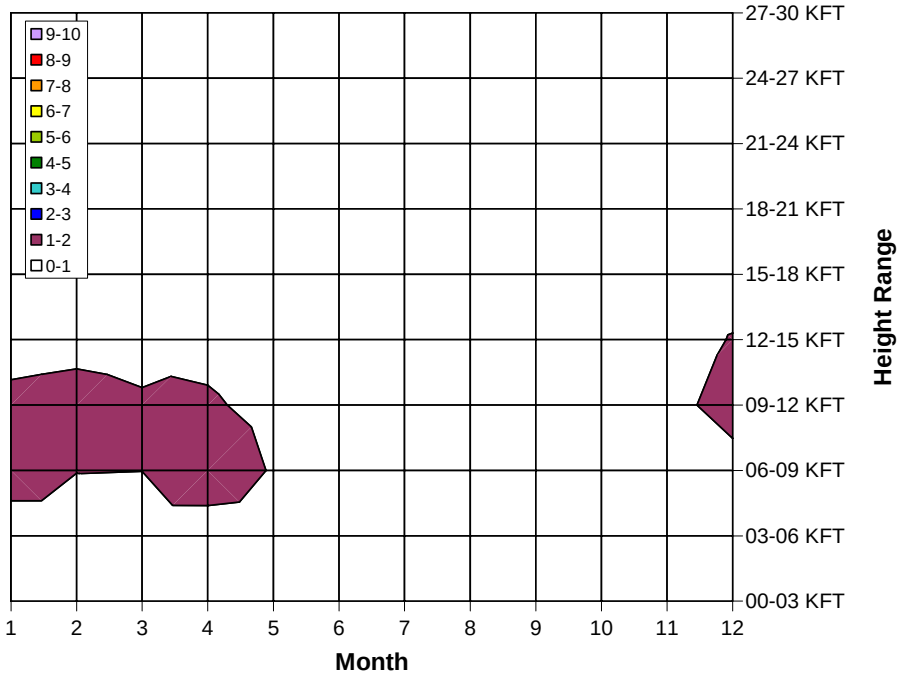

Color intervals are every 4% for icing and 1% for SLD.

FIGURE 9i. TIME-HEIGHT DISTRIBUTION OF INFERRED ICING AND SLD FREQUENCY (%) FOR THE INDIVIDUAL STATION OF LISBON, PORTUGAL

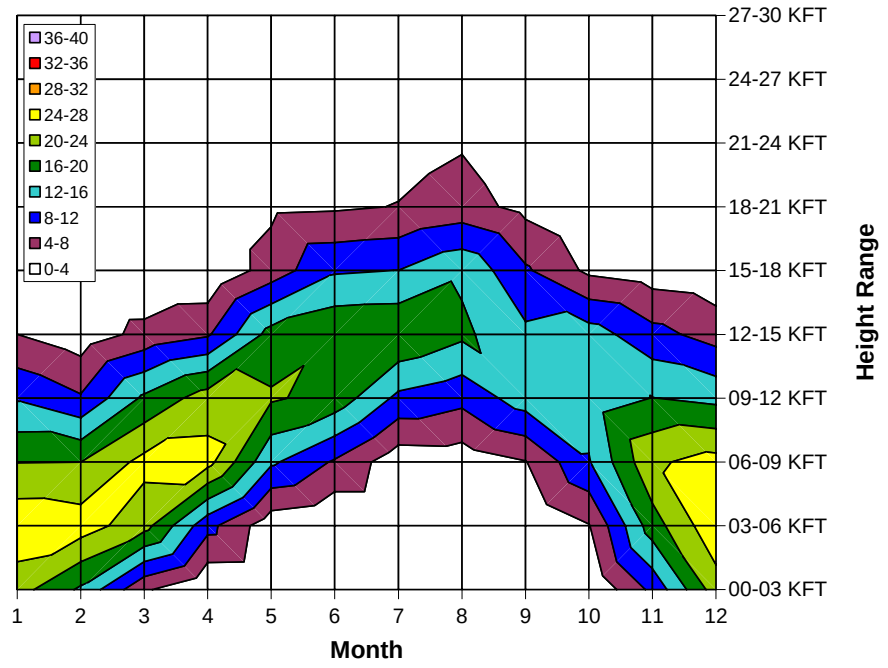

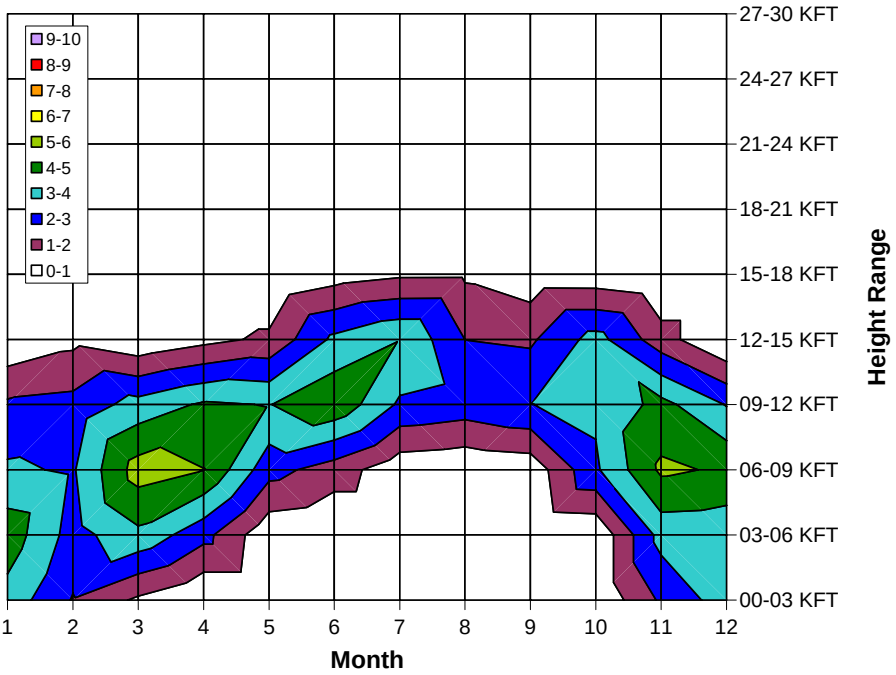

Color intervals are every 4% for icing and 1% for SLD.

FIGURE 9j. TIME-HEIGHT DISTRIBUTION OF INFERRED ICING AND SLD FREQUENCY (%) FOR THE INDIVIDUAL STATION OF VIENNA, AUSTRIA

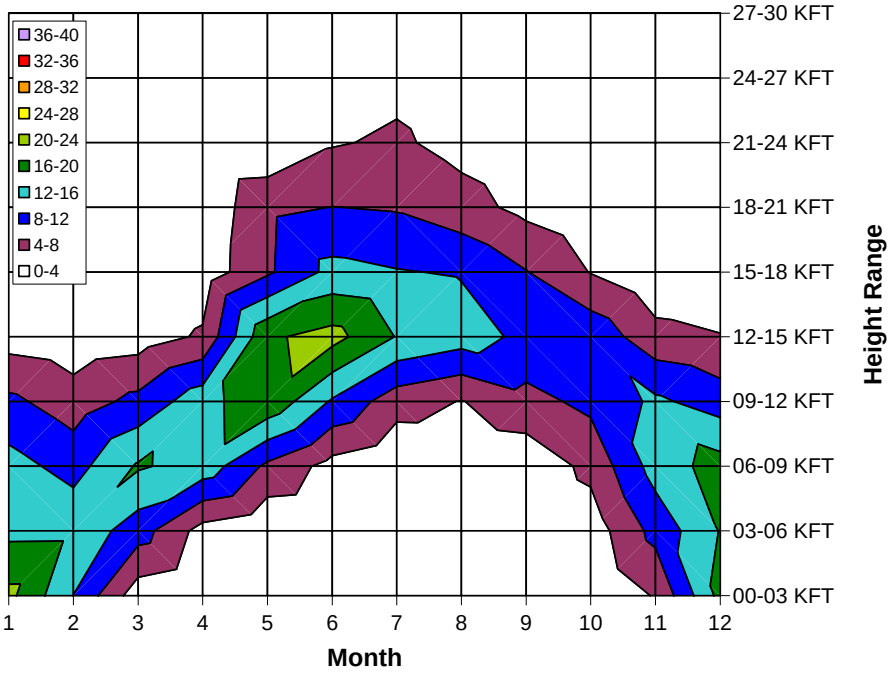

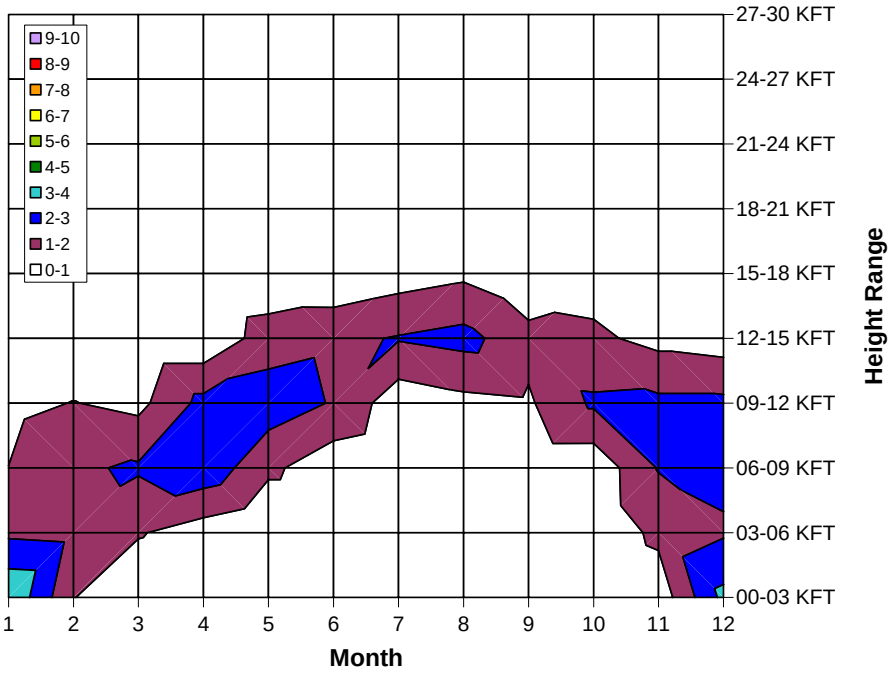

Color intervals are every 4% for icing and 1% for SLD.

FIGURE 9k. TIME-HEIGHT DISTRIBUTION OF INFERRED ICING AND SLD FREQUENCY (%) FOR THE INDIVIDUAL STATION OF BUDAPEST, HUNGARY

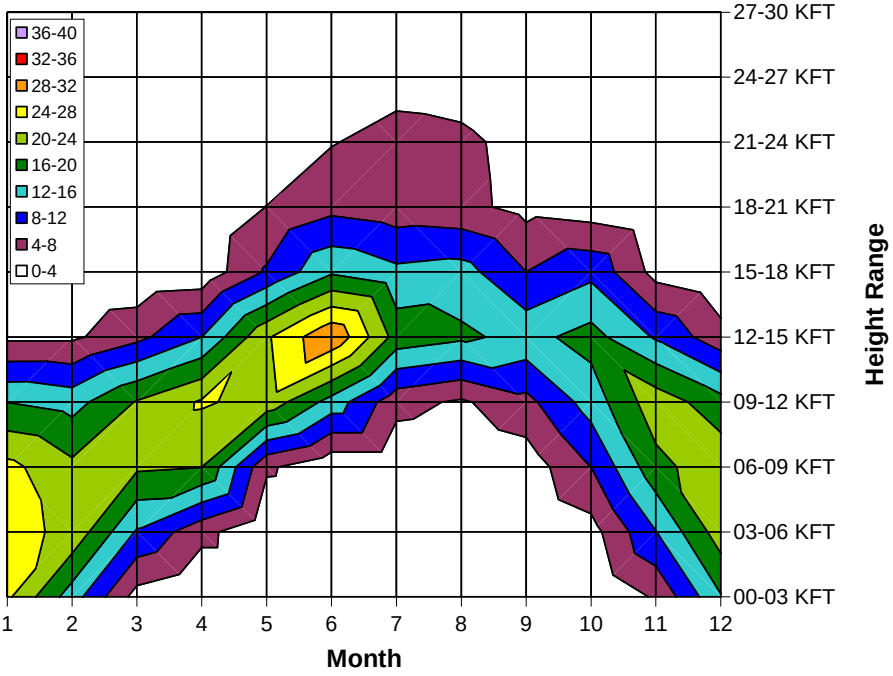

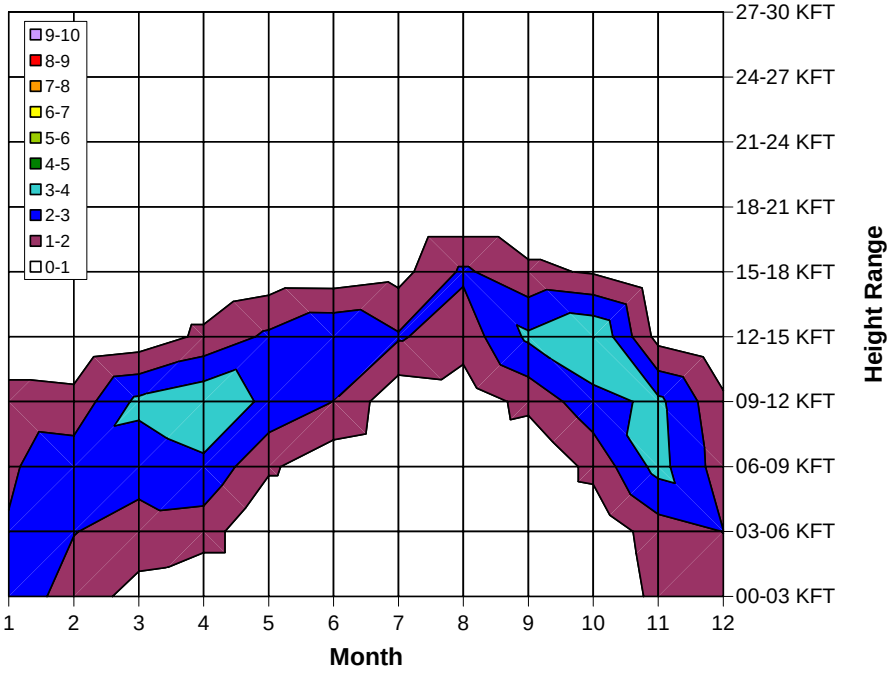

Color intervals are every 4% for icing and 1% for SLD.

FIGURE 9l. TIME-HEIGHT DISTRIBUTION OF INFERRED ICING AND SLD FREQUENCY (%) FOR THE INDIVIDUAL STATION OF BELGRADE, YUGOSLAVIA

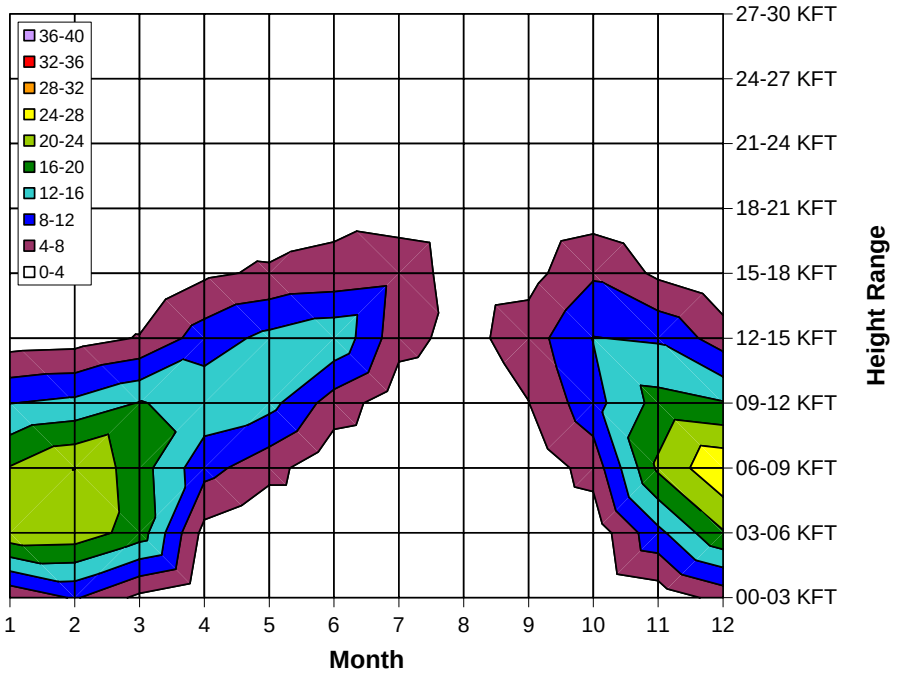

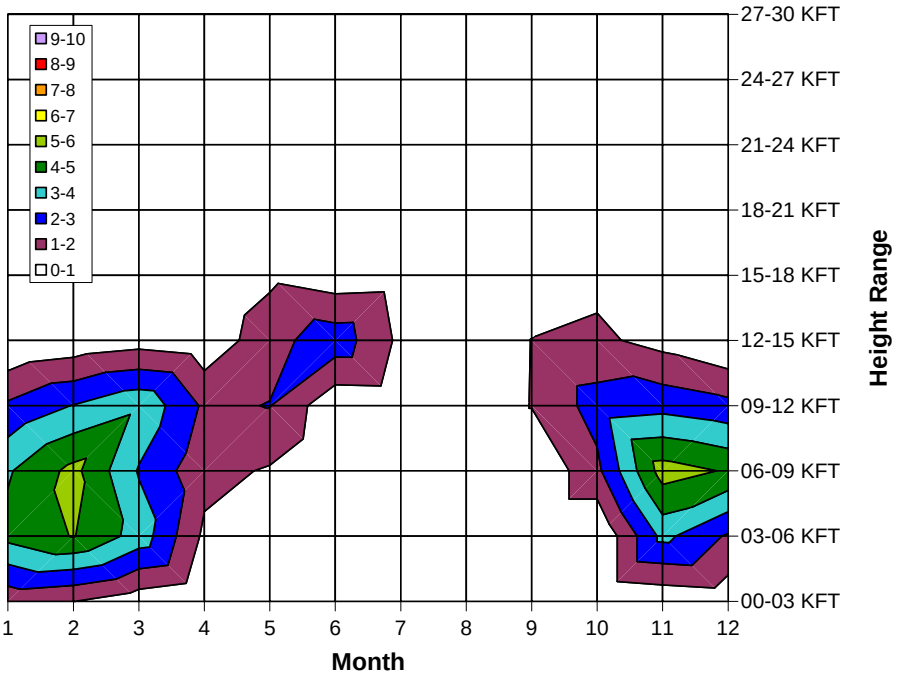

Color intervals are every 4% for icing and 1% for SLD.

FIGURE 9m. TIME-HEIGHT DISTRIBUTION OF INFERRED ICING AND SLD FREQUENCY (%) FOR THE INDIVIDUAL STATION OF ISTANBUL, TURKEY

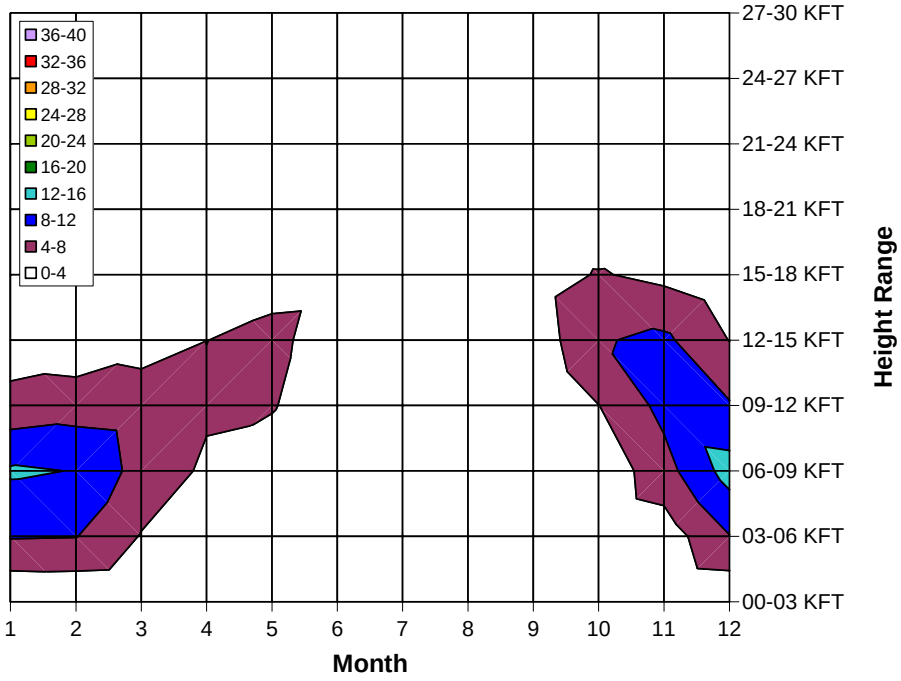

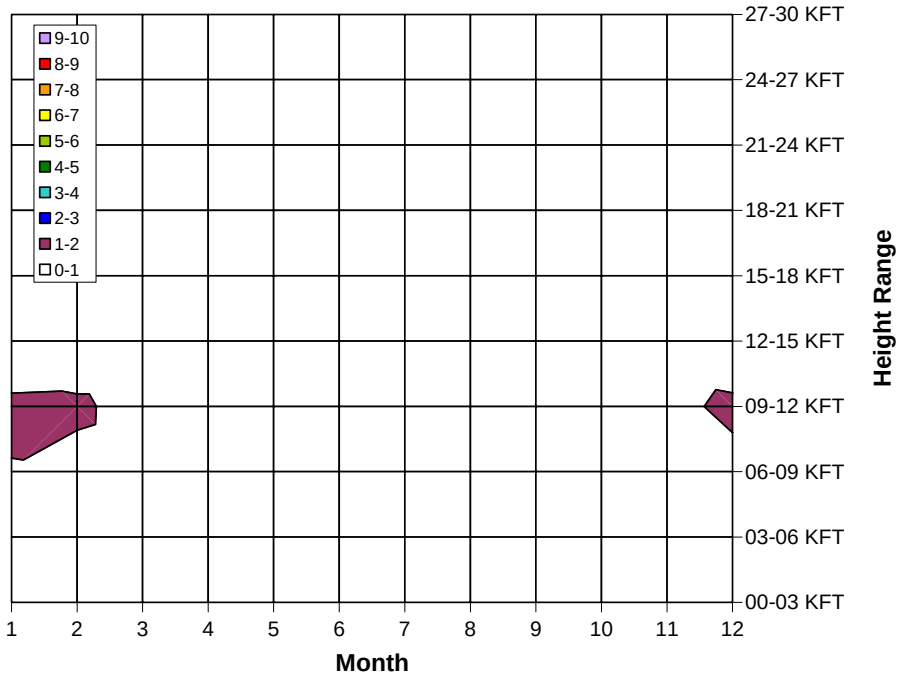

Color intervals are every 4% for icing and 1% for SLD.

FIGURE 9n. TIME-HEIGHT DISTRIBUTION OF INFERRED ICING AND SLD FREQUENCY (%) FOR THE INDIVIDUAL STATION OF ATHENS, GREECE

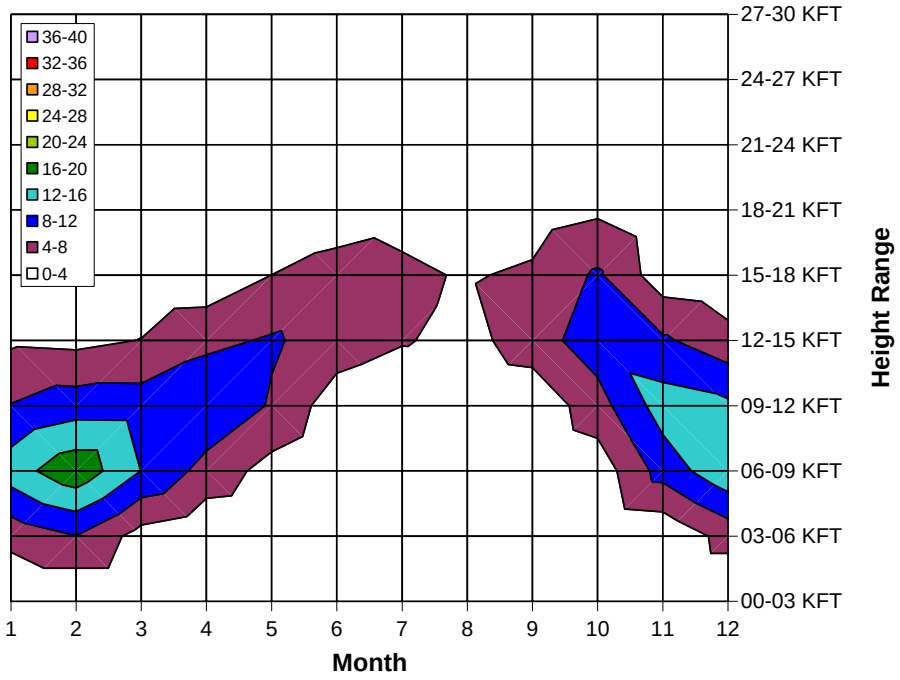

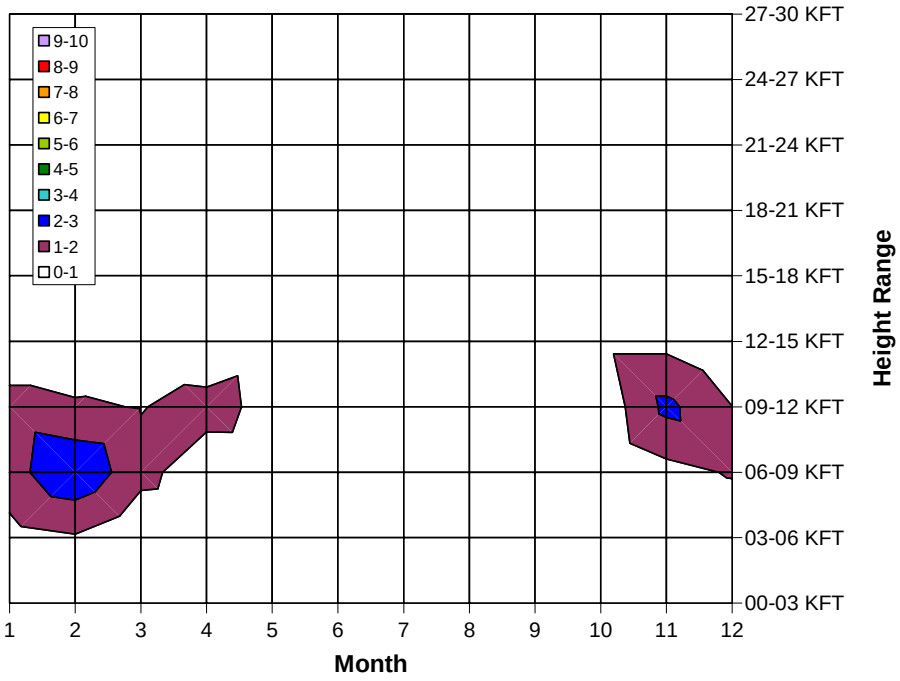

Color intervals are every 4% for icing and 1% for SLD.

FIGURE 9o. TIME-HEIGHT DISTRIBUTION OF INFERRED ICING AND SLD FREQUENCY (%) FOR THE INDIVIDUAL STATION OF BRINDISI, ITALY

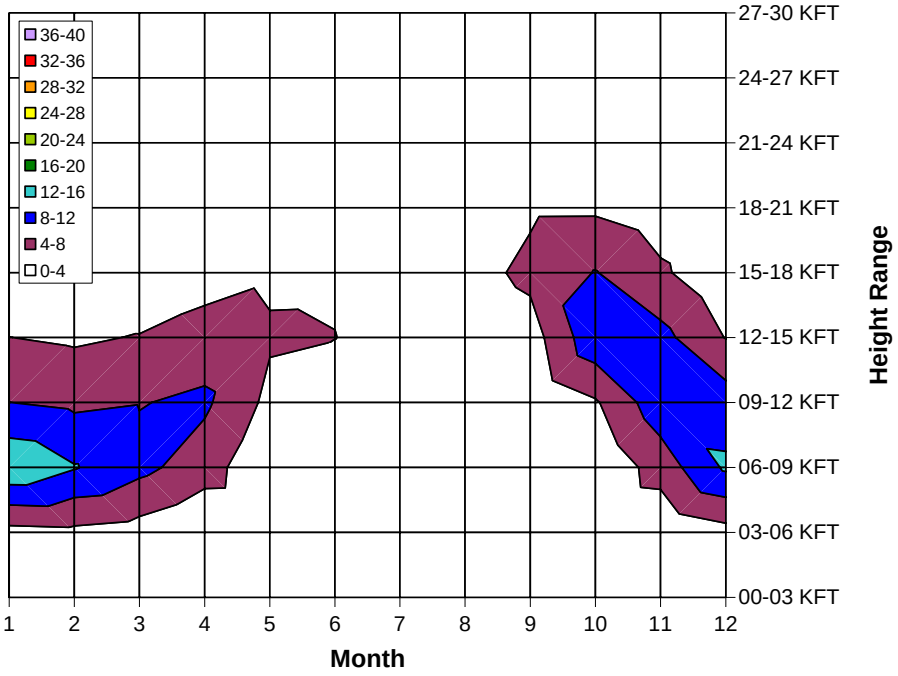

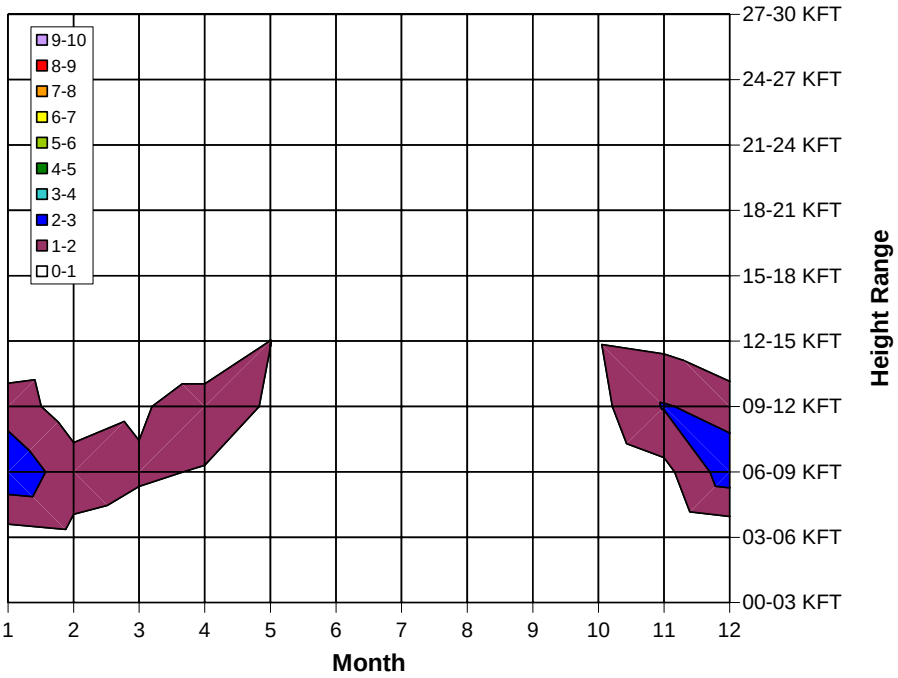

Color intervals are every 4% for icing and 1% for SLD.

FIGURE 9p. TIME-HEIGHT DISTRIBUTION OF INFERRED ICING AND SLD FREQUENCY (%) FOR THE INDIVIDUAL STATION OF TRAPANI, SICILY

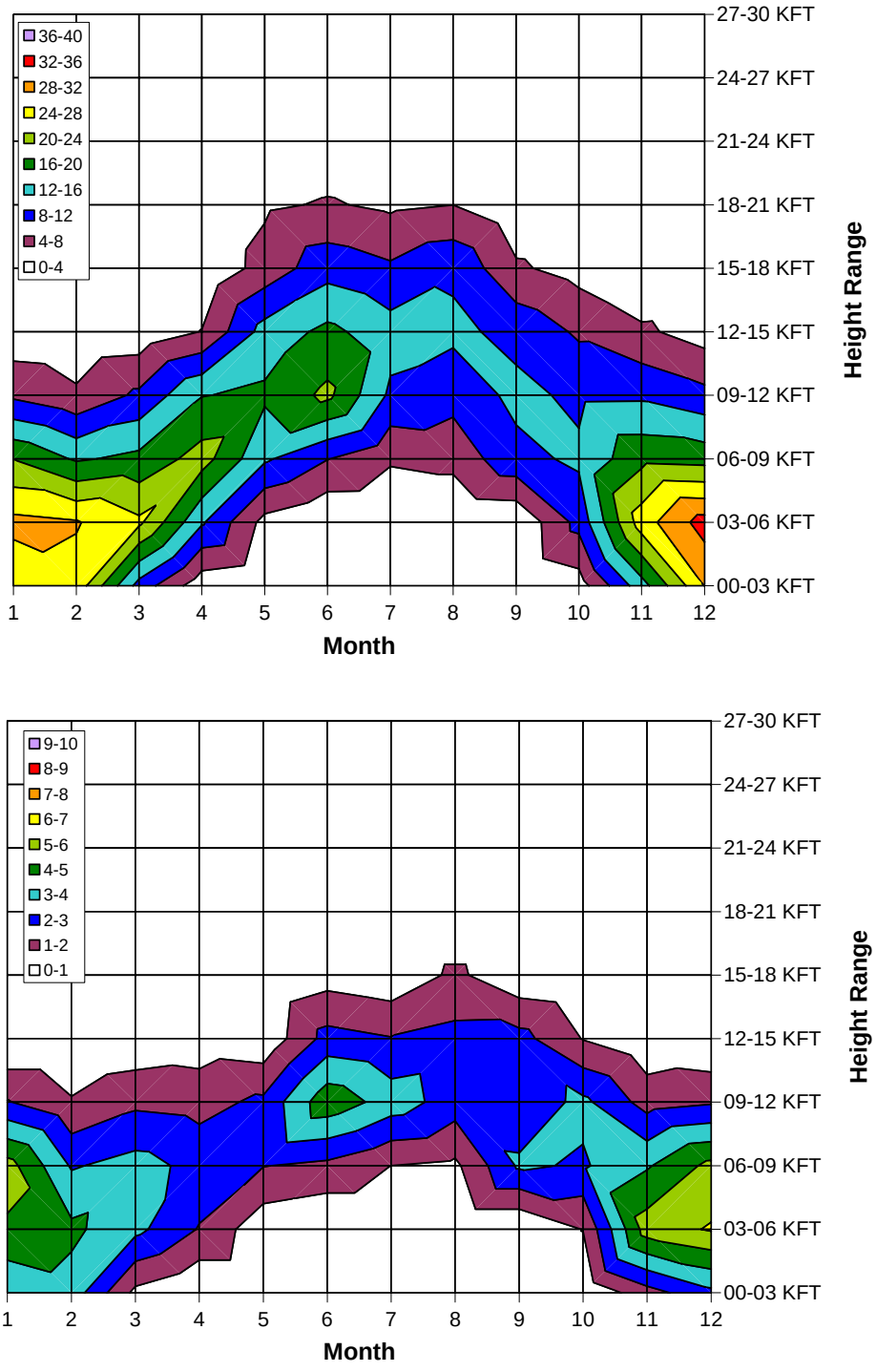

Color intervals are every 4% for icing and 1% for SLD.

FIGURE 9q. TIME-HEIGHT DISTRIBUTION OF INFERRED ICING AND SLD FREQUENCY (%) FOR THE INDIVIDUAL STATION OF WARSAW, POLAND

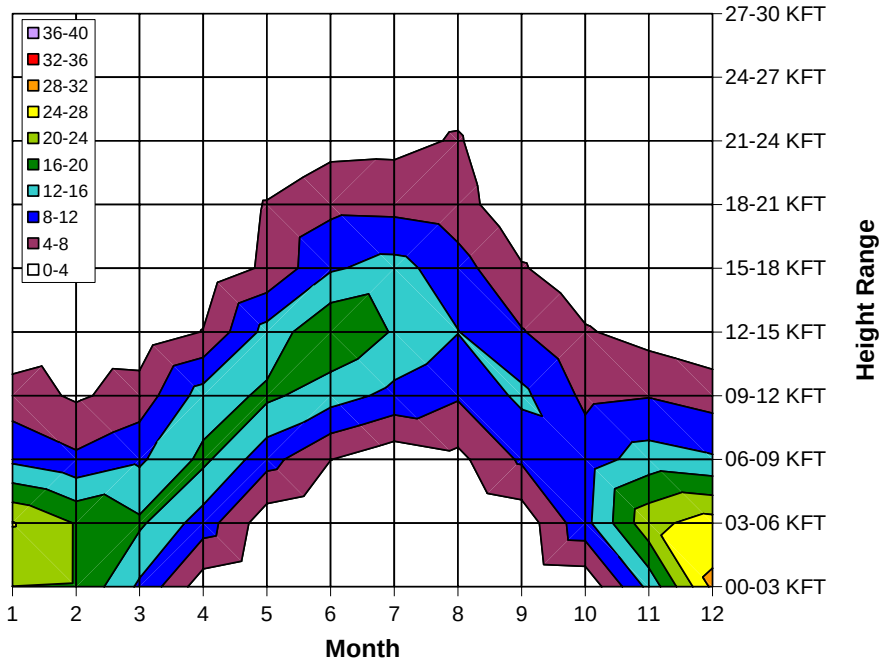

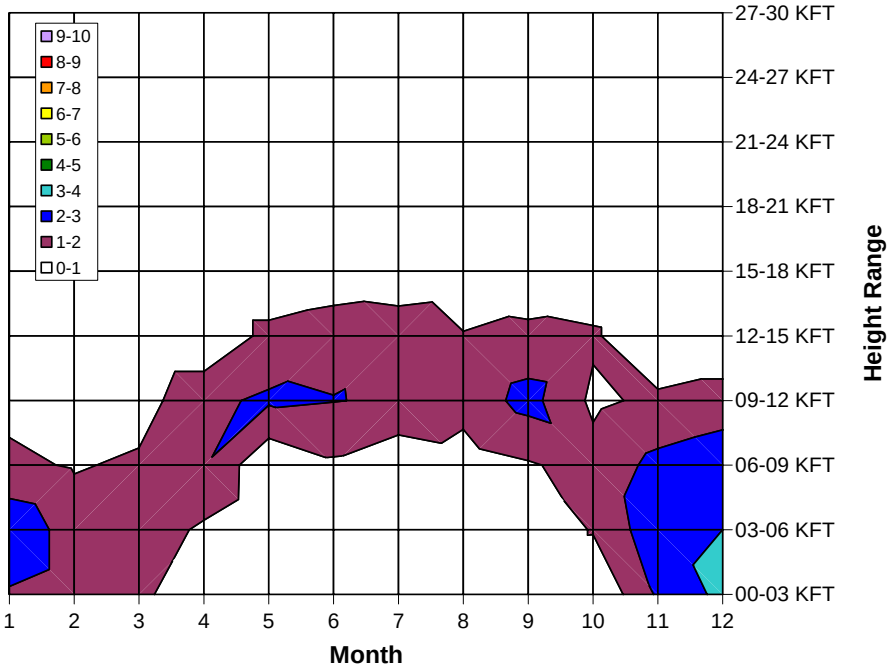

Color intervals are every 4% for icing and 1% for SLD.

FIGURE 9r. TIME-HEIGHT DISTRIBUTION OF INFERRED ICING AND SLD FREQUENCY (%) FOR THE INDIVIDUAL STATION OF KIEV, UKRAINE

To the north of the continental maximum, SLD patterns were very different. Though icing frequencies were quite substantial near the Arctic Circle, SLD frequencies were relatively low. It was during the warm season that adequately warm temperatures were present to support nonglaciated clouds. A good example of this was the annual pattern from Bjornoya Island, Norway (located at 74.5° north latitude), where SLD was most often found between June and August and icing was most common during April-June and September-October, all at altitudes below 6000 ft (figure 9s; see figure 1a for the location of station S). At such northern latitudes, clouds tend to be more glaciated during the very cold winter months. Similar SLD patterns were seen along the Arctic coast in the North American study. It was interesting to note that the summertime, low-altitude maximum was not evident across most of the northern coast of Russia, where one might also expect it. One clear exception was at Murmansk, which is very close to the border with Finland (figure 9t; see figure 1a for the location of station T). Ramalyekar and Radikson Island (not shown) also had summertime maxima, but they were quite weak. Pocora, to the southeast, has a distinct peak in August and September just preceding the icing maximum, found in the September-November time frame (figure 9u; see figure 1a for the location of station U). It is interesting to note that such a mismatch in timing of the icing and SLD patterns was found at several Arctic stations, but not over most of the rest of Europe. In the Arctic, icing peaks tended to occur during the spring and fall, while SLD peaks often occurred during the summer. Monthly frequencies of precipitation types were not created as part of this climatology, but based on these results, it is likely that liquid precipitation was most common during the summer in the Arctic.

A gradual transition from the Arctic pattern to one more like the European average pattern was evident as one looks southward along the west coast of Norway at Bodovi and Orland (figures 9v and 9w; see figure 1a for the location of stations V and W). SLD still occurred at fairly low altitudes and was most common during the warm season, especially early fall. The icing and SLD timing mismatch was also present, but not as pronounced. These stations represent a transition from the Arctic summer peak to the winter peak found to the south. Compared to those to the west, SLD frequencies were relatively low in Oslo and Stockholm, though icing frequencies were only slightly low (figures 4a and 4b). Stockholm and nearby Jokioinen, Finland still featured somewhat of a fall peak in SLD occurrence (figures 9x and 9y; see figure 1a for the location of stations X and Y). These sites also represent the transition toward the southwest from the Arctic summertime maximum in northwestern Russia to the continental maximum.

To the northwest of the continental maximum, SLD frequencies were high throughout most of the year, with peak icing and SLD values exceeding 32% and 9%, respectively, during October, November, and February at Keflavik, Iceland, an important international airport near the capital of Rejkavik (figure 9z; see figure 1a for the location of station Z). Icing and SLD were consistently found in the 3,000- to 6,000-ft range throughout the year, but briefly climbed to 6,000 to 12,000 ft during the summer. This is the only time of year when surface temperatures at Keflavik climb to +10°C or so. Similar patterns are found over the Faeroe Islands (not shown) and in northern Scotland (figure 9aa; see figure 1a for the location of station AA). Again, stations to the south exhibited a shift toward the cool season and higher altitudes, overall. This is quite evident as one compares Stornoway, Scotland to London, England and Brest, France (figures 9aa-9ac; see figure 1a for the location of stations AA, AB, and AC).

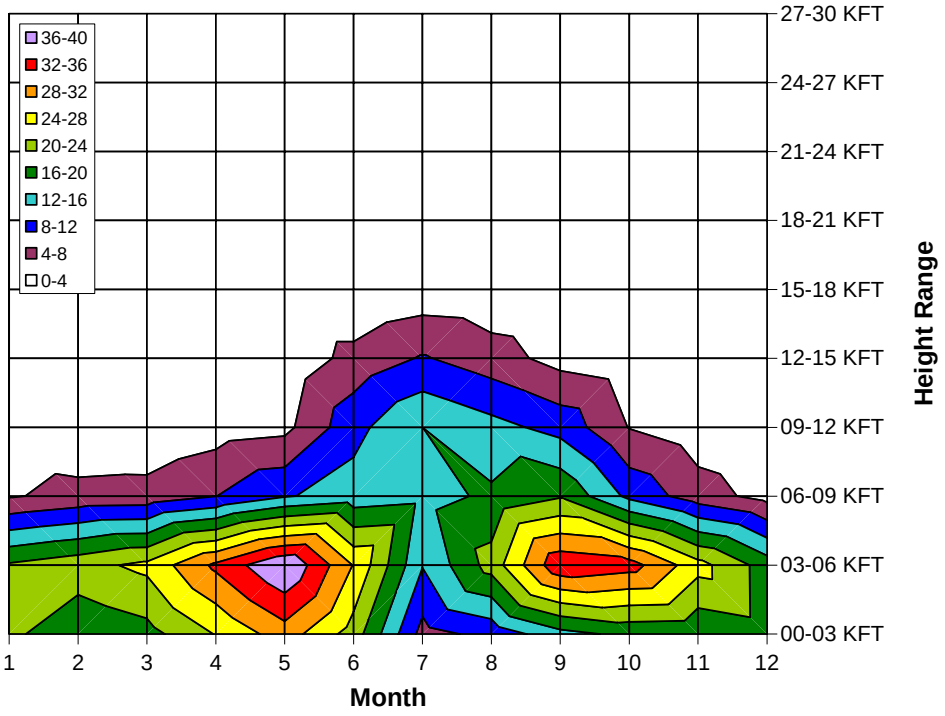

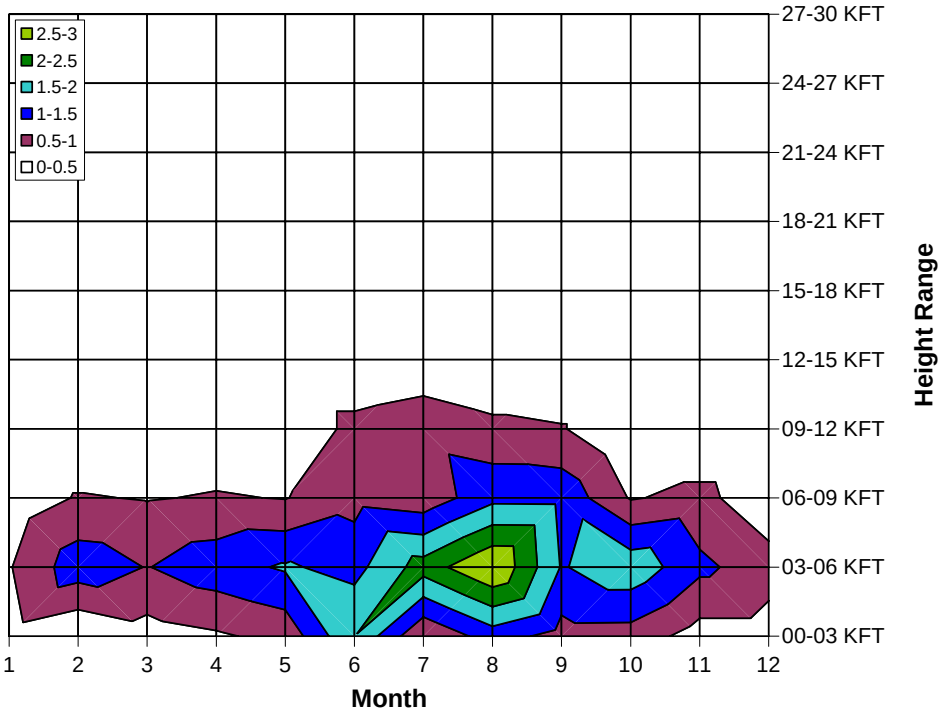

Color intervals are every 4% for icing and 1% for SLD.

FIGURE 9s. TIME-HEIGHT DISTRIBUTION OF INFERRED ICING AND SLD FREQUENCY (%) FOR THE INDIVIDUAL STATION OF BJORNOYA ISLAND, NORWAY

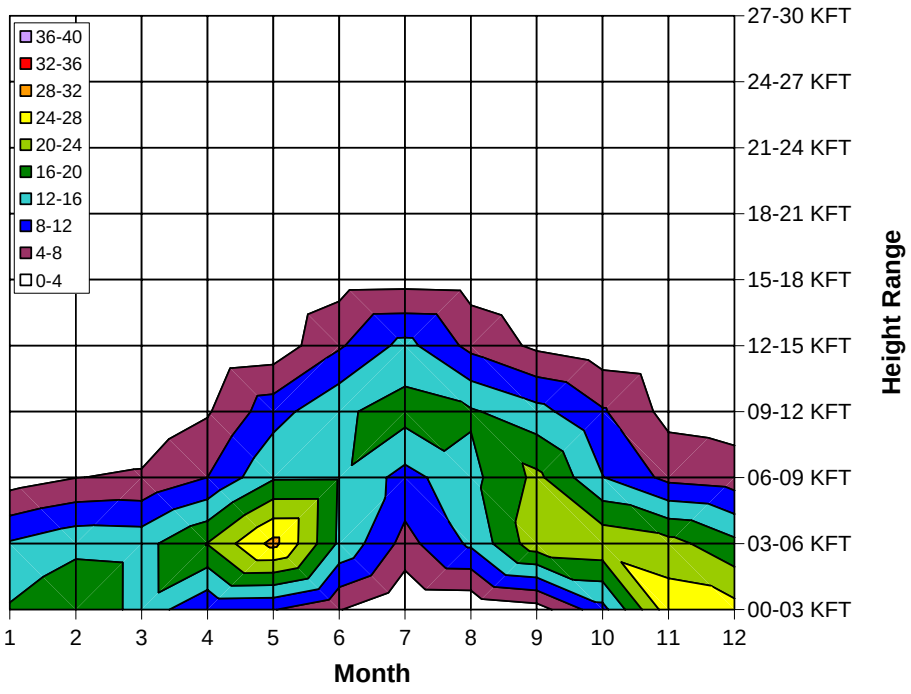

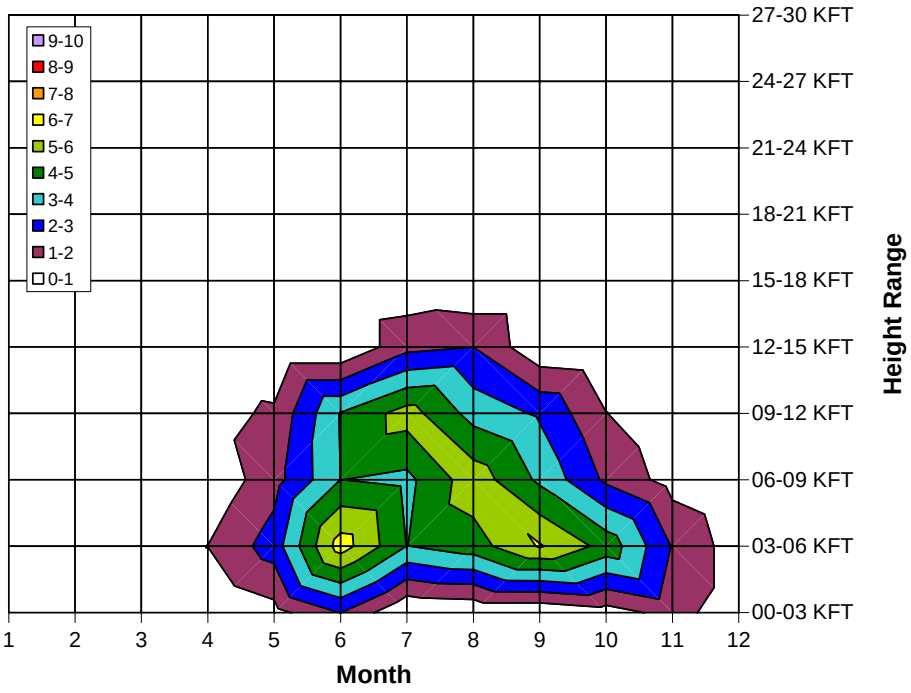

Color intervals are every 4% for icing and 1% for SLD.

FIGURE 9t. TIME-HEIGHT DISTRIBUTION OF INFERRED ICING AND SLD FREQUENCY (%) FOR THE INDIVIDUAL STATION OF MURMANSK, RUSSIA

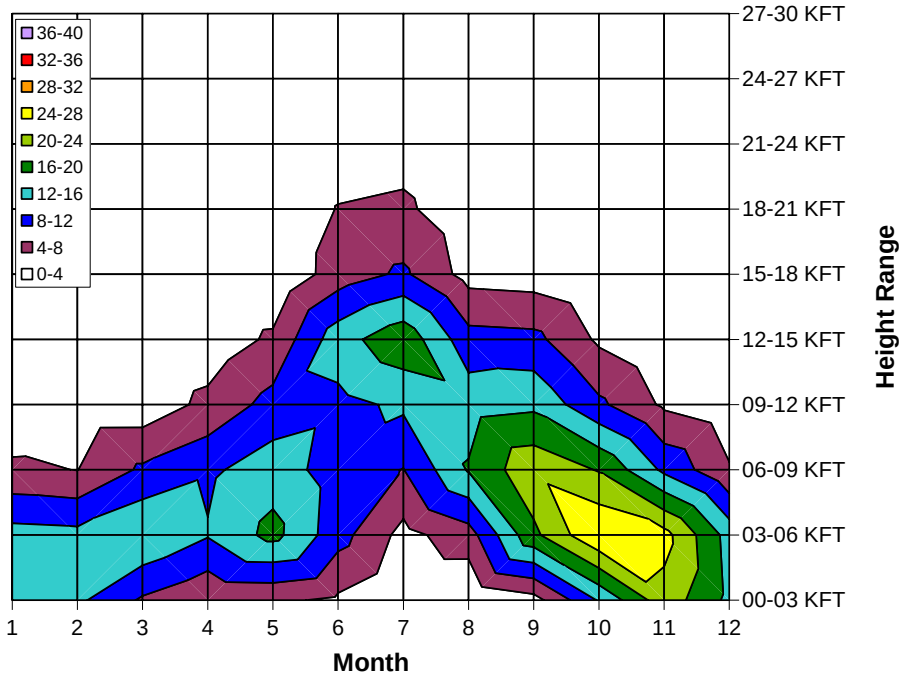

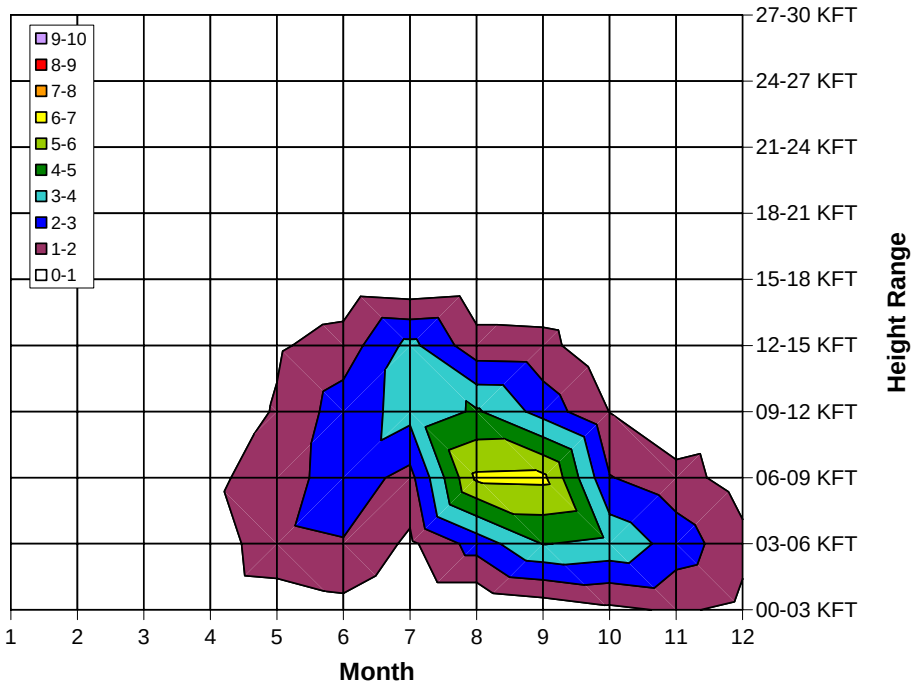

Color intervals are every 4% for icing and 1% for SLD.

FIGURE 9u. TIME-HEIGHT DISTRIBUTION OF INFERRED ICING AND SLD FREQUENCY (%) FOR THE INDIVIDUAL STATION OF POCORA, RUSSIA

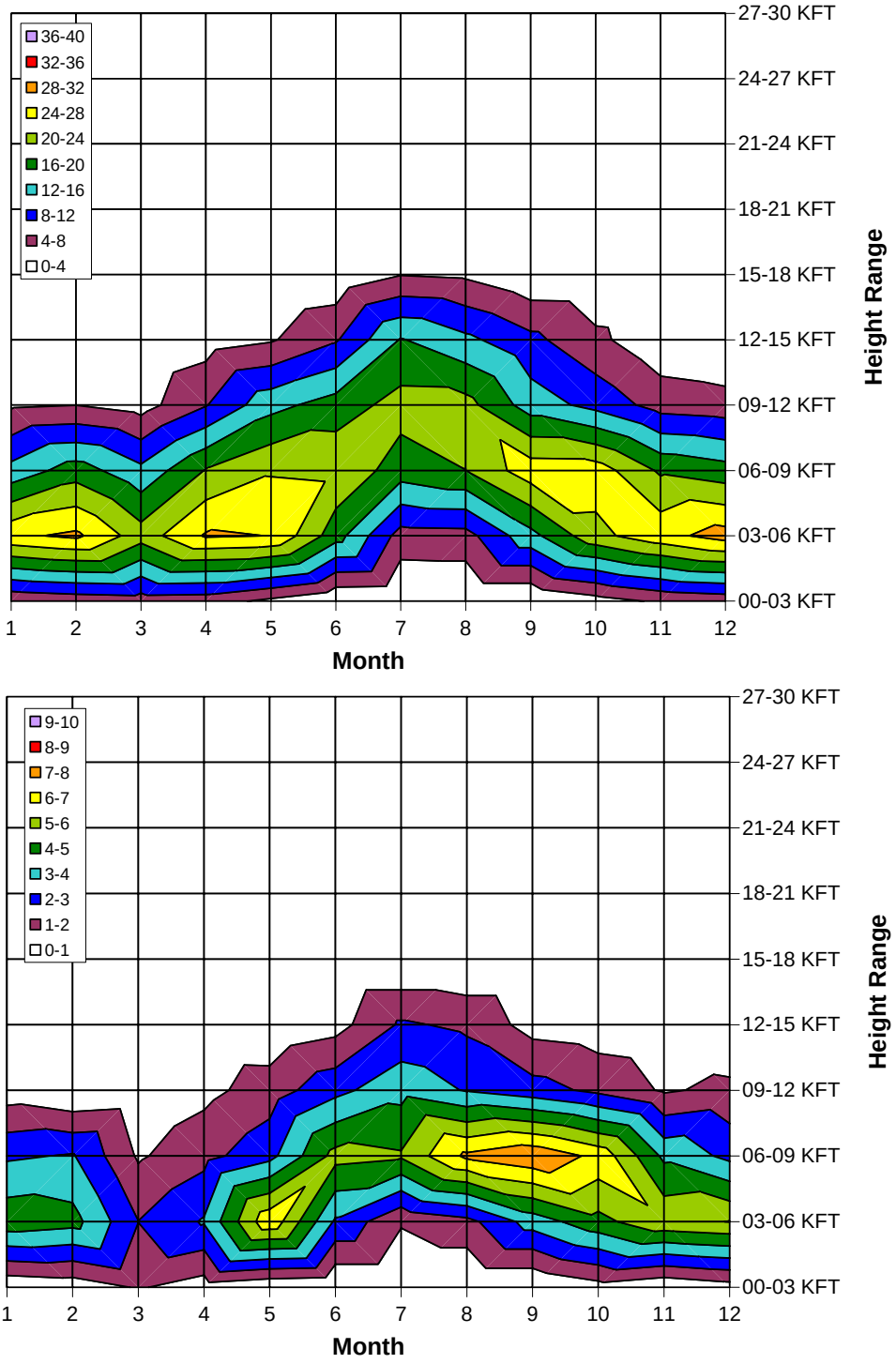

Color intervals are every 4% for icing and 1% for SLD.

FIGURE 9v. TIME-HEIGHT DISTRIBUTION OF INFERRED ICING AND SLD FREQUENCY (%) FOR THE INDIVIDUAL STATION OF BODOVI, NORWAY

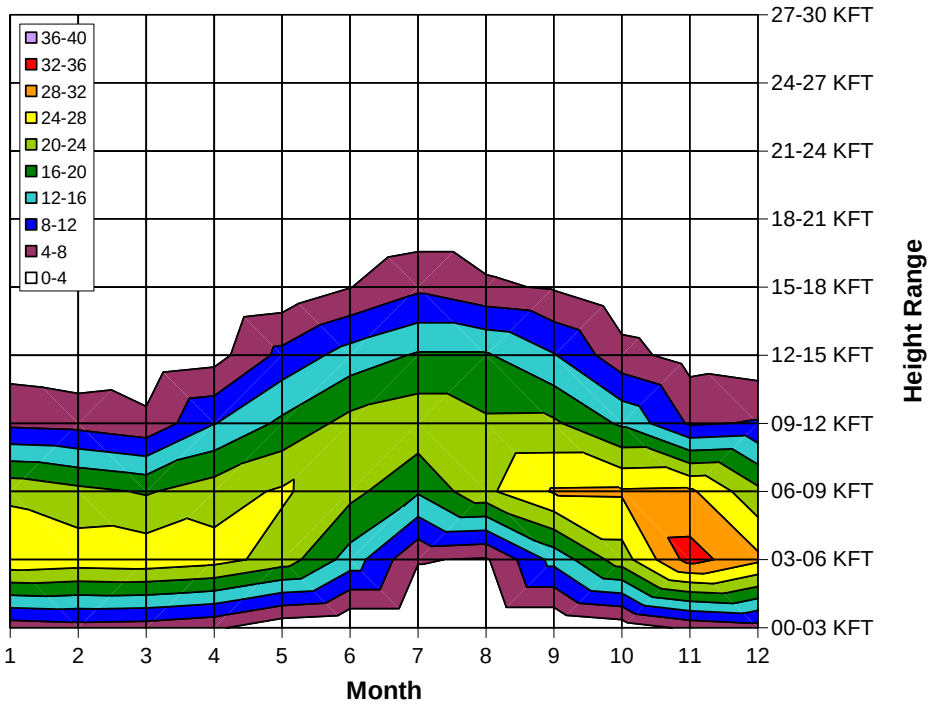

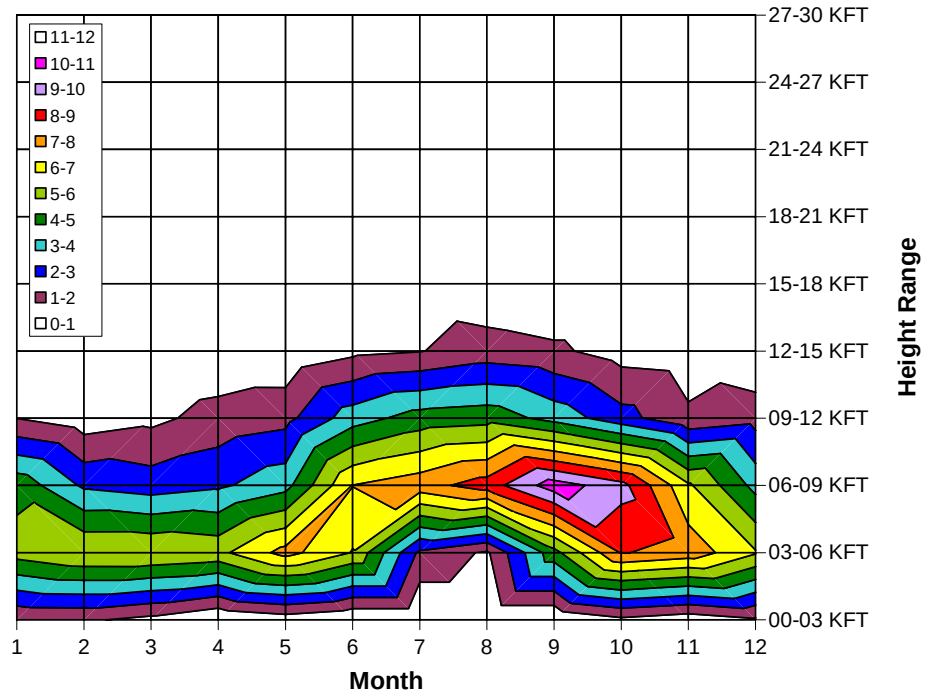

Color intervals are every 4% for icing and 1% for SLD.

FIGURE 9w. TIME-HEIGHT DISTRIBUTION OF INFERRED ICING AND SLD FREQUENCY (%) FOR THE INDIVIDUAL STATION OF ORLAND, NORWAY

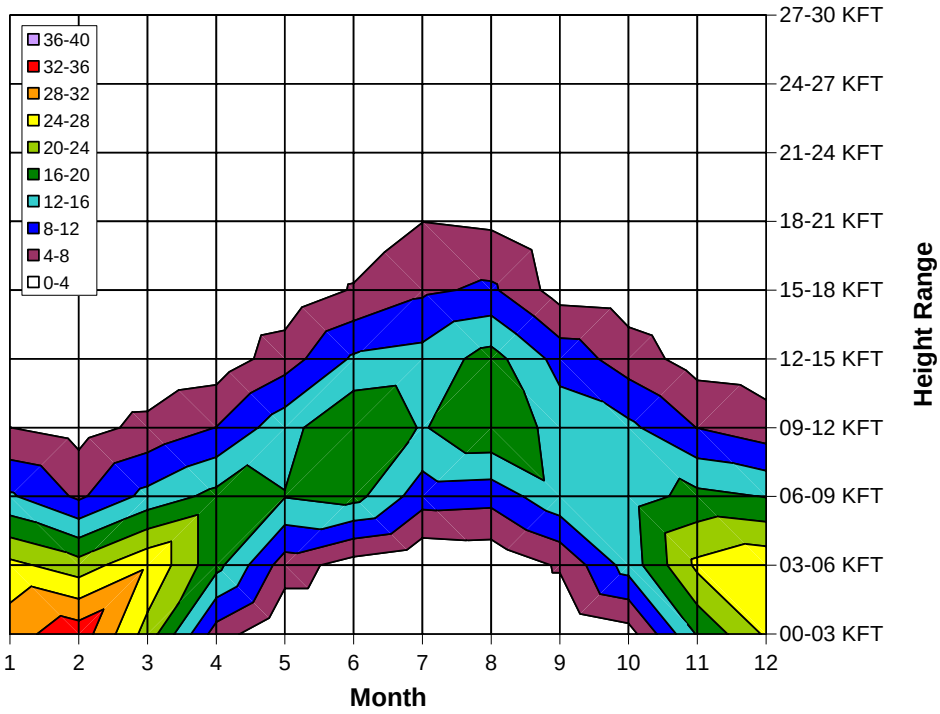

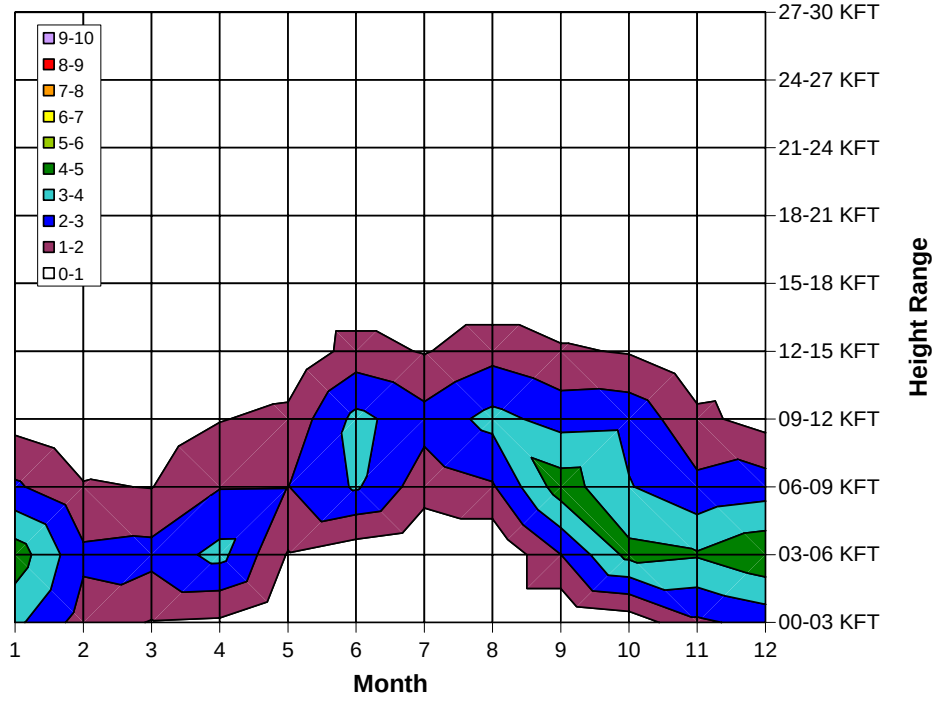

Color intervals are every 4% for icing and 1% for SLD.

FIGURE 9x. TIME-HEIGHT DISTRIBUTION OF INFERRED ICING AND SLD FREQUENCY (%) FOR THE INDIVIDUAL STATION OF STOCKHOLM, SWEDEN

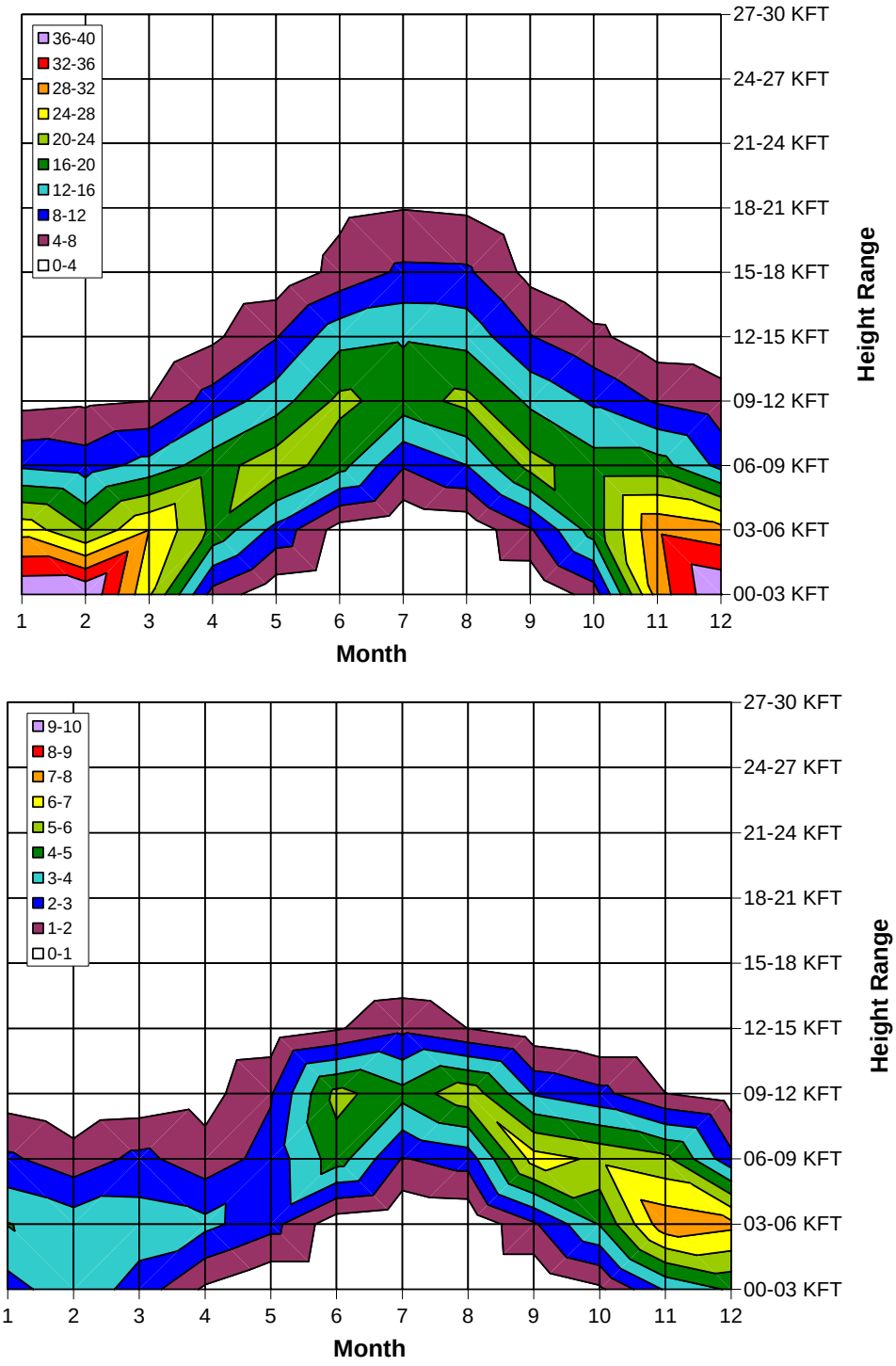

Color intervals are every 4% for icing and 1% for SLD.

FIGURE 9y. TIME-HEIGHT DISTRIBUTION OF INFERRED ICING AND SLD FREQUENCY (%) FOR THE INDIVIDUAL STATION OF JOKIONEN, FINLAND

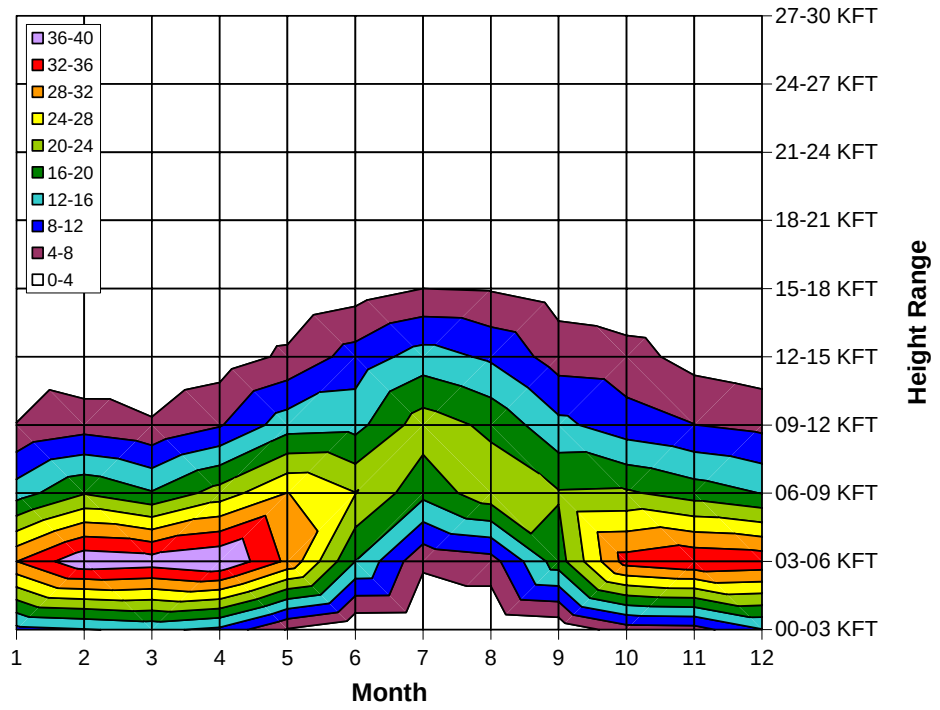

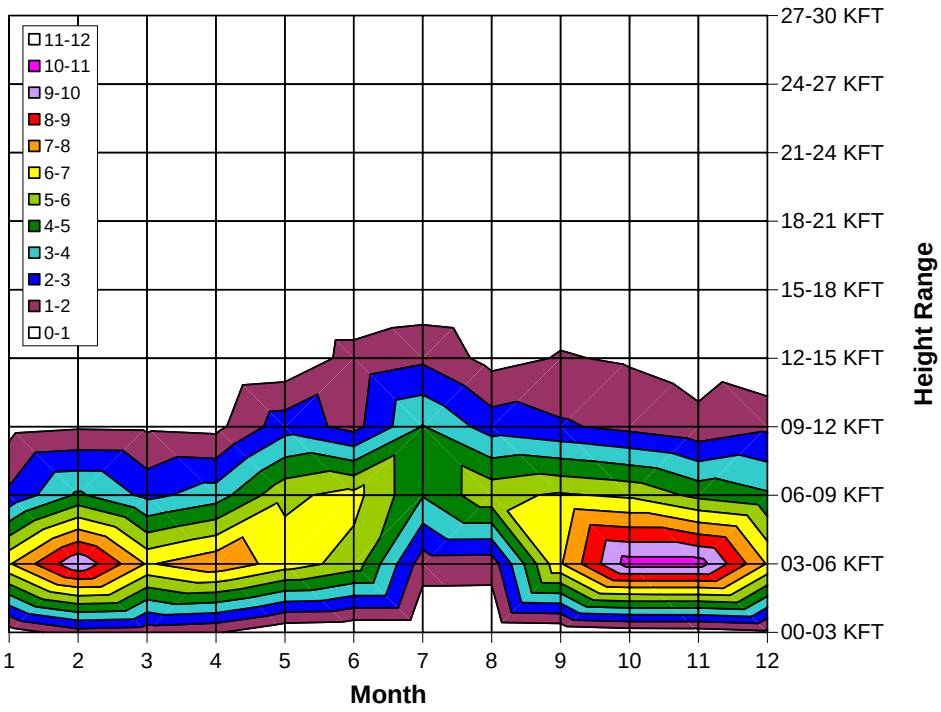

Color intervals are every 4% for icing and 1% for SLD.

FIGURE 9z. TIME-HEIGHT DISTRIBUTION OF INFERRED ICING AND SLD FREQUENCY (%) FOR THE INDIVIDUAL STATION OF KEFLAVIK, ICELAND

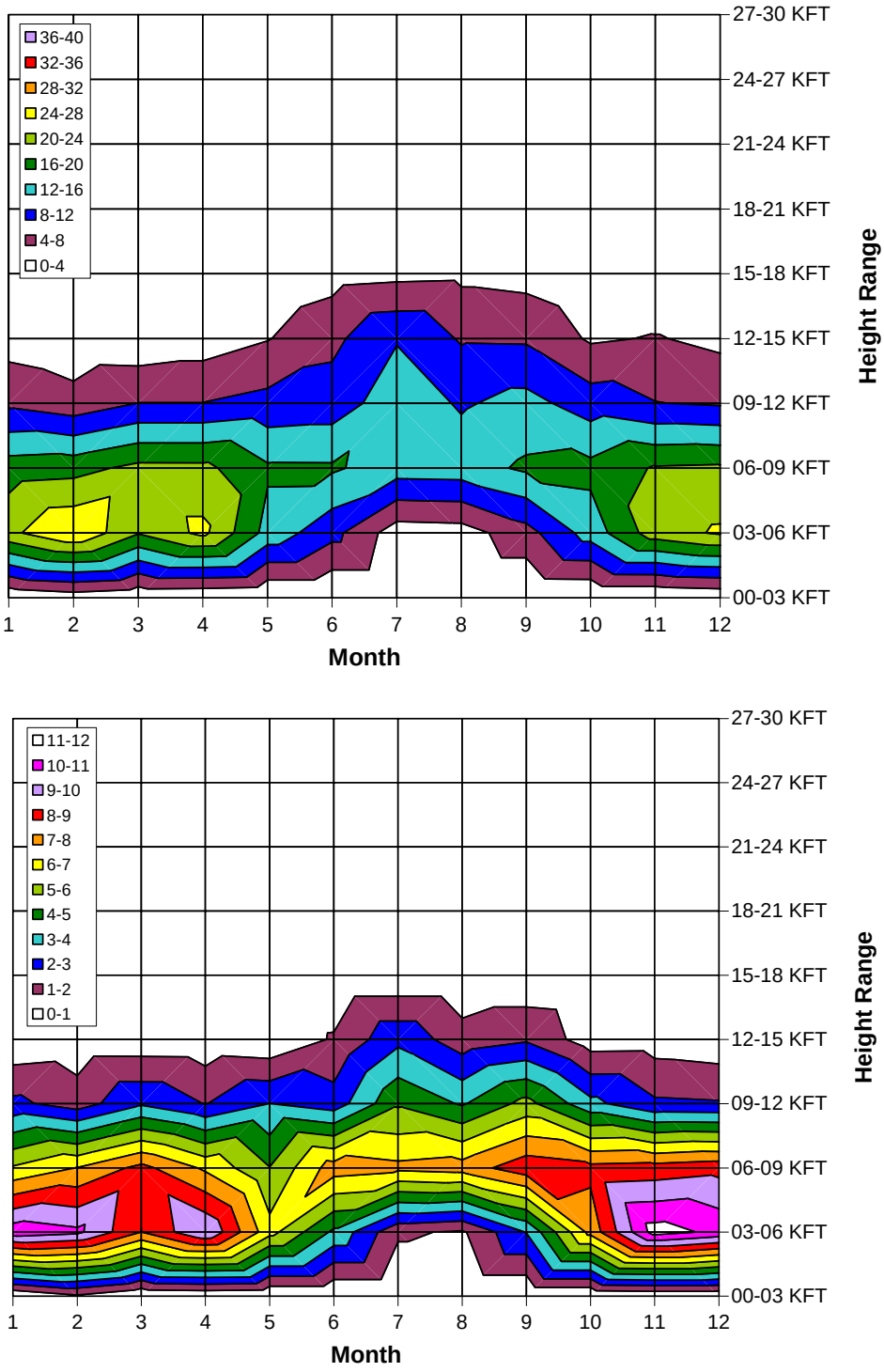

Color intervals are every 4% for icing and 1% for SLD.

FIGURE 9aa. TIME-HEIGHT DISTRIBUTION OF INFERRED ICING AND SLD FREQUENCY (%) FOR THE INDIVIDUAL STATION OF STORNOWAY, SCOTLAND

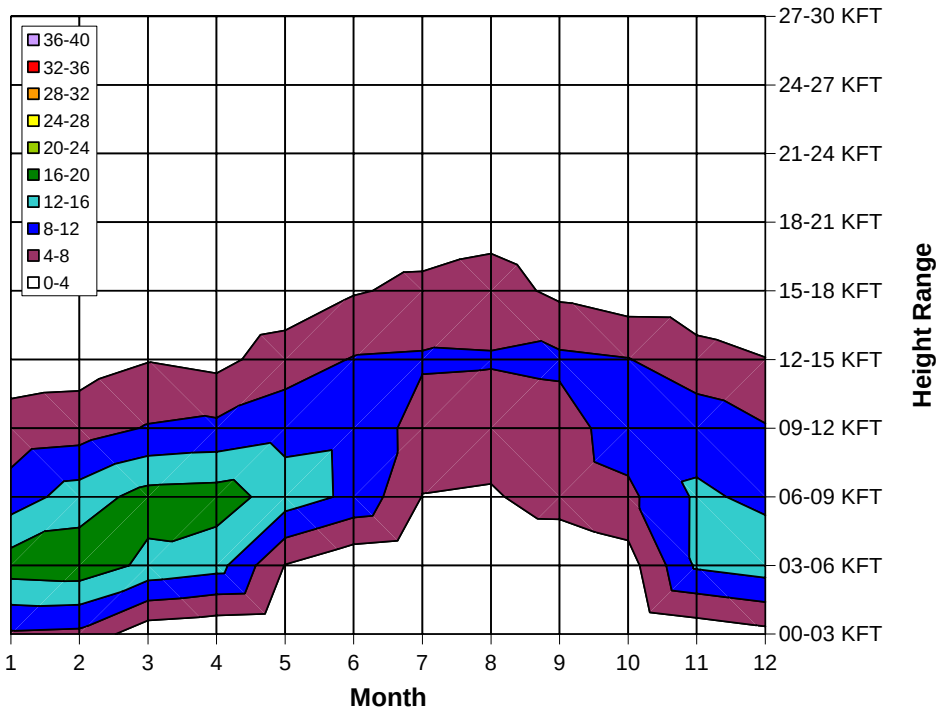

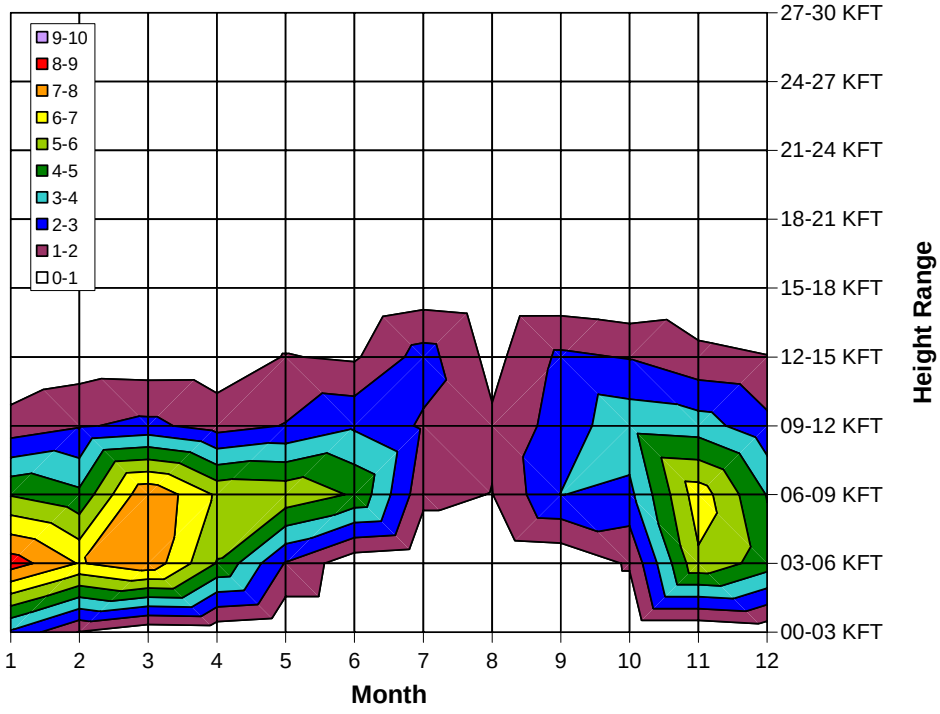

Color intervals are every 4% for icing and 1% for SLD.

FIGURE 9ab. TIME-HEIGHT DISTRIBUTION OF INFERRED ICING AND SLD FREQUENCY (%) FOR THE INDIVIDUAL STATION OF LONDON, ENGLAND

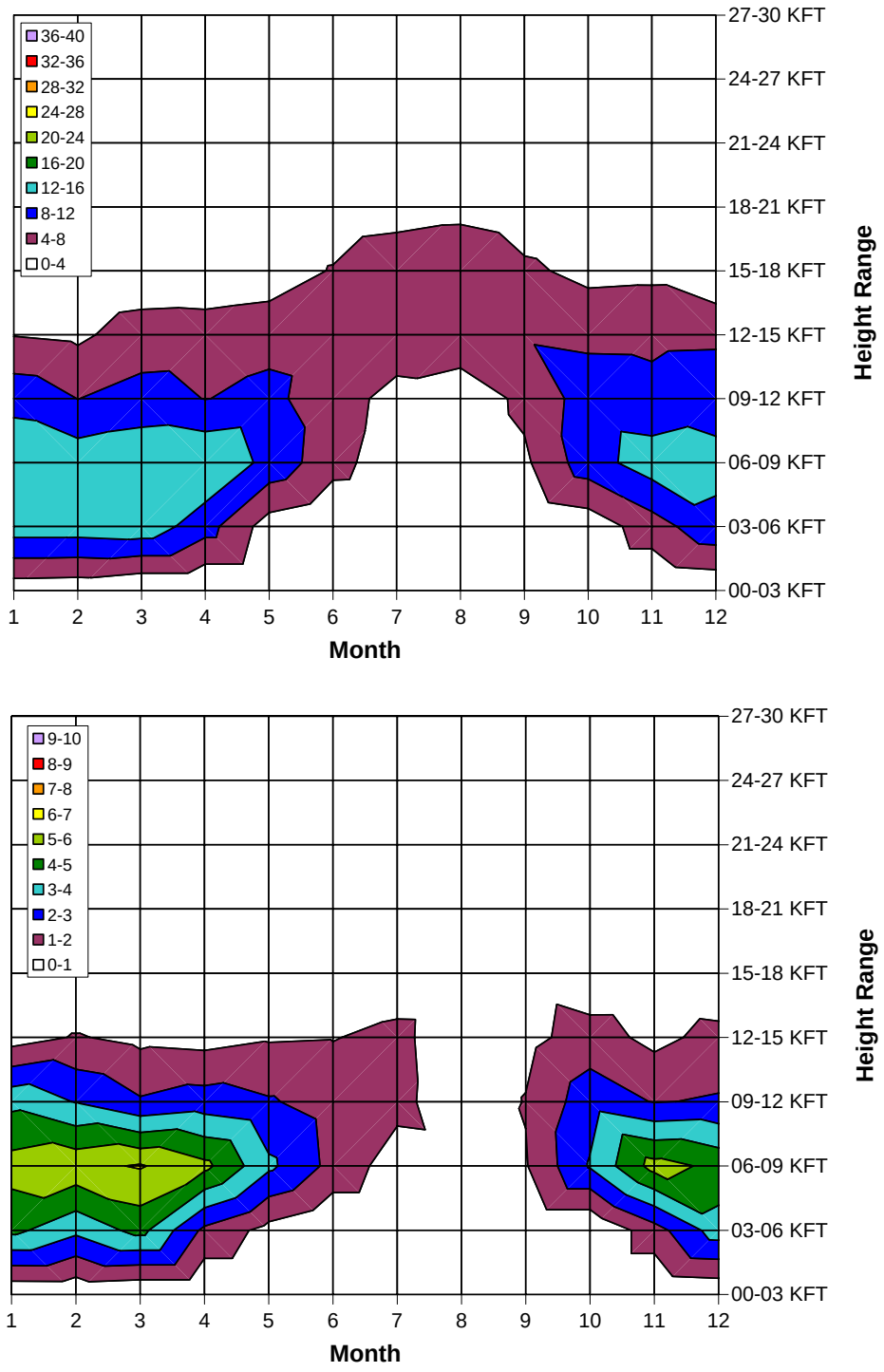

Color intervals are every 4% for icing and 1% for SLD.

FIGURE 9ac. TIME-HEIGHT DISTRIBUTION OF INFERRED ICING AND SLD FREQUENCY (%) FOR THE INDIVIDUAL STATION OF BREST, FRANCE

3.3 SUPERCOOLED LARGE DROPLET LAYER DEPTHS.

SLD layers occurred over a wide range of depths, and their distribution was dependent on the formation mechanism. For classical SLD, the peak occurred at <500 ft (<~150 m; figure 10). About 25% of all classical SLD events fell into this range, while about half were less than 1000 ft (~330 m) deep, ~90% were less than ~2500 ft (~800 m) deep, and ~99% were less than 4000 ft deep. Nonclassical SLD events were deeper, in general, with the peak in the distribution at 1500-2000 ft (~450-600 m). About 20% of all nonclassical SLD events fell into this range, about half were less than ~1800 ft (~600 m), ~90% were less than ~4500 ft (~1350 m) deep, and ~99% were less than 7000 ft deep. The deepest event may have been as much as 15,000 ft deep. It is important to recall that such an estimate was based on the assumption that nonclassical SLD proliferated throughout the lower cloud deck, so the top of the layer was often assumed to be at cloud top. Sounding by sounding estimates of SLD layer depths were likely not as accurate as those calculated for North America because of the relative lack of vertical resolution in the European data. This may have inflated layer depths somewhat, but to what extent, it is difficult to say. However, results are consistent with those from North America, so the distributions are likely reasonable. SLD layers documented by research aircraft over Canada, the Great Lakes and Colorado had depths that reasonably matched the distributions found in the climatology [2, 23, 24, and 25].

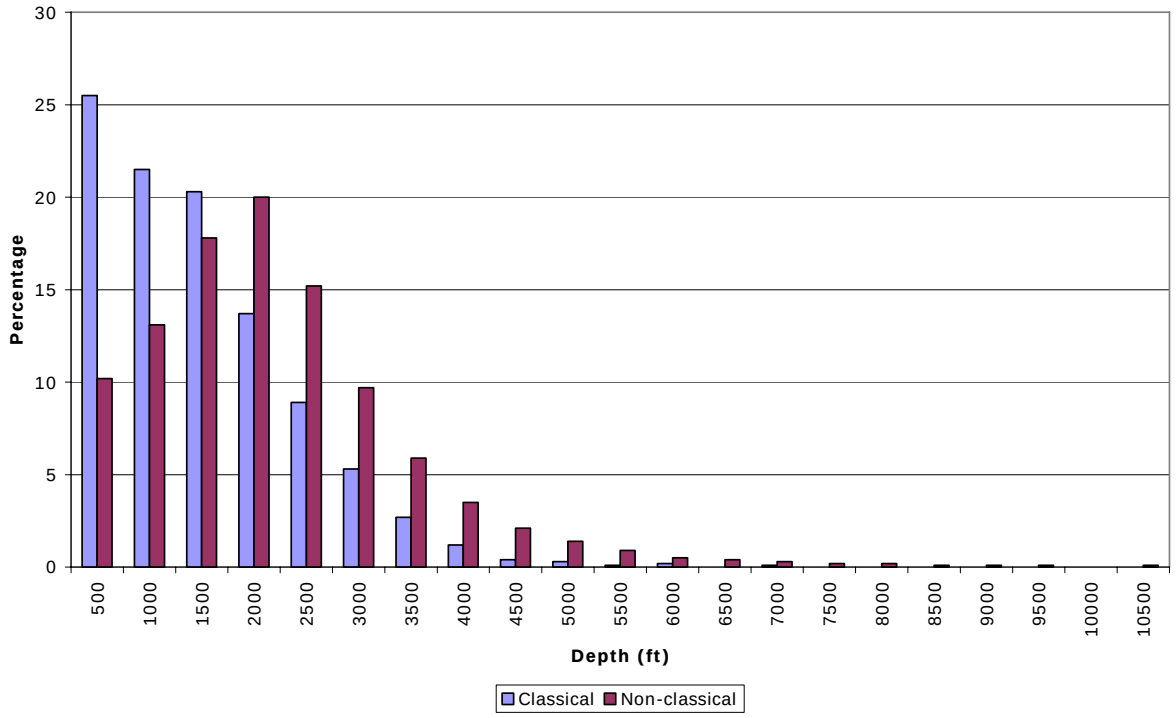

X axis values are the max in the bin.

FIGURE 10. SUPERCOOLED LARGE DROPLET LAYER DEPTH DISTRIBUTIONS FOR CLASSICAL (BLUE) AND NONCLASSICAL (PURPLE) STRUCTURES

4. COMPARISON WITH PAST EUROPEAN CLIMATOLOGIES.

For Europe, one SLD and four icing climatologies were found in the historical literature. An initial sounding-based icing climatology by Katz [7], later updated by Heath and Cantrell [8] showed similar patterns to those found here. Icing migrated latitudinally and vertically with season. Frequencies were calculated at standard pressure levels (e.g., 850 mb), rather than in altitude bins and for the whole column, and the data used were from a few years surrounding 1950, rather than the larger 15 year climatology presented here. To compare the new results with the pressure-based results, a separate test was run on the new data, calculating icing frequencies at the standard pressure levels. Absolute values were reasonably similar, overall, but were sometimes 2-4 times larger and smaller at individual locations, altitudes, and times of the year. The same was true in comparisons with an analysis of reconnaissance aircraft observations of subzero cloud taken over the UK and surrounding areas by the British military during and following World War II [14]. Two-dimensional maps of icing-free conditions compiled from two winters of output from the Meteo-France SIGMA icing algorithm [7] showed similar (but inverted) patterns to those found here for their domain (UK, eastern Spain, France, and bordering areas to the east). Only the Meteo-France study included a climatology of SLD, based solely on surface observations of FZDZ and FZRA from the years 1995-98. The results were, again, comparable with similar absolute frequencies. FZDZ maxima were found in parts of Germany and at significantly elevated stations, and FZRA maxima in eastern France, southern Germany and some parts of the Balkans.

5. IMPLICATIONS FOR COMMUTER FLIGHTS.

Short-range commuter aircraft, in particular, have a good chance of encountering icing and even SLD conditions during flights over Europe. Such aircraft complete many flights per day, and because of their short routes, spend a relatively large percentage of their flight time at altitudes below 20,000 ft where nonconvective icing and SLD are most common. The frequency of exposure is certainly impacted by flight location. Aircraft spending most of their time flying close to the Mediterranean will likely encounter such conditions much less frequently than those flying into Scandinavia, central Europe, the Baltics, Balkans, and western Russia (icing only for the latter three regions). Pilots flying within the icing-prone regions should be particularly aware of the hazard, since they are more likely to encounter it over the course of a flight career. Of course, the vast majority of these events do not result in accidents, otherwise icing-related accidents would happen frequently. A very unique combination of meteorological conditions and aviation parameters must occur for the icing to contribute to an accident. The results presented in this document only represent an estimate of the meteorological part of the equation.

Given the typical range of altitudes for icing and SLD, most encounters are likely to occur during hold, descent, or climb. Summertime encounters may occur above 12,000 ft, especially in deep convection. Most SLD events appear to be less than 2000 ft deep, so escape may only require a change in altitude of a few thousand feet. In the deepest cases, however, such an altitude change may not result in an exit from the conditions. Knowledge of the altitudes of the freezing level (if it is above ground, which it usually is over Europe) and cloud top may prove to be critical in these situations.

6. CONCLUDING REMARKS.

The results described here were based on the inferred presence of icing and supercooled large droplets (SLD) aloft, based upon coincident surface observations of cloud cover and precipitation type and balloon-borne soundings of temperature and dew point. The techniques applied have important limitations. First, icing and SLD associated with thunderstorms was not considered. This was done because aircraft specifically avoid flight into thunderstorms due to the many hazards they present, such as hail and lightning. Thus, their inclusion would have incorrectly inflated the inferred exposure rate. Second, any SLD aloft that was not reflected as freezing or liquid precipitation at the surface was missed. Since there is no reliable method to determine the presence of such situations from climatological data when liquid precipitation is not reported, this was an unavoidable shortcoming of the study. Third, a 100-km-radius circle was used to find surface reports in the vicinity of balloon launches. Appropriate precipitation types were often observed by a subset of all stations within the circle. Thus, only a portion of the 100-km-radius cylinder may have contained SLD. One must consider this when estimating the actual chances that an aircraft flying over a given location would be exposed to SLD. Fourth, the choice of a threshold of 0.4 permits most SLD will be captured, but may result in an over diagnosis in some cases when conditions for SLD are somewhat marginal. Increases (decreases) in threshold choice would result in decreases (increases) in frequencies. Most icing and SLD aloft should have been captured by the methodologies and thresholds applied here.

Regardless of their frequency, depth, and mechanism, when combined with the wrong set of circumstances, encounters with SLD events can result in significant performance effects and even disaster. It is imperative that pilots are aware of the presence or expectation of such conditions along their flight route and know the appropriate escape routes to allow for a quick exit from the conditions.

7. REFERENCES.

1. Marwitz, J.D., M.K. Politovich, B.C. Bernstein, F.M. Ralph, P.J. Neiman, R. Ashenden, and J. Bresch, “Meteorological Conditions Associated With the ATR-72 Aircraft Accident Near Roselawn, Indiana on 31 October 1994,” *Bull. Amer. Meteor. Soc.*, 78, pp. 41-52, 1997.

2. Cober, S.G., G.A. Isaac, and J.W. Strapp, “Characterizations of Aircraft Icing Environments That Include Supercooled Large Drops,” *J. Appl. Meteor.*, 40, pp. 1984-2002, 2001.

3. Miller, D., T. Ratvasky, B. Bernstein, F. McDonough and J.W. Strapp, “NASA/FAA/NCAR Supercooled Large Droplet Icing Flight Research: Summary of Winter 96-97 Flight Operations,” *36th Aerospace Science Meeting and Exhibit*, AIAA, Reno, NV, 12-15 January 1998.

4. Bernstein, B.C., F. McDonough, and R. Bullock, “An Inferred Climatology of Supercooled Large Droplet Icing Conditions for North America,” *39th Aerospace*

Sciences Meeting and Exhibit, 6-10 January 2003: American Institute of Aeronautics and Astronautics, Washington, D.C., paper AIAA-2003-0563, 10 pp, 2003.

5. Fowler, T.L., M. Crandell, and B.G. Brown, "An Inferred Icing Climatology—Part III: Icing Airmets and IIDA," in compendium of preprints for the *10th Conference on Aviation, Range and Aerospace Meteorology*, Portland, OR, 12-15 May 2003, pp. J25-J28, 2003.

6. Young, G.S., B.G. Brown, and F. McDonough, "An Inferred Icing Climatology—Part I: Estimation From Pilot Reports and Surface Conditions," in compendium of preprints for the *10th Conference on Aviation, Range and Aerospace Meteorology*, 12-15 May 2003, Portland OR, pp. J17-J20, 2003.

7. LeBot, C. and J. Carriere, "Two Approaches for an Icing Climatology Over Europe: Surface Freezing Precipitations and Altitude Icing Areas Based on the SIGMA System," *FAA In-flight Icing/Ground De-icing International Conference*, June 16-20, 2003, Chicago, Illinois, paper 2003-01-2118, 2003.

8. Katz, L.G., "Climatological Probability of Aircraft Icing," Air Weather Service Technical Report No. 194, available from the Environmental Technical Applications Center (ETAC), USAF, Bldg 159, Navy Yard Annex, Washington, DC 20333, 1967.

9. Heath, E.D. and L.M. Cantrell, "Aircraft Icing Climatology for the Northern Hemisphere," Air Weather Service Technical Report No. 220, available from the Environmental Technical Applications Center (ETAC), USAF, Bldg 159, Navy Yard Annex, Washington DC 20333, 1972.

10. Stuart, R.A. and G.A. Issac, "Freezing Precipitation in Canada," *J. Atmos. Oceanic Technol*., **37-1**, pp. 87-102, 1999.

11. Carriere, J., C. Lainard, C. LeBot, and F. Robart, "A Climatological Study of Surface Freezing Precipitation in Europe," *Meteor. Appl.*, **7**, pp. 229-238, 2000.

12. Bernstein, B.C., "Regional and Local Influences on Freezing Drizzle, Freezing Rain, and Ice Pellet Events," *Wea. Forecasting*, **15**, pp. 485-508, 2000.

13. Ryerson, C.C., "Atmospheric Icing Climatologies of Two New England Mountains," *J. Appl. Meteor*., 27, pp. 1261-1281, 1988.

14. Roach, W.T., D.A. Forrester, M.E. Crewe, and K.F. Watt, "An Icing Climatology for Helicopters," Royal Meteorological Office Special Investigations Memorandum 112, 1984.

15. Politovich, M.K. and T.A.O. Bernstein, "Aircraft Icing Conditions in Northeast Colorado," *J. Appl. Meteor*., 41, pp. 118–132, 2002.

16. Grelson, E.F., “A Climatology of Conditions Known to Lead to In-Flight Aircraft Icing Across North America,” M.S. Thesis, University of Nebraska, Lincoln, Nebraska, pp. 131, 1997.

17. Bernstein, B.C., T.A. Omeron, F. McDonough, and M.K. Politovich, “The Relationship Between Aircraft Icing and Synoptic Scale Weather Conditions,” *Wea. Forecasting*, 12, pp. 742-762, 1997.

18. Bernstein, B.C., F.M. McDonough, M.K. Politovich, B.G. Brown, T.P. Ratvasky, D.R. Miller, and C.A. Wolff, “The Current Icing Potential (CIP),” submitted to *J. Appl. Meteor*., 2004.

19. Wang, J.W. and W.B. Rossow, “Determination of Cloud Vertical Structure From Upper-Air Observations,” *J. Appl. Meteor*., 34, pp. 2243-2258, 1995.

20. Hanesiak, J.M. and R.E. Stewart, “The Mesoscale and Microscale Structure of a Severe Ice Pellet Storm,” *Mon. Wea. Rev*., 123, pp. 3144-3162, 1995.

21. Korolev, A.V. and G.A. Isaac, “Drop Growth Due to High Supersaturation Caused by Isobaric Mixing,” *J. Atmos. Sci.*, 57, pp. 1675-1685, 1995.

22. Rasmussen, R.M., I. Geresdi, G. Thompson, K. Manning, and E. Karplus, “Freezing Drizzle Formation in Stably Stratified Layer Clouds: The Role of Radiative Cooling of Cloud Droplets, Cloud Condensation Nuclei, and Ice Initiation,” *J. Atmos. Sci.*, 59, pp. 837-860, 2002.

23. Bernstein, B.C., “Analysis of the Meteorology Associated With the 1998 NASA Glenn Twin Otter Flights,” NASA CR-2000-209413, 2000.

24. Politovich, M.K. and B.C. Bernstein, “Production and Depletion of Supercooled Liquid Water in a Colorado Winter Storm,” *J. Appl. Meteor*., 34, pp. 2631-2648, 1995.

25. Rasmussen, R.M., B.C. Bernstein, M. Murakami, G. Stossmeister, J. Reisner, and B. Stankov, “The 1990 Valentine’s Day Arctic Outbreak, Part I: Mesoscale and Microscale Structure and Evolution of a Colorado Front Range Shallow Upslope Cloud,” *J. Appl. Meteor*., 34, pp. 1481-1511, 1995.